

UNIVERSITÀ DEGLI STUDI DI NAPOLI “FEDERICO II”

Dottorato in Scienze ed Ingegneria del Mare

in consorzio con

**SECONDA UNIVERSITÀ DI NAPOLI
UNIVERSITÀ “PARTHENOPE” NAPOLI**

in convenzione con

**ISTITUTO PER L’AMBIENTE MARINO COSTIERO – C.N.R.
STAZIONE ZOOLOGICA “ANTON DOHRN”**

XXV Ciclo

Tesi di Dottorato

**Particulate trace metals chemistry: new
constraints for the Si budget in the
Mediterranean sea**

Candidato: Dott.ssa Barbara Capuozzo

Tutor: Prof. Maurizio Ribera D’Alcalà

Co-Tutor : Dott. Mario Sprovieri

Il Coordinatore del Dottorato: Prof. Alberto Incoronato

ANNO 2013

INDEX

ABSTRACT

OVERVIEW

CHAPTER . 1 **THE MASS BALANCE OF SILICA IN THE MEDITERRANEAN SEA**

1.1	The Mediterranean basin.....	p. 3
1.1.1	Basin characteristics.....	p. 3-4
1.1.2	Circulation and ocean dynamics.....	p. 4-8
1.1.2.1	Water exchange through the Strait of Gibraltar and the Strait of Sicily...	p. 9
1.1.3	The Mediterranean Climate.....	p. 10
1.1.4	Biogeochemical cycles in the Mediterranean Sea	p. 10-12
1.2	Silicon in seawater.....	p. 12
1.2.1	Silicon and Marine Cycle.....	p. 12-14
1.2.2	The river inputs and the Si distribution patterns in the Mediterranean Sea.	p. 14-15
1.2.3	The atmospheric contribution to Silicon patterns in the Mediterranean Sea.	p. 15-16
1.2.4	Kinetics Dissolution of Silicon from marine particulate.....	p. 16-18
1.3	The mass balance of Si in the Mediterranean sea: a state of the art.	p. 19
1.3.1	Mass Balance.....	p.19
1.3.2	Budget of Si in the Mediterranean Sea.....	p. 19-21
1.3.3	Objective of this research work.....	p. 22

CHAPTER. 2 MATERIALS AND METHOD

2.1	Sampling activities: nutrients and trace metals in seawater.....	p. 23
2.1.1	The sampling area.....	p. 23
2.1.2	CTD Rosette sampling.....	p. 26
2.1.3	Sampling techniques	p. 26-27
2.2	Analytical procedures for nutrients, and trace elements.....	p. 27
2.2.1	Nutrients.....	p. 27-28
2.2.2	Analytical procedures for analysis of trace elements in particulate phase	p. 28
2.2.2.1	Analytical procedures for analysis of trace elements in particulate phase	p. 28

CHAPTER . 3 RESULTS

3.1	Nutrients.....	p. 30
3.1.1	Silicates -the Bonifacio_2010 cruise.	p. 30-31
3.1.2	Silicates - the Aeolian_2010 cruise	p. 31-32
3.2	Trace Metals in the particulate phase.....	p. 33
3.2.1	Aluminium (Al).....	p. 34
3.2.2	Iron (Fe).....	p. 34-35
3.2.3	Zinc (Zn).....	p. 35-36
3.2.4	Copper (Cu).....	p. 36-37
3.2.5	Vanadium (V).....	p.37-38
3.2.6	Distribution of trace elements in particulate: comparison with literature information.	p. 38-39
3.2.6.1	Distribution of particulate Aluminum.....	p. 39-41
3.2.6.2	Distribution of particulate Iron.....	p. 41-43
3.2.6.3	Distribution of particulate Zinc.....	p. 43-45
3.2.6.4	Distribution of particulate Copper.....	p. 45-47
3.2.6.5	Distribution of particulate Vanadium.....	p. 47-48

CHAPTER . 4 DISCUSSION

4.1	Distribution of particulate in the Mediterranean sea	p. 50-55
4.2	Estimation of dust deposition at basin scale	p. 55-59
4.3	Hydrographic characteristics at the Strait of Sicily: new	p. 59-61

observations for the silicon balance

4.4 Particulate chemistry and source areas p. 62-67

4.5 Enrichment factors P 67-70

CHAPTER. 5 CONCLUSION

REFERENCE

APPENDIX I Chemical analysis of Nutrients_ Bonifacio Cruise

APPENDIX II Chemical analysis of Nutrients_ Aeolian Cruise

APPENDIX III Chemical analysis of Trace Metals_ Bonifacio Cruise

APPENDIX IV Silicon and Aluminum concentrations in the suspended particulate matter of the Rhone river

[Ollivier 2011]

Abstract

Silicon plays a key role in the ocean biogeochemical cycles by its direct link with the carbon cycle through the chemical weathering of silicate minerals and transfer of carbon dioxide from the atmosphere to the lithosphere and the massive transfer of carbon from the surface to the deep seawater through sinking of marine siliceous phytoplankton such as diatoms.

Despite the great importance of silicon in biogeochemical cycles budgets of this element at the scale of marginal seas, as Mediterranean sea, which are among the main contributors to the global ocean, are scarce. On the other hand Mediterranean sea is well suited to monitor elemental fluxes towards the open ocean because of the narrow connection with it. Recent observations evidence that the silica cycle in the Mediterranean sea is characterized by a net deficit of silicon. Observed fluxes are only partially able to compensate net losses, and suggest a net accumulation in the western basin and a deficit in the eastern basin.

This research presents a review of the mass balance of the silicon through the exploration of the potential role played by the atmospheric dust and particulate forms from river inputs, taking into account also of the dynamic biogeochemical of the basin.

In addition, analysis of trace elements chemistry in seawater particulate, provides a good tool to investigate on natural and anthropogenic sources influencing different area of the Mediterranean basin.

The resulting contribution to dissolved Si contribution from atmospheric and river particulates, shows a relatively low impact, in relation to the strongly variability of the system, meant as a variation of atmospheric flows and river flows. There are considerable difficulties associated with the assessment of the role of the particulate in the budget of the silicon, therefore further investigations are needed to better constraint the silicon budget by more specific data collection of particulate in seawater associated to estimates of atmospheric deposition from satellite observations.

However the revisited budget based on an updated mass fluxes, specifically of deep waters, at the Sicily strait , allows us to formulate a new hypothesis concerning biogeochemical behavior of silicon in marine systems.

Overview

Silicon is the second most abundant element in the Earth's crust, and is a main constituent in a variety of matrices such as soils, sediments, phytoplankton, plants, natural waters, primary and secondary minerals.

The continental silicate crust is exposed to the atmosphere and hydrosphere and thus to the physical and chemical disintegrative processes of weathering. The products of leaching occur in particulate and dissolved form and are carried by wind and by rivers into the sea. The two forms of reactive Si considered are dissolved silicate (DSi) and biogenic silica (bSiO₂). Because of biological activity, surface waters throughout most of the marine realm are depleted in dissolved silicate, reaching values as low as a few micromoles per liter. When organism from the siliceous biota die, their skeletons settle through the water column, where more than 90% of the silica is regenerated via inorganic dissolution. Part of the bSiO₂ is deposited in riverine sediments, but a significant fraction reaches the coastal waters thus contributing to the total riverine input of silica to the sea [Conley, 1997].

The Mediterranean basin is an effective receptor of matter; it receives atmospheric and river inputs of considerable importance for the biogeochemistry of the basin, which appear strongly associated with the hydrodynamic patterns, with a close relationship between chemical parameters and water mass distribution.

Estimates of flows in and out the straits [Ribera d'Alcala' *et al.*, 2003] have shown that the Mediterranean basin is characterized by a net loss of silicon in the eastern and western Mediterranean.

Recently, Lavezza, (2010) provided a new elaborated composite profiles of Si along the water column and different budgets for the Mediterranean basin, also taking into account more updated estimates of river inputs [Ludwig *et al.*, 2009]. In particular, it was observed that influxes are only partially able to compensate net losses, and the new estimate has revealed a net accumulation in the western basin and a deficit in the eastern basin.

Aim of this work is to improve the knowledge of the silicon mass balance in the Mediterranean Sea and to understand what is the potential role played by the atmospheric and river particulate on the Si budget at basin scale.

The main objectives of this research effort can be synthesised as follows:

- ✓ To contribute through new datasets of i) nutrients, ii) trace metals in the particulate phase collected from key areas of the Mediterranean sea to a revised budget of Si at basin scale;
- ✓ To explore the different sources of silicon in the Mediterranean basin and in particular the role played by the atmospheric dust and river particulate in terms of basin scale mass balance;
- ✓ To explore the role played by the transitional Eastern Mediterranean Deep Water in terms of Si transport from the deep Eastern to the deep Western basin;
- ✓ To discriminate influences of natural and anthropogenic sources of atmospheric dust in terms of chemical signatures, on the Mediterranean sea.

Chapter 1

THE MASS BALANCE OF SILICON IN THE MEDITERRANEAN SEA

1.1-The Mediterranean basin

1.1.1- Basin characteristics

The Mediterranean sea is the largest semi-enclosed sea on the Earth, its surface being similar to that of the largest semi enclosed [e.g., the Gulf of Mexico] and open marginal sea [e.g., the Caribbean Sea] of the ocean [Meybeck *et al.*, 2007]. The Mediterranean Sea is a concentration basin; evaporative losses [E] exceed the freshwater inputs resulting from precipitation [P] and river runoff [R] [Béthoux, 1980; Garret, 1996; Gilman and Garret, 1994].

Its surface is approximately 2.51 million Km² and has a width of about 6000 Km. It is a paradigm of semi-enclosed seas with specific characteristics that makes its study an exciting oceanographic issue from many points of view. This intercontinental sea is connected to the Atlantic Ocean to the west, across the Strait of Gibraltar, and on the other side, the Dardanelles/Marmara Sea/Bosporus straits system connects the Mediterranean basin to the Black Sea [Theocharis *et al.*, 1999; Malanotte-Rizzoli *et al.*, 1997].

The Mediterranean Sea is divided by the Strait of Sicily into two main sub-basins [Figure 1.1] the western and eastern Mediterranean. It is bordered by Europe to the North, Asia to the East and Africa to the south.

The western basin is formed by the Alboran and Algero-Provencal basins and the Tyrrhenian Sea. The eastern basin includes the Adriatic Sea, the Ionian Sea, the Levantine basin and the Aegean Sea. In the western basin there are external forcing that affect the eastern basin; the latter is subjected to the influence of the dynamics of the Adriatic and Aegean.

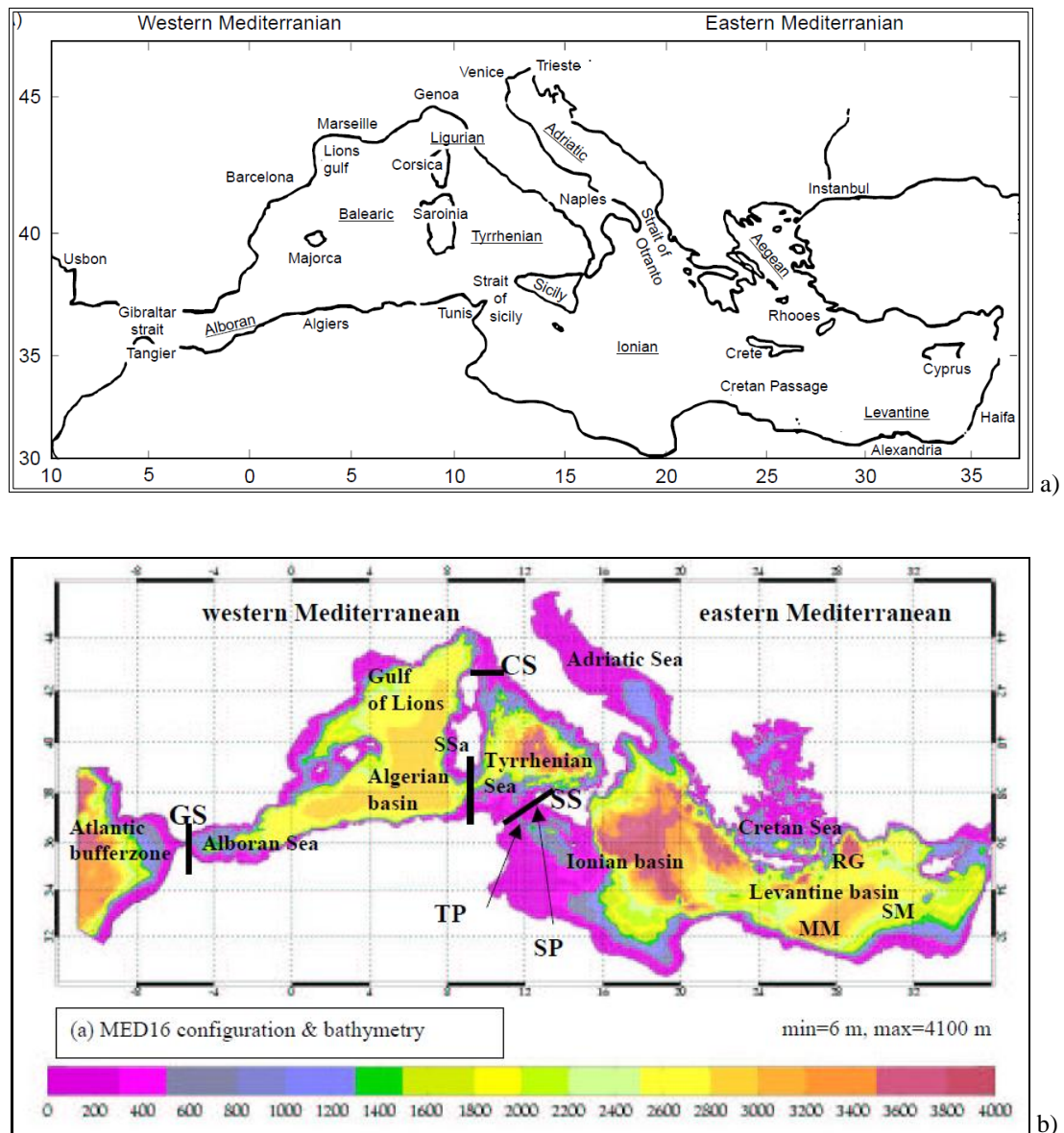


Figure 1.1: The geography of the Mediterranean Sea and nomenclature of the major sub-basins and straits (a) and bathymetry (b).

1.1.2- Circulation and ocean dynamics

The Mediterranean sea is considered a miniature ocean basin extremely suitable for investigating process occurring at global scale. Also, being relatively small, the Mediterranean is a test basin for general circulation and dynamic studies.

The general circulation of the basin is composed by three predominant and interacting spatial scales: the basin scale (including the thermohaline –3D circulation), the sub-basin scale, and the meso-scale. Complexity and dynamic scales arise from the multiple driving forces, from strong topographic and coastal influences, and from internal dynamical processes. There exist: free and boundary currents and jets which bifurcate, meander and grow and shed ring vortices; permanent

and recurrent sub-basin scale cyclonic and anticyclonic gyres, and small but energetic mesoscale eddies.

The circulation of the Mediterranean Sea is usually described in a schematic way as an open thermohaline cell with two closed secondary cells, one for each sub-basin [Figure 1.2].

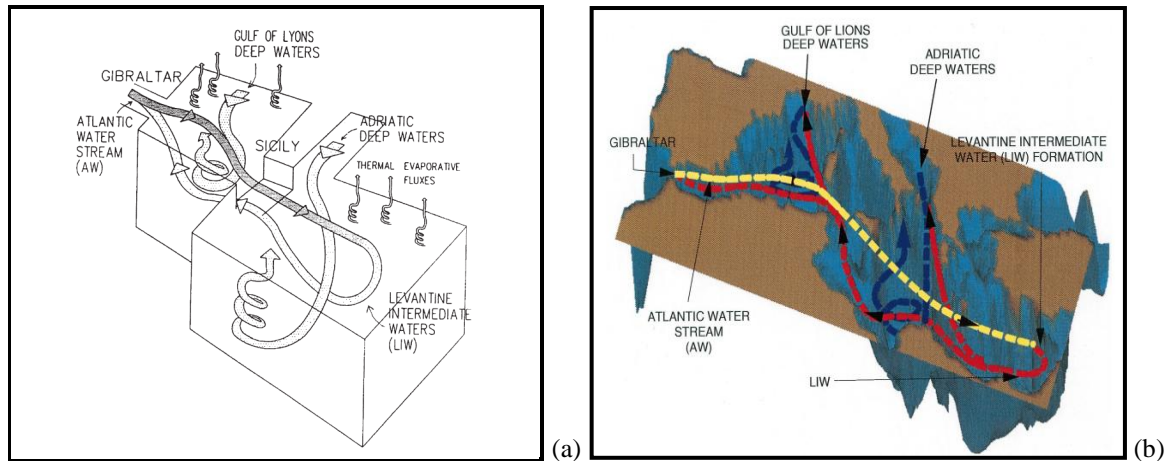


Figure 1.2: Schematic representation of the thermohaline circulation in the Mediterranean Sea (Lascaratos et al; 1999) (a); (Pinardi e Masetti 2000) (b).

The principal cell describes the transformation of the surface Atlantic Water [AW] to the Levantine Intermediate Water [LIW], which is the main contributor to the Mediterranean outflow into the Atlantic. The two secondary cells describe the transformation of the surface and intermediate waters to the Western Mediterranean Deep Water [WMDW] and to the Eastern Mediterranean Deep Water [EMDW]. The existence of an intermediate depth cell is mainly controlled by the presence of the two relatively shallow sills [*Gibraltar and Sicily Straits*] [Ribera et al 2003]. Furthermore, the sill in the Strait of Sicily prevents a direct communication between the EMDW and WMDW; coupling is achieved via the LIW layer.

Surface waters in the Mediterranean have their origin in the inflow of Atlantic waters through the Strait of Gibraltar; they are warmed up by solar irradiation and evaporation causes a steady increase in salinity. As the inflowing waters, by now known as Modified Atlantic Water, arrive in the easternmost Mediterranean, the salinities are very high reaching more than 39 salinity units, compared with about 36 in the original Atlantic inflow, or with the global ocean's average salinity of 35. The high salinity in the easternmost Mediterranean would cause a high density, which is partially compensated by very high temperatures, which in summer reach 26°C or more [Rohling 2001; Lascaratos 1999].

Crucially, winter cooling reduces sea surface temperatures in the general easternmost Mediterranean to around 17°C; the density increase due to the high salinity is now no longer compensated by temperature and as a consequence, deep water formation takes place in

the area between Cyprus and Rhodes. This water does not sink all the way to the bottom, but settles between 150/200 and 600 m depth and is normally called Levantine Intermediate Water. The formation of this water mass (known to be formed around Rhodes cyclonic gyre in the NW part of the Levantine Basin) is essentially driven by a salinity increase to >38 psu. The Levantine Intermediate Water is found everywhere in the Mediterranean. Spilling through the Strait of Sicily at depth, it is also distinctly present in the western Mediterranean, and represents the largest contribution of outgoing water from Gibraltar.

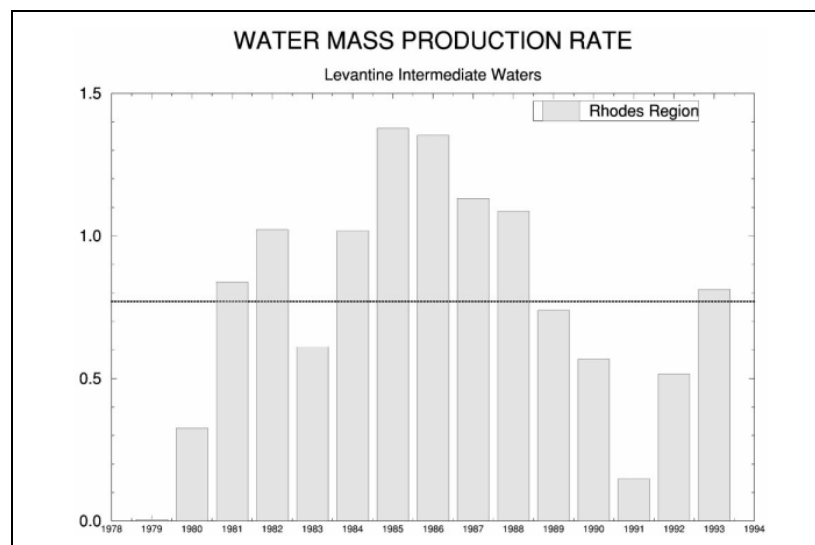


Figure 1.3: The water mass production rate in the Rhodes gyre region as a function of years for the PE4 interannual experiment (Pinardi and Masetti, 2000).

The interannual variability of LIW fluxes is very large, ranging from a minimum of 0.1 Sv in 1991 to a maximum of 1.4 Sv in 1985–1986. [Figure 1.3].

Thus, the amplitude of the interannual variability of the formation rate, is larger than the average value, indicating that the vertical water mass structure in the upper thermocline is varying in terms of volume of water renewed every year [Pinardi and Masetti, 2000].

Most of this flow returns to the Atlantic Ocean as Levantine Intermediate Water (LIW), formed during winter convection in the Levantine sub-basin, while another part is transformed into Eastern Mediterranean Deep Water (EMDW) in the Adriatic and the Aegean sub-basins and into Western Mediterranean Deep Water (WMDW) in the Gulf of Lions; the cold temperatures and strong winds in the northern part of the basin allow for the formation of these dense waters also in the Gulf of Lions and in the Northern and Southern Adriatic.

The deep waters of the eastern Mediterranean (EMDW) are formed in the southern Adriatic [Pollak 1951]. The Adriatic Sea has historically been considered as the most relevant contributor to the deep waters of the Ionian and Levantine basin. Most deep waters in the east Mediterranean

come from the south Adriatic Sea (but see below), with small contributions of waters from the northern part of the basin that become denser during winter time by effect of cooling and evaporation associated to local meteorological conditions, mainly associated to the sudden wind blowing of the cold Bora.

The deep waters of the western Mediterranean (WMDW), are formed during periods of strong Mistral. The intermediate water in the Gulf of Lion, thanks to the presence of a cyclonic turn, is brought at the surface; excessive cooling and evaporation winter makes this water cold and saltier and falls to the bottom.

The Tyrrhenian Sea, is another important source of dense waters, as the mixing of LIW with WMDW, creates the deep water of the Tyrrhenian Sea, coming out of the channel of Sardinia.

New experimental data [Astraldi *et al.*, 1996], have demonstrated that the Eastern Mediterranean outflow is actually composed of two different water types [Figure 1.4], one of which is the classical LIW while the other is a colder water that was observed to flow at the bottom of the Sicily Channel all year round, following approximately the same route as LIW.

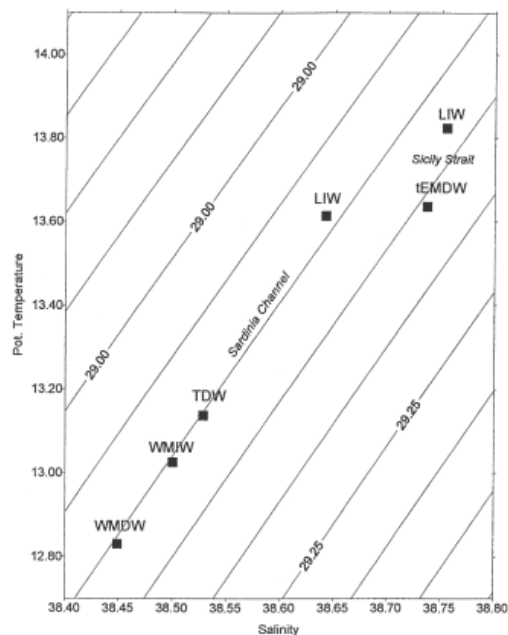


Figure 1.4: T-S diagram relative to the intermediate and deep waters in the Sardinia Channel and in the Sicily Strait in January 1997 (Astraldi *et al.* 1999).

This dense water, fresher and colder than the LIW, is present in the Ionian Sea filling the transitional layer between LIW and Eastern Mediterranean Deep Water. It was referred to as transitional Eastern Mediterranean Deep Water (tEMDW) [Sparnocchia *et al.* 1999].

The two masses of water move separately, while the LIW flows at the known depth, for this type of water namely between 500 and 800 m, a considerable volume of transitional EMDW was seen to sink from a depth of about 300 m in the Sicily Channel to a maximum depth of 1850 m in the

Tyrrhenian Sea, where it floats over the Tyrrhenian Deep Water TDW. The sinking is a consequence of the higher density of the incoming water $\gamma > 29.10$ with respect to that of the intermediate Tyrrhenian waters $\gamma \approx 29.00-29.05$. The entrainment resulting from the turbulent flow down the slope determines the major part of the mixing between the bottom vein and the fresher and colder resident water.

Recent observations conducted during the past two decades showed that important changes in the characteristics of the intermediate/deep waters of the Mediterranean basin had occurred; two climatic events affected the general Mediterranean circulation [Roether *et al.*, 1996; Theocharis *et al.*, 2002] the first event, called Levantine Transient (LT) occurred during the mid-sixties and early seventies [Theocharis *et al.*, 2002; Skliris and Lascaratos, 2004] in the Levantine Basin, and the second, called Eastern Mediterranean Transient (EMT), occurred during the late 80s and early 90s, and originated in the Aegean Sea [Roether *et al.*, 1996; Klein *et al.*, 1999]. Specifically, consequently to an established pattern of warming and increasing salinity of deep waters in the western basin of origin and the Levantine Intermediate Water, in the 90's there was a sudden change of the hydrological characteristics or geographical origin of Eastern basin deep water (Eastern Mediterranean Transient, EMT). This is completely distorting the vertical stratification and circulation, also modifying the hydrological characteristics of the water that enters at an intermediate level through the Strait of Sicily in the Western basin. EMT is a process of slow advection and with significant anomalies of salt and temperature.

Several theories have been formulated regarding the causes of this change, some authors attributing it to the reduction of the rainfall occurring at that time [Theocharis *et al.*, 1999], others authors showing that human activities have influenced, inputs of fresh water (for example through the construction of dams), and the thermohaline circulation [Skliris Lascaratos 2004]. EMT-induced spread through the Sicily Strait to the WMed, with Tyrrhenian sea playing a more important role than before in the dynamics of WMed [Roether and Lupton, 2011]. Indeed, a significant warming and salinification of the whole water column has been observed also in the Western Mediterranean, comparable to the EMT, both in terms of intensity and observed effects [Schroeder *et al.*, 2008]. This event of high production of anomalously warm and salty new deep water during winters 2004/2005 and 2005/2006 is now known as the Western Mediterranean Transition (WMT). Currently, thus, the subsurface distributions of temperature and salinity, as well as of most other properties in the entire Mediterranean are far from a steady state.

1.1.2.1.- Water exchange through the Strait of Gibraltar and the Strait of Sicily

The flows through the Strait of Gibraltar and the Strait of Sicily are subjects to different forcing factors: 1. the tidal component particularly active in the coastal areas [Artale *et al.*, 1989] and 2. the seasonal component as indicated by the increase of the mean energies of MAW and LIW during winter. This is clearly evidenced by current measurements reported by Manzella *et al.* (1988) that recorded a doubling of transport of LIW in winter with respect to summer (3,2 Sv in winter and 1,5 Sv in summer, respectively).

The estimation of inflows and outflows from direct observations has technical and operational limitations, and several disparate values have been reported in literature.

We report the transport of water at the two straits of the Mediterranean basin, a minimum and maximum values [Table 1.1].

<i>Strait of Sicily</i> [1 Sv = 10 ⁶ m ³ s ⁻¹]		
Authors	Inflow (Sv)	Outflow (Sv)
Moretti 1993 Bethoux and Gentili 1999	0,76 ± 3,53 AW	0,53 ± 3,47 LIW
Astraldi 1996	1 ± 1,4 AW	0,95 ± 1,35 LIW
Astraldi 1999	1 ± 1,4 AW	0,58 ± 1,1 LIW
K Shroeder 2008	1,65 AW	1,18 LIW
Sparnocchia 1999		0,2 ± 0,3 tEMDW

<i>Strait of Gibraltar</i> [1 Sv = 10 ⁶ m ³ s ⁻¹]		
Authors	Inflow (Sv)	Outflow (Sv)
Bryden 1994 Bethoux and Gentili 1999	0,76 ± 1,68 AW	0,68 ± 1,6 LIW
Bethoux and Gentili 1999; Hopkins 1999	1,28 ± 1,68 AW	1,2 ± 1,6 LIW
Bryden 1994;Lacombe and Richez 1982	0,72 ± 1,2 AW	-

Table 1.1: Water fluxes at the two main Straits of the Mediterranean Sea

1.1.3- The Mediterranean Climate

Climatologically, the Mediterranean resides at the transition between the high-to mid-latitude and the subtropical atmospheric systems, which interact and, in a way, may be regarded to compete with one another [Lionello *et al.*, 2006]. As a consequence, the Mediterranean climate depends on the latitudinal shift of these climate systems with the seasons and typically varies between mild wet winters and hot, dry summers [Eshel, 2002; Rohling *et al.*, 2008].

Specifically, the winter regime is dominated by mild and wet conditions related to the southward spreading of the temperate westerlies from central and northern Europe [Lolis *et al.*, 2002], with occasional out breaks of cold polar/continental air masses funnelled through the valleys of the northern Mediterranean margin [Maheras *et al.*, 1999].

In summer, warm and dry conditions prevail due to a northward shift of the subtropical high-pressure belt over the basin [Rodwell and Hopskins 1996; Saaroni *et al.*, 2003; Ziv *et al.*, 2004]. It is worth noting that before the anthropogenic curtailment of the freshwater discharge of the Nile River, another climate system, namely the northern African monsoon, used to have an impact on the Mediterranean system and specifically on the basin's hydrography.

The influence of the African monsoon on the Mediterranean hydrography is however indirect as there is no actual latitudinal displacement of this climate system onto this region but rather a modulation of the basin's freshwater inputs via the Nile River and other North African drainage system [Rohling and Bryden, 1992; Rohling *et al.*, 2002b, 2004; Scrivner *et al.*, 2004; Skliris and Lascaratos, 2004] [Figure 1.5] .

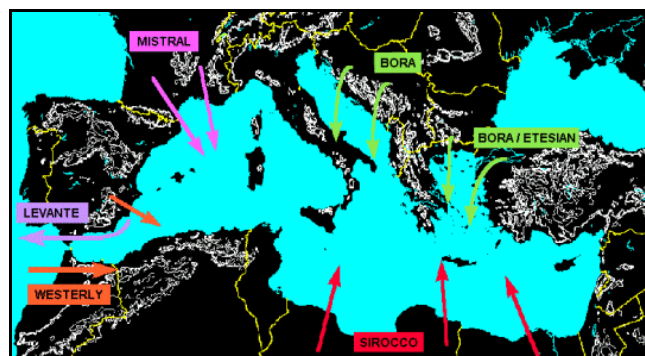


Figure 1.5: Principal winds in the Mediterranean area.

1.1.4- Biogeochemical cycles in the Mediterranean Sea

A biogeochemical cycle is the pathway by which chemical elements or molecules move through both biotic (biosphere) and abiotic (lithosphere, atmosphere, hydrosphere, cryosphere)

compartments of the Earth [Figure 1.6]. The geochemical cycle of the elements in a marine system is strongly dependent or influenced by biological activity. In effect, an element is chemically recycled, although in some cycles there may be places (called "sinks") where the element accumulates and is held for a long period of time.

The production of organic matter acts as a major process of transfer of elements from the dissolved to the particulate state as soft or hard tissues. On the other hand, respiration or biological degradation may lead to the re-dissolution of particulate species. As primary productivity is strictly limited to the photic zone and decay of organic matter is pursued in the deeper water masses of the oceanic system, the distribution of many elements exhibits a strong vertical gradient.

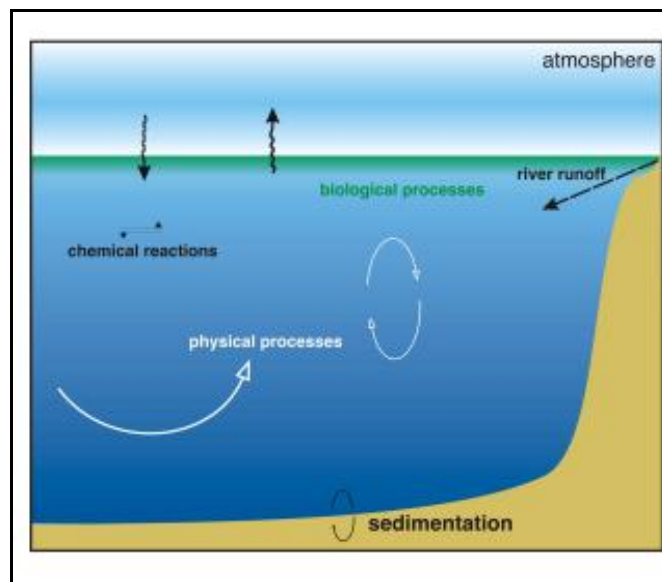


Figure 1.6: The biogeochemical cycle.

The Mediterranean basin is an active processor of matter, it receives atmospheric and river input of considerable importance for the biogeochemistry of the basin, which is strongly associated with the hydrodynamic patterns, with a close relationship between chemical parameters and water mass distribution. The Mediterranean Sea is one of the most oligotrophic oceanic systems of the World Ocean [Dugdale, 1976]; it is traditionally assumed that an eastward flow of Atlantic nutrient-poor surface waters is compensated by a deep countercurrent of Mediterranean nutrient-rich waters.

The dissolved inorganic nutrients (nitrates, phosphates and silicates) are important tracers of biological cycles, whose distribution is controlled by the physical processes of convection, advection, mixing and diffusion (as mentioned before), but also by biogeochemical processes.

In the Mediterranean sea there are few studies on the distribution and budgets of nutrients [Ribera d'Alcala' et al 2003; Bethoux et al 2002] and few studies on the fluxes through the Straits of Sicily and Gibraltar [Bethoux et al 1998].

During the last century, the eastern Mediterranean basin has also become increasingly oligotrophic since the construction of the Aswan Dam on the river Nile, whereas the western basin remains well supplied by the Rhone and Po river inputs and entering Atlantic surface waters [Bethoux et al., 1998].

After building the Aswan Dam in 1964, the river with the largest drainage basin and water load in the Mediterranean until the early 1960s, was dramatically reduced. Damming of the Nile River, represents an efficient silica trapping, that should have reduced the Si delivery to the Mediterranean by $100 \cdot 10^3 \text{ t yr}^{-1}$ [Nixon, 2003].

Skirris and Lascaratos [2004] observed through modeling, what was the impact of Nile river damming. The model results show that the absence of the Nile freshwater input induces a saltier surface layer in the vicinity of the Rhodes Gyre thus favoring the preconditioning for the formation of the Levantine Intermediate Water (LIW). This results in about 30% increase of the LIW formation rate. Intermediate waters become saltier, and as they are transported westward they reduce the stability of the water column in the deep water formation sites, namely the South Adriatic and the Gulf of Lions. Thus, saltier and larger amounts of dense waters are formed filling the deep parts of the Mediterranean Sea.

1.2-Silicon in seawater

1.2.1- Silicon and Marine Cycle

Silicon is the second most abundant element in the Earth's crust, 27% by weight [Faure, 1986], exceeded only by oxygen. The position of silicon in the periodic table of elements shows a clear relationship with carbon, sharing the same possible valence states [p4, p2 and p4]. In natural environments, however, Si is most stable in the p4 form, in which it is found in various forms of solid silicon dioxide [silica, SiO_2], as mineral silicates and as the dissociated anions of silicic acid [H_4SiO_4].

During silicate weathering dissolved soil CO_2 is used in a reaction where ortho-silicic acid [H_4SiO_4] is dissolved and released from the crystalline structure of silicate minerals. In the environment dissolved silicate [Dsi], i.e. ortho-silicic acid [H_4SiO_4], is transported through soil and exported to rivers and eventually the ocean [Meybeck, 1994]. The silicate weathering process

consumes CO₂, for example, in the weathering of anorthite [over kaolinite] to gibbsite, DSi is produced and CO₂ is consumed [*Stumm and Morgan, 1970*]:



Silicon is a very important nutrient in the ocean; the dissolved silicate in the ocean is converted by various plants and animals into particulate silicate (SiO₂), which serves primarily as a structural material (i.e., the biota's hard part).

The marine biogeochemical cycle of silica thus depends on the weathering of rocks on the continents. This temperature dependent process releases dissolved silica [DSi] into ground waters and rivers and DSi plays an important role in the production of phytoplankton and the burial of carbon in the coastal zone and in deep-sea sediments [*Ragueneau et.al 2006*].

All along the transport route over the continents, the dissolved silica may be used by fresh water diatoms and plants to build up biogenic forms of silica [bSiO₂] [*Conley and Schelske 1997*]. When organisms from the siliceous biota die, their skeletons settle through the water column, where more than 90% of the silica is regenerated via inorganic dissolution. The reason silicate cycling has received particular scientific attention is because diatoms are one of the dominant forms of phytoplankton responsible for the export production from the surface ocean [*Dugdale et al; 1995*]. Export production (called New Production), is the transport of particulate material from the euphotic zone (where photosynthesis occurs) down into the deep ocean.

The relevance of this process can be appreciated because it takes dissolved inorganic carbon from surface ocean waters, where it is exchanging with carbon dioxide in the atmosphere, turns it into particulate organic matter, and then transports it to depth, where most of it is regenerated back into dissolved form.

This process, called the biological pump along, is along with deep ocean circulation, responsible for the transfer of inorganic carbon into the deep ocean, where it is unable to exchange with the atmosphere for hundreds or even thousands of years.

Silicate and silica play an important role in the carbon cycle, which affects the world's climate through greenhouse feedback mechanisms.

Briefly the silica cycle can be represented in this way [**Figure 1.7**]

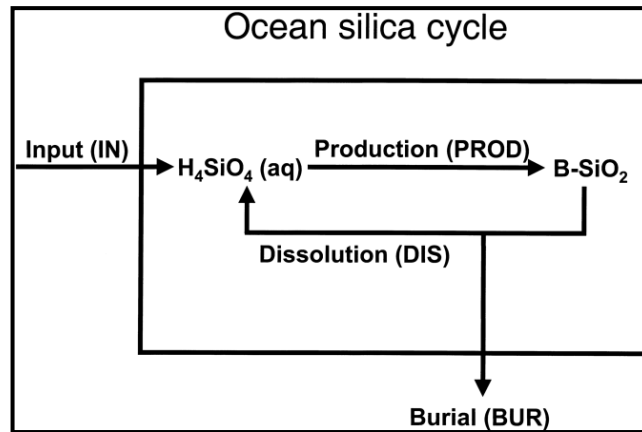


Figure 1.7: Marine silica cycle.

$$IN = BUR$$

$$PROD = IN + DIS \quad (\mathbf{a})$$

Furthermore, we can define the dissolution (or recycling) efficiency

$$\alpha = DIS / PROD \quad (\mathbf{b})$$

where $0 < \alpha < 1$. In the modern ocean, α is on the order of 0.97, reflecting very efficient silica recycling. Combining Equations (a) and (b) it is possible to obtain

$$PROD = IN / (1 - \alpha) \quad (\mathbf{c})$$

The denominator in Equation (c), $(1 - \alpha)$, can also be viewed as the ocean-wide biogenic silica preservation efficiency. The numerator and denominator on the right-hand side of Equation (c) are related to processes such as silicate weathering, volcanic-seawater interaction, dissolution plus ageing of biosiliceous shells, and sediment burial. In other words, Equation (c) links the global rate of silica biomineralization in the oceans to geological and geochemical processes that regulate the oceanic sources and sinks of silica.

For a proper balance within the basin it is necessary to take into account inputs of silicon within the Mediterranean basin, with respect to the silicon from different sources, which are due to river inputs, atmospheric inputs, diatoms and hydrothermal flows.

1.2.2- The river inputs and the Si distribution patterns in the Mediterranean Sea

Rivers have a significant impact on the hydro geography and biogeochemistry of the Mediterranean Sea. Indeed, external inputs from the coasts play a significant role in the Mediterranean Sea. The Si exists in rivers in particulate and dissolved form; silica is largely transported in dissolved form while only a small part of the particles contain soluble forms (biogenic particulate silica), contributing to about 10-20% of the total silica flux [Conley 1997; Conley and Schelske 2001; Garnier et al 2002; Sferratore et al 2006].

There are only three major rivers, the Po in the North Adriatic Sea, the Rhone in the Gulf of Lions and the Nile in the South East Levantine Sea. The Nile, however, has suffered a dramatic decrease in water transport over the last decades, possibly suggesting a concurrent, though not proportional decrease in nutrient inputs. In fact, the relevance of riverine runoff to overall nutrient fluxes is still uncertain, despite several general [e.g., Ludwig *et al.*, 2009] and regional studies [e.g., Degobbis and Gilmartin, 1990; Skoulikidis and Gritzalis, 1998; Cruzado *et al.*, 2002; Moutin *et al.*, 1998].

Due to the presence of rivers, the concentrations of silicon are different. Concentrations in coastal areas are higher than in open sea.

A reduction of the river freshwater discharge implies a reduction of the fluxes associated with the elements. Also human activities [damming, land use practices, deforestation] are affecting the natural terrestrial cycle of silica and its delivery to the ocean [Conley *et al.*, 1993; Humborg *et al.*, 2000; Ragueneau *et al.*, 2005]. The temporal evolution of the river Si load could influence the marine productivity, as Si is considered as a limiting nutrient for diatoms, for which the Redfield Ratio can be written as C:N:Si:P=106:16:16:1.

Ribera d'Alcala' *et al.*, 2003, summarized the variation of the ratios N:P and Si:N in the intermediate waters of the Mediterranean. In particular, the eastern basin appears characterized by higher values in the two relationships relative to the western basin. The same trend, with lower values, has been documented for the deep waters. The situation proposed by Ribera d'Alcalà *et al.*, 2003 shows a marked imbalance in the ratio of Redfield especially in the eastern Mediterranean. Actually the two basins can be considered as two microsystems, characterized by different input; changes in Mediterranean riverine inputs are potential driver for long term changes in the marine ecosystems.

1.2.3- The atmospheric contribution to Silicon patterns in the Mediterranean Sea

Dust plays an important role in terrestrial and oceanic biogeochemical cycles.

The deposition of atmospheric dust at the sea surface is important, although it is extremely difficult to reliably quantify that due to the limited sampling sites distributed at basin scale and dedicated to exploration of dust deposition from atmosphere. Furthermore, dust aerosol distribution has a high spatial and temporal variability, and large uncertainties exist in quantitative estimates of large-scale dust loads. Modern global dust distribution and properties can be characterized by satellite data and by concentration measurements at surface stations. So far, quantitative estimates of dust optical thickness by satellites are possible only over ocean

surfaces, although qualitative patterns of dust distribution can be observed over land, for example, by the Total Ozone Mapping Spectrometer satellite instrument [*Herman et al. 1997*].

In contrast, surface station measurements of dust concentrations [e.g., *Prospero and Lamb 2003*] and deposition flux measurements are too sparse to obtain regional averages through extrapolation of the local observations.

Recently, some studies have focused on the importance of dust transport to the Mediterranean in terms of biogeochemical cycles and additional source of nutrients. Despite the associated uncertainties, budget calculations [*Ribera d'Alcalà et al., 2003; Krom et al., 2004*] and, more recently, isotopic data [*Krom et al., 2004; Sandroni et al., 2007; Schlarbaum et al., 2009*] suggested that atmospheric inputs support a significant amount of new production, especially in the Eastern Mediterranean Sea (EMS).

Other authors [*Volpe et al., 2009*] provided new information on modes and frequencies of Mediterranean Dust events and associated impacts on phytoplankton biomass and blooming. Through Satellite observations it is possible to investigate the phytoplankton-dust linkage on various space and timescales, and to establish the reproducibility of the effect. The Sea-viewing Wide Field-of-view Sensor (SeaWiFS) provides estimates of chlorophyll, a widely used proxy for phytoplankton biomass, and aerosol optical thickness (AOT) and offers reliable constrain to a deeper exploration of impact of atmospheric particulate and associated deposited marine particulate on the biogeochemical balance at basin scale.

Silicon can be transported through the atmosphere associated with airborne particles; flying ash produced by industrial burning can contain Si, and those particles are abundant in heavily industrialized areas, but reliable and accurate global estimates of industrial Si emissions are not available.

There are two important sources of dust and associated Si in the Mediterranean sea, from southern “Sahara dust” and from northern “industrialized European countries”. The origin of the source depends on the winds. In summer and fall, atmospheric cyclonic systems develop over the African continent, thereby mobilizing and transporting dust, making it the dominant aerosol over the MED; in winter, the meteorological conditions tend to favor aerosol transport from the north where anthropogenic pollutants are dominant [*Alpert et al., 1990; Israelevich et al., 2002*].

1.2.4- Kinetics Dissolution of Silicon from marine particulate

Different experiments have been conducted to test the effects of sea water dissolution of clay minerals. Studies of the distribution of clay minerals in near-shore marine environments [*Grim et*

al., 1949 ; *Grim and Johns, 1954 ; Powers, 1954, 1957*] suggest that diagenesis of such minerals may occur when they are transferred from fresh-water to sea-water by river action.

Silicon is transported to the sea as particulate loads of rivers, as biogenic silica and as atmospheric dust.

How much of flux of particulate silica (lithogenic and biogenic) actually dissolves remains unknown. Whereas the lithogenic component of this flux is fairly insoluble, the amorphous, largely biogenic component (phytoliths, freshwater diatoms, sponge spicules) is easily dissolvable.

The exact mechanism of any changes that take place is not known, but a first stage must involve reactions of the cations and anions in sea-water with the minerals through exchange.

During the reaction of clay minerals with seawater small amounts of SiO₂, Al₂O₃, and Fe₂O₃ are dissolved by sea-water, but it is not known if this solubility is due to a surface effect as indicated by Nash and Marshall (1956), to the solubility of SiO₂ and Al₂O₃ (the latter is slightly soluble at pH 8.0) at the pH of sea-water [*Correns, 1949 ; Krauskopf, 1956*], or to the release of Al₂O₃ from H-clays by a saline solution [*Mukherjee, Chatterjee and Ray, 1948*].

Carroll and Starley have examined these effects by allowing seawater to remain in contact with the minerals for certain periods of time; small amounts of SiO₂ and Al₂O₃, for a total of less than 1 percent of the sample, were removed from these clay minerals.

The dissolution of biogenic silica produced in surface waters is strongly influenced by intrinsic factors such as temperature, structure, degree of silicification, and trace metals within organic coatings and within the opal matrix such as Al [*Van Bennekom et al., 1988; Van Cappellen and Qiu, 1971*].

The nanostructural nature of biogenic silica commonly is described as globular spheres constructed of colloidal silica. Mineralogically biogenic silica is commonly called opal-A. The solubility of biogenic silica is highly temperature dependent varying from 800–1,000 mM Si at 38°C to 1,500–1,700 mM Si at 23°C [*Lawson et al., 1978; Kamatani, 1982*]. Pressure also affects the solubility of biogenic silica (increasing solubility with increasing depth), but the total effect is only 200 mM (or 20%) over the depth ranges commonly observed in the ocean [*Willey, 1974*]. The solubility of biogenic silica can be affected by the adsorption of cations on its surface [*Lewin, 1961*], which is why “acid- cleaned” biogenic silica commonly has higher solubilities (and a more rapid rate of dissolution) than those from natural siliceous assemblages of phytoplankton [*Lawson et al., 1978*]. The solubility of biogenic silica also is affected by its aluminum content. *Van Bennekom et al. (1991)* reported that the Al/Si atomic ratio in siliceous material collected from various marine environments varied from $0.6 \cdot 10^{-3}$ to $7 \cdot 10^{-3}$ with a

corresponding change in silica solubility from 1,080 μM to 660 μM . The amount of aluminum incorporated into siliceous skeletons during growth appears to be dependent on the Al/Si ratio in the surrounding water as well as the particular species of siliceous biota.

The mineral composition of dust particles reflects the mineralogy of the rocks at the earth's surface, and the percentage of particulate Si that dissolves in the seawater from dust depends on the mineral composition. How much dissolves is difficult to estimate because of large differences in the solubility of the varieties of lithogenic and biogenic silica that constitute dust [*Durr et al. 2011*].

Silicon solubility ranges from 0.02% to 1.1% for Saharan dust, which is mainly quartz [*Baker et al. 2006*]. However, 10% of silicon may be soluble from feldspar dust [*Harrison 2000*], and even more may be soluble from biogenic silica present in dust.

Several authors have investigated the solubility of silicon from the dust. In particular, *Treguer et al. (1995)* assume that 5-10 percent of the silica transported to the ocean surface by Aeolian dust dissolved in the surface water; *Guerzoni et al 1999* report 1 percent solubility for Si in Sahara dust samples collected at Sardinia, *Gehlen et al 2003* assume a 3 percent solubility of aluminosilicates in seawater in their model investigation.

Taking these studies into account, it is possible to assume that the solubility of particulate Si from dust ranges between 1-10 percent.

1.3 -The mass balance of Si in the Mediterranean sea: a state of the art

1.3.1- Mass Balance

Many processes may act to control the distributions of chemicals in the ocean. The method of putting these processes together in a model utilizes the principle of mass balance applied to the system as a whole or some parts of it (control volumes). The system as a whole is linked to the environment by external inputs and outputs. Box models are especially useful for understanding geochemical cycles and their dynamic response to change. Describing a model first requires choosing a system, that is, the division between what is "in" and what is "out". The second step involves choosing the complexity of the description of the "internal" system. The goal in modelling is to analyze all the relevant processes simultaneously. The concept of mass balance serves as a way to link everything together. To use the idea of a mass balance, the system is first divided into one or several "control volumes" which are connected with each other and the rest of the world by mass fluxes. A mass balance equation is written for each control volume and each chemical. *The Change IN = Sum of all Inputs + Sum of Internal Sources – Sum of Outputs – Sum of all Internal Sinks*

1.3.2- Budget of Si in the Mediterranean Sea

Despite the great importance of silicon there are currently not many studies on this element's budget at the basin scale.

A first estimate on the budget of the silicon in the Mediterranean was made by *Schink 1976*, which showed the flows of silicates in Gibraltar as substantially balanced.

A subsequent study on the balance of silicon was carried out by Ribera d'Alcala' et al. (2003), trying to balance the flows into and out of the two straits; the Strait of Gibraltar and the Strait of Sicily.

The values for the mass transport of water used by Ribera d'Alcala' et al. (2003) and the values of concentrations of silicates are indicated in the table [see Table 1.2].

Strait of Gibraltar			Strait of Sicily		
In	[Sv]	0.76 ^(a) - 1,68 ^(c,d)	In	[Sv]	0.58 ^(b) - 3.52 ^(e)
	[mmol m ⁻³]	1.27 - 2.40		[mmol m ⁻³]	0.69 - 1.20
Out	[Sv]	0.68 ^(a) - 1.60 ^(c,d)	Out	[Sv]	0.53 ^(b) - 3.47 ^(c)
	[mmol m ⁻³]	7.61 - 8.40		[mmol m ⁻³]	6.00 - 7.15

Table 1.2: Concentrations and Transports of Si at the Two Main Straits of the MED; (a)- Bryden et al [1994] (b)- Moretti et al [1993] , (c) - Bethoux [1980], (d)- Bethoux and Gentili [1999], (e)- Bryden and Stommel [1984]

From the estimation of atmospheric inputs [Guerzoni *et al.* 1999 - Herut and Krom 1996-Loye Pilot *et al.* 1990] and considering river inputs [Moutin 1998 - Balboni *et al.* 1999 - Schink 1957] a budget deficit was recorded in both the western and eastern basins [Table 1.3].

	WMED		EMED	
	Si in/out Min	Si in/out Max	Si in/out Min	Si in/out Max
Atmospheric input	0,709	2,2	0,009	5,1
Rivers input	11,5	39,2	12,2	78,7
Input (Tot)	12,2	42,1	12,8	83,8
Sicily	179	304	-179	-304
Gibraltar	-288	-424		
Input TOT	-109	-120	-179	-304
Deficit	-97	-77,9	-166	-220

Table 1.3: Silicon budget in the Mediterranean Sea (by Ribera d’Alcala’ *et al.*, 2003)

Recently, Lavezza (2010) showed a different budget situation, especially taking into account more recent estimates of river inputs to the Mediterranean from 1960-2000 proposed by Ludwig *et al.*, 2009. In particular he has presented an extensive datasets on the nutrients in the Mediterranean basin, through a recovery and reorganization of available silicon data and other nutrients from two different sources (oceanographic cruises and data published).

The database used by Lavezza is summarized in **Table 1.4**.

Source	Cruises	Stations
MEDAR	50	1704
MATER	28	327
SESAME	125	3396
Report Cruises	18	669
ToT	221	6096

Table 1.4: Database (cruise oceanographic and data published from 1960-2000) used by Lavezza

The basin was divided into 14 homogeneous areas [Figure 1.8] and for each area a quality control of data sets has been carried out; the data have been reorganized in a single matrix and validated, using statistical parameters as maximum, minimum, mean and standard assuming a normal distribution of the data.

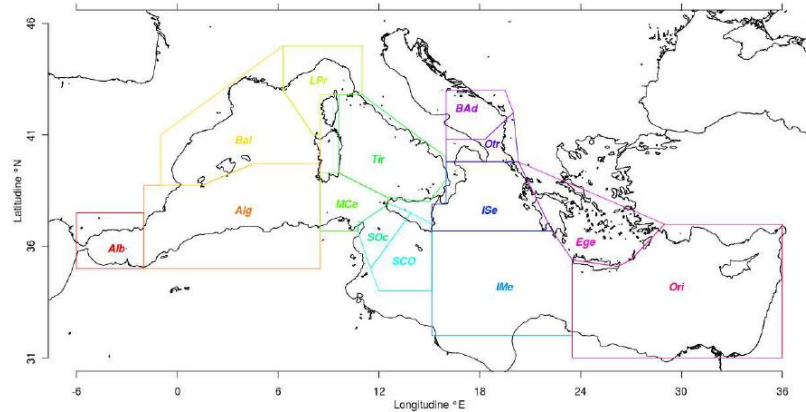


Figure 1.8: Mediterranean area(Lavezza 2010).

It was observed that inputs were only partially able to compensate net losses, and a new estimate has revealed an accumulation in the western basin and a deficit in the eastern basin [Table 1.5]. A possible interpretation would be that the basin is slowly losing silicon; however from statistics analysis reported by Lavezza it is evident that, despite recorded deficits of silicon in the east basin, the trend is not negative, so we can interpret this situation to be due to underestimated inputs in the system.

	WMED		EMED	
	Si in/out Min	Si in/out Max	Si in/out Min	Si in/out Max
Atmospheric input	0,709	2,2	0,009	5,1
Rivers input	11,7	13,1	21,2	23,5
Input (Tot)	12,4	15,3	21,2	28,8
Sicily	165	235	-165	-235
Gibraltar	-147	-199		
Input TOT	18	36	-165	-235
Deficit	30,4	51,3	-143,8	-206,4

Table 1.5: Silicon budget in the Mediterranean Sea (by Lavezza 2010)

1.3.3 Objective of this research work

Starting from the available basic information, our aim is to understand what is really causing the recorded deficiency of Si in the eastern Mediterranean basin and to understand whether and how dust potentially affects the mass balance of silicon at basin scale.

Several authors have attempted to estimate the atmospheric flows of metals for ocean's surface [Chester *et al.*, 1989;. Guieu *et al.*, 1991;. Migon *et al.*, 1991; Guerzoni *et al.*, 1993; Migon *et al.*, 1997] and have focused their attention on deposition patterns and source signature of Saharan aerosols, collecting samples in a variety of sites around the Mediterranean Sea. However, there are many gaps in the data of the silicon in the atmosphere, so in addition to the lack of knowledge of this element we have to consider that the available data on silicon are actually few. The only data particularly useful to our work, concerning a study over the Gulf of Aquaba, by Chen 2008, during which are monitored the concentrations of aerosol trace elements, during a two years period (August 2003- to September 2005). Back trajectories of the air masses over the Gulf, were calculated and categorized into six characteristic source sectors, to identify the source of trace elements.

However to have a reliable information on the magnitude and the geographical distribution of the dust deposition on seawater, the use of a credible numerical model is considered as essential, because the use of satellite images and/or analyses of ground in sampling sites, to measure the amount of dust that covers the Mediterranean, are actually powerful tools because it allows a regular temporal and spatial coverage, but has a limit, it is not certain that dust measured in the air is deposited on the surface of the sea.

We decided to observe the dust phenomenon through atmospheric modeling that in the last two decades has experienced important improvements.

We considered the Earth Sciences Department at BSC-CNS (Barcelona Supercomputing Center – Centro Nacional de Supercomputación) conducts modelling research and developments for short-term prediction as well maintains dust forecast operations with BSC-DREAM8b. Since May 2009, BSC-DREAM8b [Pérez *et al.* 2006a, Pérez *et al.* 2006b] provides the operational dust forecast at BSC-CNS; its main improved features include a more detailed size bin distribution and the inclusion of dust-radiation interactions.

In order to achieve the goal and to understand what is really causing the recorded deficiency of Si in the eastern Mediterranean basin it is necessary to be aware of high difficulty of the problem. The actual condition of the system is difficult to determine because the Mediterranean is subject to interannual variability which is difficult to predict and influenced by the dynamics of the straits, internal dynamics and by the redistribution of water masses.

Chapter 2

MATERIALS AND METHODS

2.1- Sampling activities: nutrients and trace metals in seawater

Seawater samples were collected and analysed for nutrients and trace elements concentration in dissolved and particulate phases during two oceanographic cruises in the central Mediterranean.

2.1.1- The sampling area

Seawater samples were collected in the Mediterranean sea during the oceanographic cruise BONIFACIO_2010, in November 2010 on board of the N/O Urania.

Samples were collected for analysis of trace elements (dissolved and particulate phases), and nutrients [Figure 2.1; Table 2.1].

During the oceanographic cruise “AEOLIAN_2010 in May 2010 on board of the N/O UraniaV, seawater samples were collected for analysis of nutrients [Figure 2.2; Table 2.2].

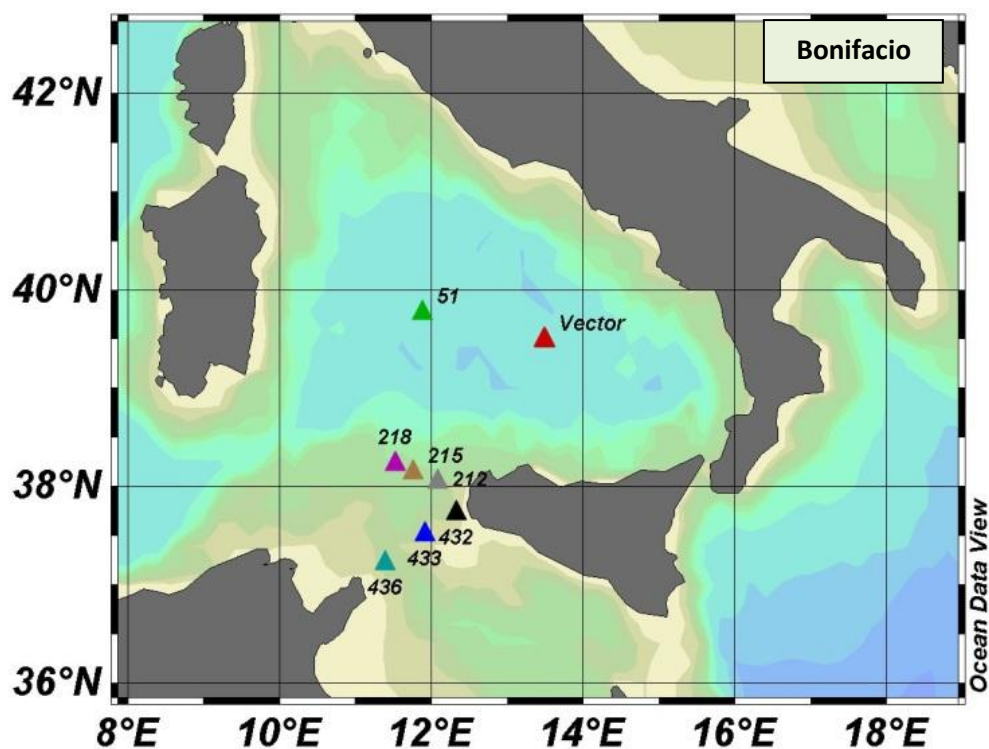


Figure 2.1 : Sampling sites from the BONIFACIO_2012 Cruise.

CRUISE	STATION	LAT	LONG	DEPTH (m)	METALS	NUTRIENTS
Bonifacio 2010	VECT	39°29.995'N	13°29.968'E	3250	X	X
Bonifacio 2010	51	39°46.428'N	11°53.264'E	3498	X	X
Bonifacio 2010	212	38°02.986'N	12°05.442'E	190		X
Bonifacio 2010	215	38°08.743'N	11°45.960'E	1199	X	X
Bonifacio 2010	218	38°13.912' N	11°31.870'E	228		X
Bonifacio 2010	432	37°44.002'N	12°19.959'E	160	X	X
Bonifacio 2010	433	37°30.850'N	11°55.358'E	105		X
Bonifacio 2010	436	37°13.575'N	11°23.803'E	412	X	X

Table 2.1 :Summary of samples collection during the Bonifacio_2010 cruise

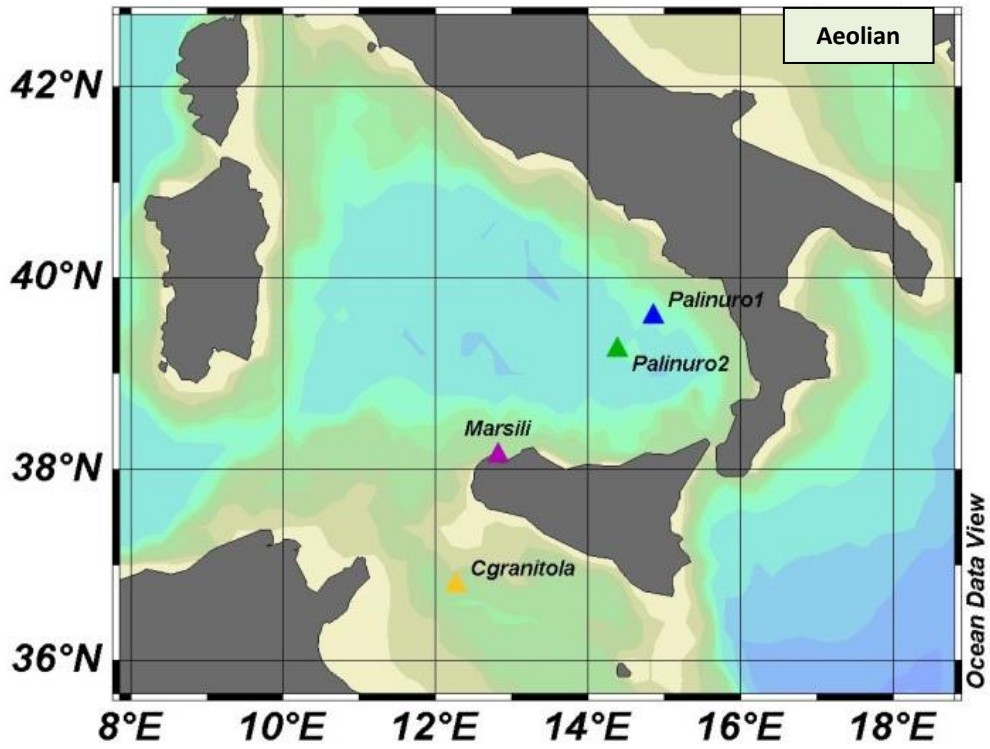


Figure 2.2 Sampling sites from the AEOLIAN_2010 cruise.

CRUISE	STATION	LAT	LONG	DEPTH (mt)	NUTRIENTS
Aeolian 2010	Palinuro1	39°36.239'N	14°51'356'E	1760	X
Aeolian 2010	Marsili	39°15.00'N	14°23.40'E	2793	X
Aeolian 2010	Palinuro2	38°07.890'N	12°49.627'E	2760	X
Aeolian 2010	Capogranitola	36°47.375'N	12°16.128'E	1240	X

Table 2.2 : Summary of samples collection during the Aeolian_2010 cruise

2.1.2- CTD Rosette sampling

Data of temperature, salinity during the two oceanographic cruises BONIFACIO_2010 and AEOLIAN_2010 were collected by a CTD Rosette; Niskin bottles were used to collect seawater samples [Figure 2.3].



Figure 2.3 : Niskin bottles fitted on a rosette with CTD instrumentation.

2.1.3- Sampling techniques

On board, samples for nitrate, nitrite, phosphate and silicate analyses were kept in 60 ml HDPE bottles no filtration was employed nutrient sample were stored at -20°C .

In order to minimise any contamination risk for trace elements analysis of seawater, all apparatus with potential contact with seawater samples (bottles, pipette tips, filtration system etc.) was pre-conditioned [as described by *Scelfo, 1997*]. Plastic bottles for seawater sampling were filled up with HNO_3 10% and placed under hood for 4 days at room temperature. After this time, the bottles were rinsed 2-3 times with ultrapure water and, after drying, singularly, were stored in polyethylene bags until final sampling.

Polycarbonate membrane filters, for particulate collection, were stored in petri dishes for the transport. Samples for trace metals were collected in 1L polyethylene pre-cleaned bottles and then filtered through 47 mm, $0.4\ \mu\text{m}$ pore size, polycarbonate membrane filters or cellulose acetate. Samples, for total dissolved trace metal analysis, were acidified to a pH ~ 2 with suprapur HNO_3 and stored at room temperature. These samples, filtered and acidified, were returned to its

original bottle contained within a plastic bag, while the polycarbonate membrane filters were kept at $T = -20^{\circ}\text{C}$ [Figure 2.4].

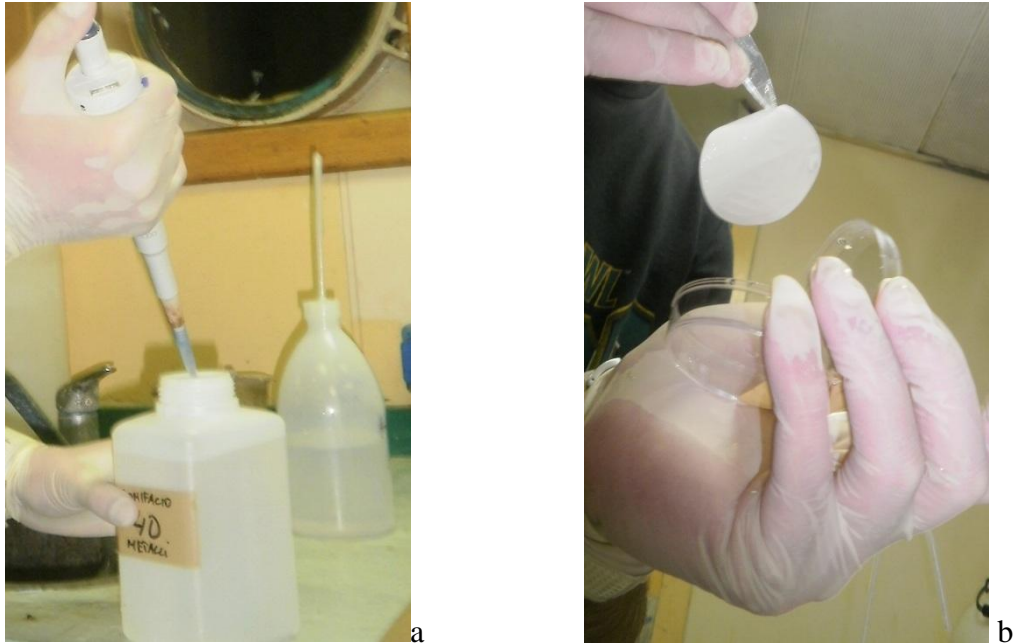


Figure 2.4: Sampling techniques for trace elements analysis; a) filtration on $0,4\ \mu\text{m}$ nucleopore PC membrane and acidified with HNO_3 ; b) membrane stored at -20°C .

2.2 Analytical procedures for nutrients and trace elements

2.2.1- Nutrients

The dissolved nutrient concentrations have been determined in the laboratory of CNR-Capo Granitola, using Auto Analyzer Sial (QUAATRO), following classical methods [Grasshoff *et al.*, 1999].

The multi-channel AutoAnalyzer allows the simultaneous and continuous orthophosphate, nitrate, nitrite, nitrate and silicate dissolved. The chemical procedures followed for the analytical determination of dissolved nutrients are based on classical methods [Grasshoff *et al.*, 1999] adapted to automated measurement systems. The samples, taken from an automatic sampler, slide one after the other, interspersed with washing water and are mixed with the various reagents injected in the flow under controlled conditions by means of peristaltic pumps. The chemical reactions leading to the final formation of colored compounds, whose intensity of staining is proportional to the concentration of the nutrient present in the sample. A colorimeter allows the measurement of the concentration values at specific wavelengths through interferential filter.

The dissolved silicates that are determined by following the procedure [Grasshoff *et al.*, 1999]: dissolved silicates react, in an acid medium, with a solution of molybdate forming silicomolybdic acid which is reduced, with the addition of ascorbic acid, to a colored complex (molybdenum blue), whose concentration is quantified by determining absorbance at 820 nm.

2.2.2- Analytical procedures for analysis of trace elements in particulate phase

2.2.2.1- Analytical procedures for analysis of trace elements in particulate phase

The particulate phase is all that remained on polycarbonate filter when the sample were filtered by vacuum through 0.45 μm

All apparatus and all samples were treated under a laminar air flow hood to minimize the contamination risks.

The filters are subjected to acid digestion in a microwave oven (CEM MARS-5); the method is simple and fast. Mixtures of HNO_3 , HCl , HF and H_2O_2 are commonly applied:

Nitric acid (HNO_3): It has a strong oxidant power and a remarkable ability to form soluble salts with most of the elements. Furthermore, it does not generate significant interference in ICP-MS.

Hydrochloric acid (HCl): It is a strong acid, with reducing power under conditions of high temperature and pressure. These features make it capable to attack oxides, hydroxides, carbonates and sulphates forming soluble compounds in water.

Hydrofluoric acid (HF): It dissolves also the more resistant crystal silicate phases.

H_2O_2 . This is, such as HNO_3 , a strong oxidant.

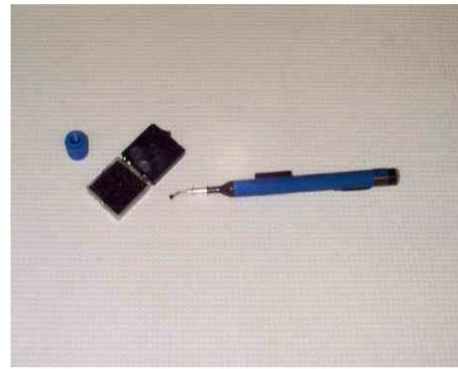
Filters, for particulate matter analyses, were put in Teflon vessels with a mixture of 3,0 ml of HNO_3 , 1,0 ml of HCl , 50 μl of HF and 2,0 ml of H_2O_2 and brought in a CEM Microwave Mars at 96°C for 3 h [Figure 2.5]

A number of precautions should be taken for safe operation of the microwave system: the vessels are placed in the support modules with the load distributing caps, and tightened with a torque wrench to 5 ft*lbs. Blue pressure caps (with pressure membranes inserted) are to be hand tight.

Pressure sensor and Thermowell must be attached to the control vessel. Support modules are placed on the carousel and the top ring attached. During microwave digestion, temperature and pressure are controlled. The metals thus obtained can be analyzed with inductively coupled plasma mass spectrometry (ICP-MS) or with inductively coupled plasma optical emission spectrometry (ICP-AES).



(a)



(b)

Figure 2.5: (a) From left to right; control vessel in the support module with pressure sensor attached and fiber optic temperature sensor inserted, a typical reaction vessel in a support module, and an assembled reaction vessel showing the explosion-proof Kevlar sleeve and the load distributing cap piece placed on the vessel lid. (b) From left to right; threaded blue cap that fits on the reaction vessel lid and into which a pressure membrane (in the black box) is placed with the pen-sized suction device.

Chapter 3

RESULTS

3.1- Nutrients

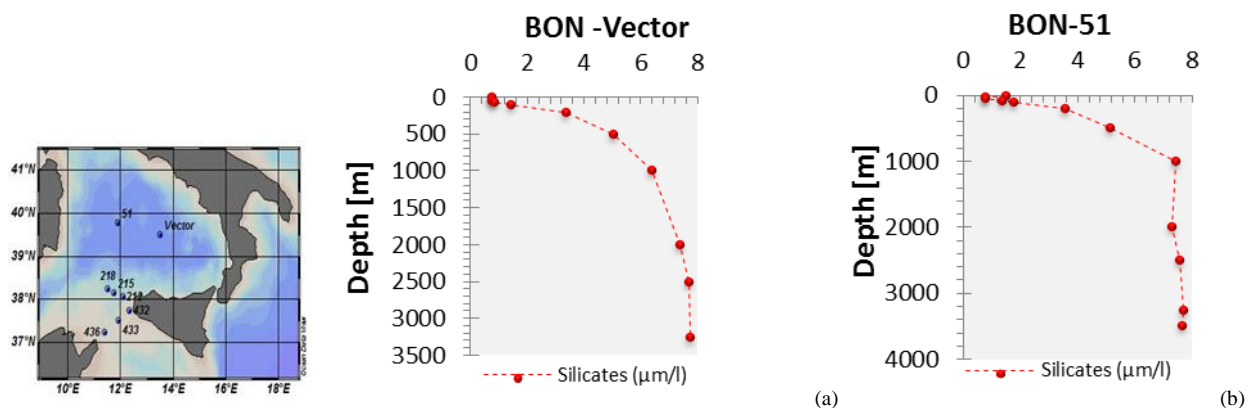
3.1.1- Silicates - the Bonifacio_2010 cruise

The distribution patterns of silicates, [Figure 3.1] from the sampling sites of the Bonifacio_2010 cruise show maximum concentration in the intermediate and deep waters (800-1200 m depth interval). The strong reduction of concentrations in the surface waters is due to the effects of assimilation by phytoplankton in the euphotic zone. The chemical analysis are reported in Appendix I.

The concentrations of silicates in the stations Vector and 51 (both in the Tyrrhenian sea) are averagely $0.90 \pm 0.30 \mu\text{mol/L}$ and $1.23 \pm 0.44 \mu\text{mol/L}$ in surface waters , 4.22 ± 1.18 and $4.36 \pm 1.12 \mu\text{mol/L}$ in intermediate waters and 7.31 ± 0.64 and $7.54 \pm 0.18 \mu\text{mol/L}$ in deep waters with values of the standard deviations which evidence relevant uniformity in deep waters [Figure 3.1 (a)(b)].

The silicate concentrations along the transect of stations 212, 215 and 218 are 1.52 ± 0.84 , 0.86 ± 0.38 and $1.50 \pm 1.22 \mu\text{mol/L}$ in surface waters [Figure 3.1 (f)(g)(h)]. The average concentrations in intermediate waters at stations 215 and 218 are respectively $4.21 \pm - (n=1)$ and $4.22 \pm - (n=1) \mu\text{mol/L}$ [Figure 3.1 (g)(h)]; the average concentration at station 215 is $6.28 \pm 0.46 \mu\text{mol/L}$ for the deep water [Figure 3.1 (g)].

The surface concentrations in the stations 432, 433 and 436 are on average $1.48 \pm 0.82 \mu\text{mol/L}$, $1.01 \pm 0.41 \mu\text{mol/L}$ and $0.73 \pm 0.13 \mu\text{mol/L}$, respectively [Figure 3.1 (c)(d) (e)].



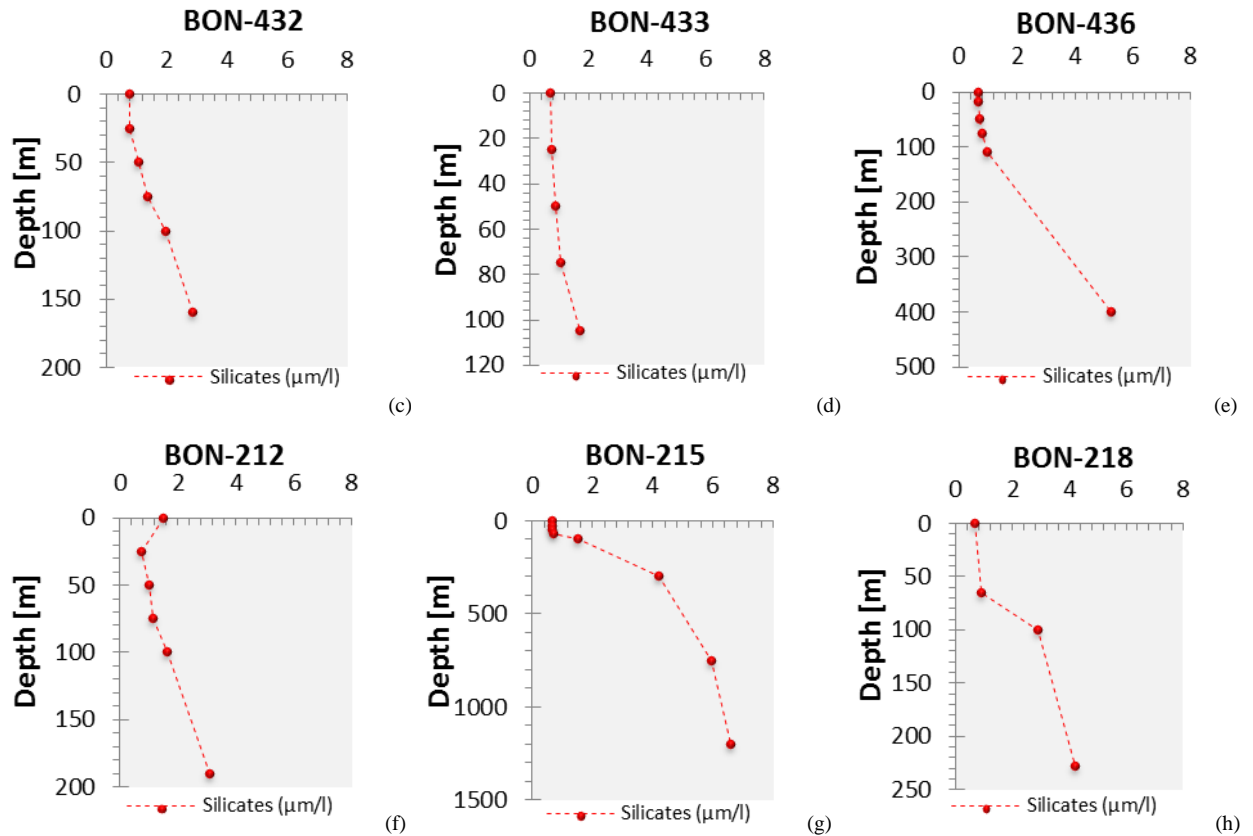


Figure 3.1 : Distribution of silicates, sampled in the Bonifacio cruise.

3.1.2- Silicates - the Aeolian_2010 cruise

The distribution patterns of silicates from sampling sites of the Aeolian_2010 cruise [Figure 3.2] again show a strong reduction of concentrations in the surface water and enriched values at the deeper levels. The chemical analysis are reported in Appendix II.

The C. Granitola station, which is located within the Sicily strait, has silicate concentrations of 0.77 ± 0.96 , 4.14 ± 1.35 , 4.64 ± 1.07 µmol/L in surface, intermediate and deep water, respectively [Figure 3.2 (a)].

In the Palinuro 1, Palinuro 2 and Marsili stations the silicate concentrations are on average 1.17 ± 0.87 , 1.50 ± 1 and 0.79 ± 0.39 µmol/L for the surface water; in the intermediate water the silicate concentrations are on average 4.41 ± 0.02 , 4.15 , and 4.18 ± 0.94 µmol/L, and they are 5.68 ± 1.83 , 6.65 ± 0.78 , 6.63 ± 0.81 µmol/L for the deep water [Figure 3.2 (b)(c)(d)].

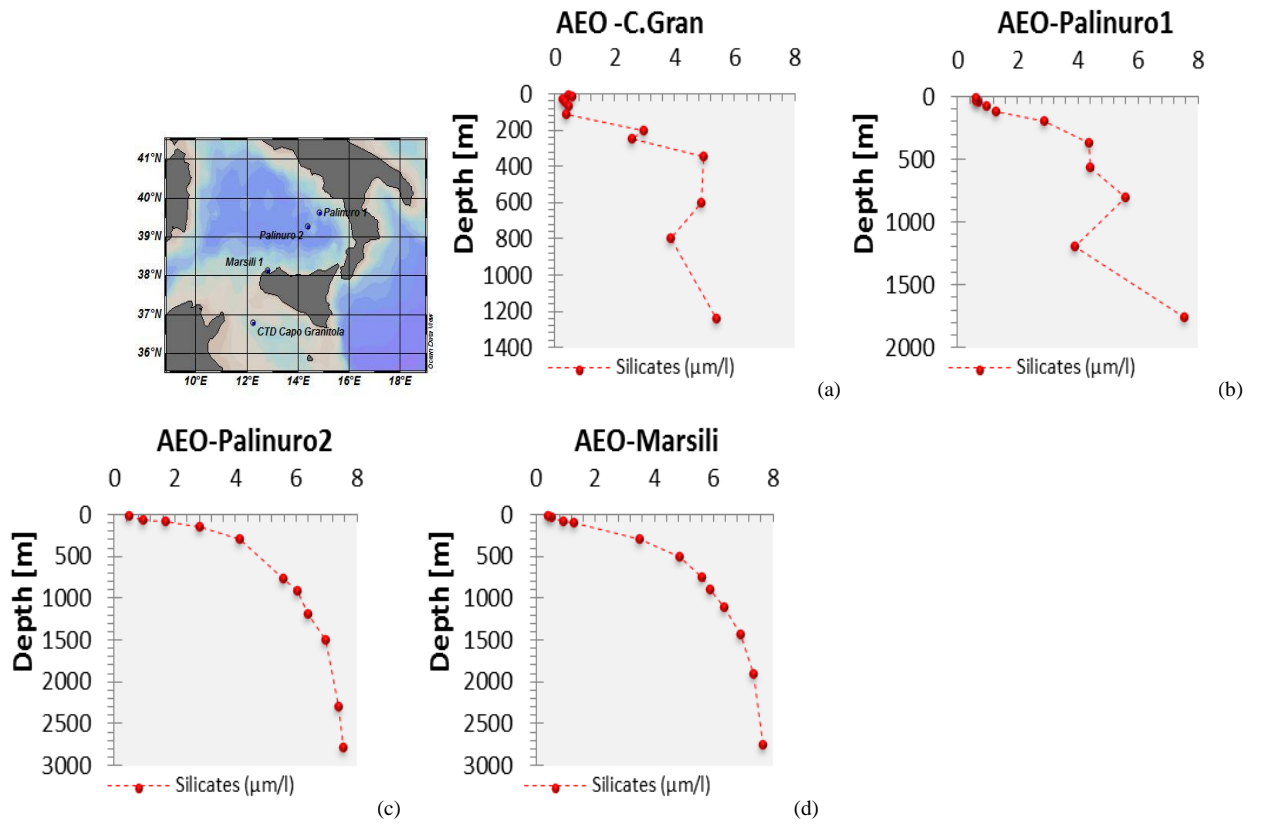


Figure 3.2 : Distribution of silicates sampled in the Aeolian cruise.

3.2- Trace Metals in the particulate phase

Chemical composition of particulate from the different sampling sites are reported in Appendix III and the graphical representation by box-wiskers plot is reported in **Figures. 3.3**.

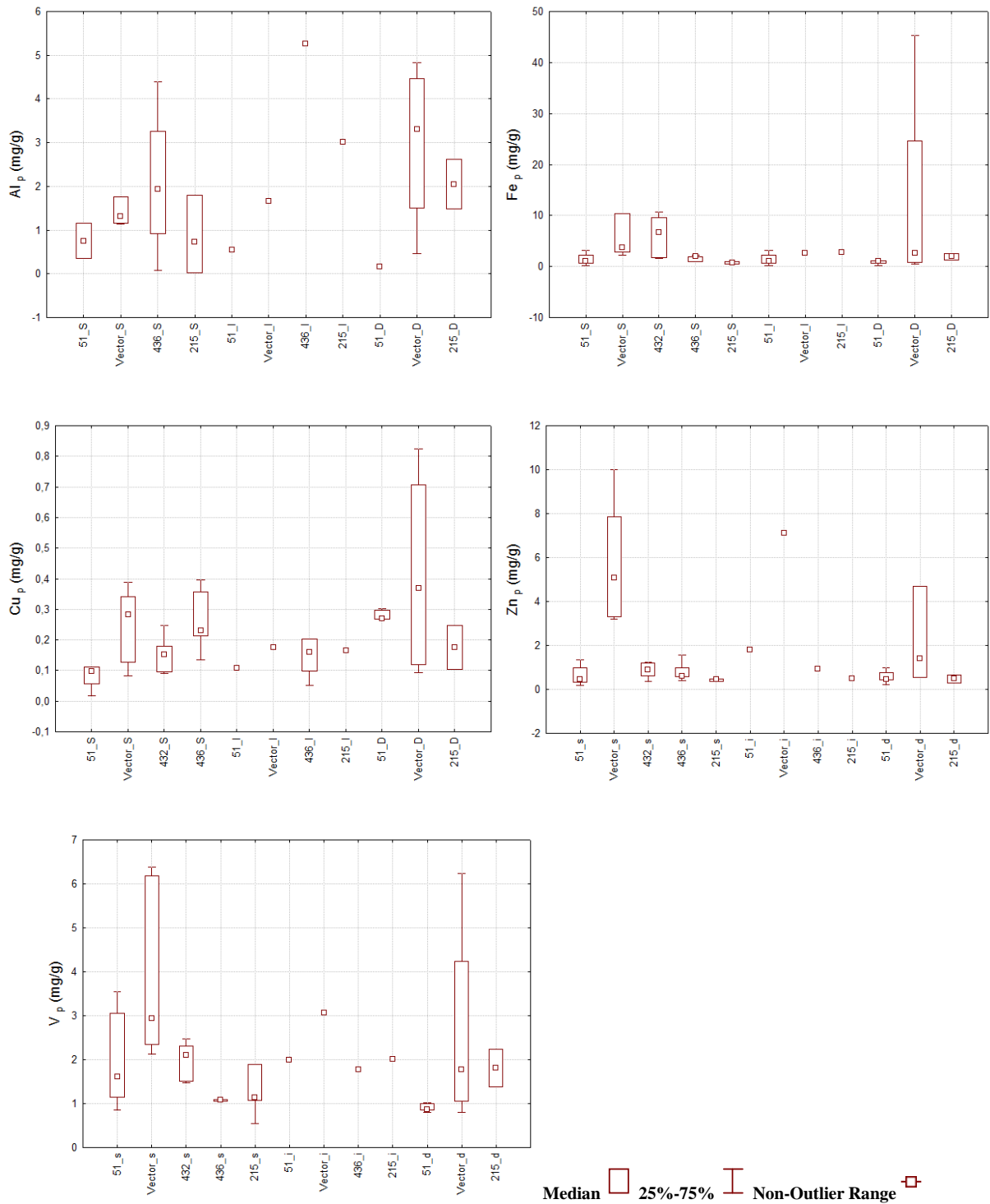


Figure 3.3: Metals particulate concentrations in seawater sample collected during Bonifacio cruise 2010.

3.2.1- Aluminium (Al)

Vertical profiles of Aluminium in particulate from the surface to the bottom water in the different sampling stations, are shown in **Figure 3.4**.

The distribution of Al_p in the surface water clearly evidence maximum of concentration at the 432 station along the column water, and at the 436 station, probably due a direct impact of the desert dust.

The Vector station, which is located in the Tyrrhenian sea, has aluminum concentrations of 2.41 ± 2.32 , 1.40 ± 0.36 , 2.98 ± 1.93 mg/g in surface (0-150 m), intermediate (150-600m) and deep water (600- bottom) [**Figures 3.4 (a)**].

Concentrations of Al in the particulate at the stations, 432 and 436 in first 150 m of the water column are respectively, 7.64 ± 6.89 , 2.08 ± 1.78 mg/g [**Figures 3.4 (b) (c)**].

In the 215 station the aluminum concentrations are on average 0.85 ± 0.89 , $3.02 \pm -$ (n=1) and 2.05 ± 0.81 mg/g in surface intermediate and deep water [**Figures 3.4 (d)**].

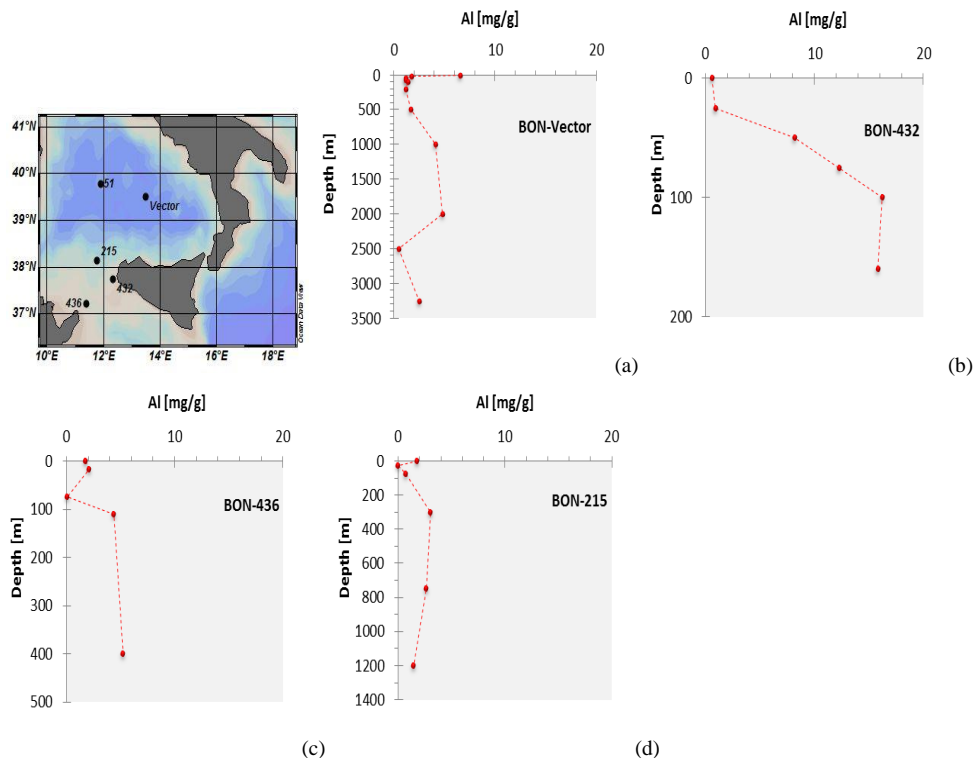


Figure 3.4: Aluminum particulate collected during Bonifacio cruise.

3.2.2- Iron (Fe)

The distribution pattern of $[Fe]_p$ particulate show the highest average surface concentrations at the Vector station (0-150m); in particular Vector station has iron concentrations of 3.21 ± 1.17 ,

2.82 ± 0.24 and 1.90 ± 1.79 mg/g in surface, intermediate and deep water respectively [Figures 3.5 (a)].

The average concentrations in surface water for the stations 432 and 436 are respectively 6.19 ± 3.88 , 1.62 ± 0.60 mg/g; there is a peak in particulate iron at station 432 that coincides with that observed for particulate aluminium [Figures 3.5 (c)(d)].

The average concentrations in surface water for the stations 51, and 215 are respectively 1.63 ± 1.02 , 1.08 ± 0.91 mg/g; the average concentrations in the intermediate water at the stations 51 are respectively, 0.74 ± 0.71 mg/g, in the deep water the average concentrations at the stations 51 and 215 are respectively, 1.09 ± 0.85 , 1.96 ± 0.92 mg/g [Figures 3.5 (b) (e)].

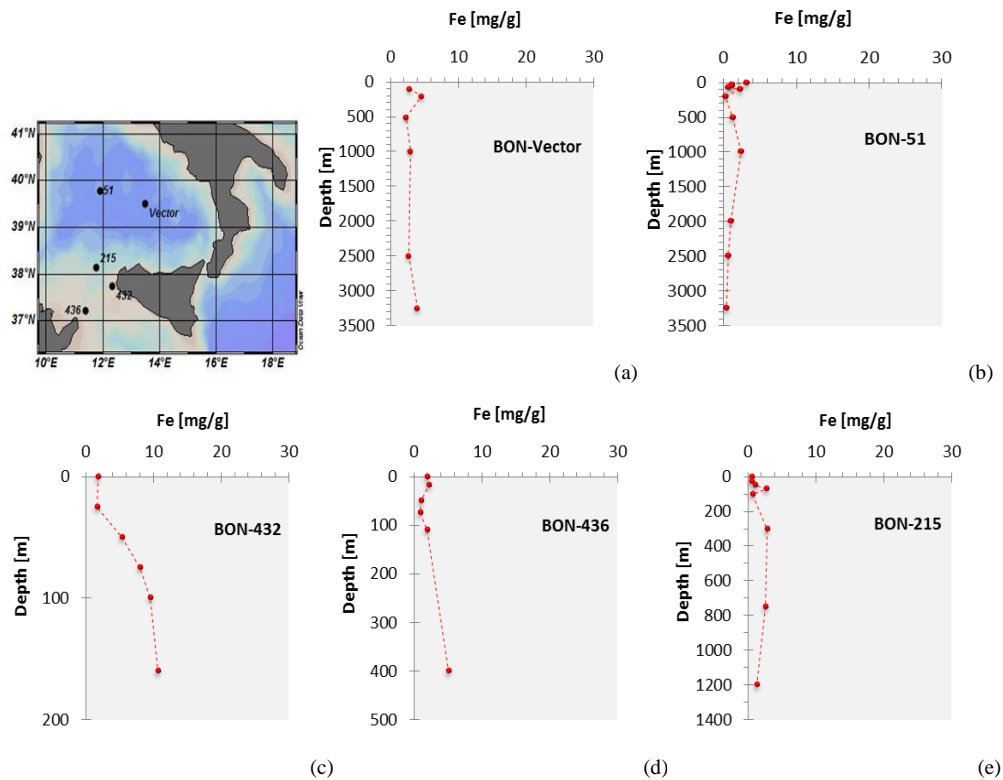


Figure 3.5: Iron particulate collected during Bonifacio cruise.

3.2.3- Zinc (Zn)

The distribution pattern of zinc in the particulate $[Zn]_p$ has the relative maximum concentration at the Vector station, while the observed concentrations are very similar in the remaining stations [Figures 3.6(a)].

The average concentrations in surface water in the stations Vector, 51, 432, 436 and 215 are respectively 4.17 ± 1.25 , 0.71 ± 0.14 , 0.86 ± 0.33 , 0.84 ± 0.41 , 0.55 ± 0.29 mg/g; the average concentrations in intermediate water in the station 51 are respectively 0.94 ± 1.05 mg/g; station

215 has an average concentration in intermediate and deep water equal to 0.51 and 0.48 mg/g respectively [Figures 3.6].

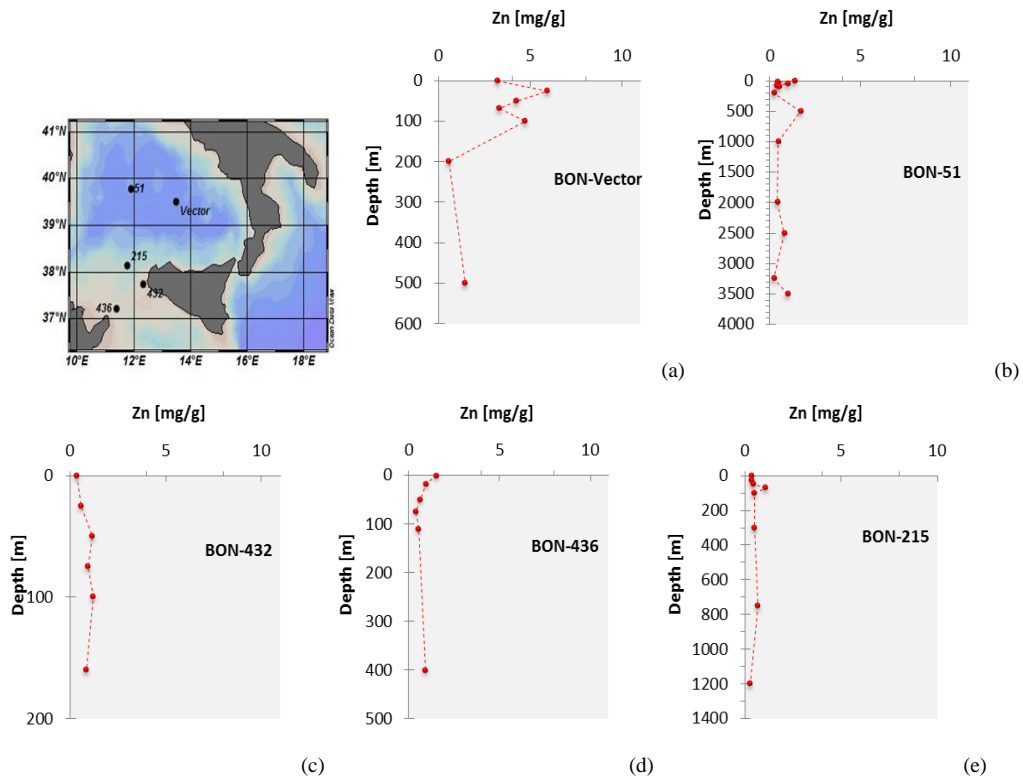


Figure 3.6 : Zinc particulate collected during Bonifacio cruise.

3.2.4- Copper (Cu)

The distribution pattern of copper in the particulate [Cu]_p shows a similar trend in the sampled stations with little variations along the water column.

The average concentrations in surface water at the stations Vector, 51, 432, 436 and 215 are respectively 0.28 ± 0.12 , 0.18 ± 0.23 , 0.15 ± 0.06 , 0.27 ± 0.11 , 0.21 ± 0.18 mg/g ; the average concentrations in intermediate water at the stations Vector and 51 are respectively 0.15 ± 0.03 , 0.08 ± 0.04 mg/g; station 215 has an average concentration in intermediate and deep water equal to $0.17 \pm - (n=0)$ and 0.18 ± 0.1 mg/g respectively [Figures 3.7].

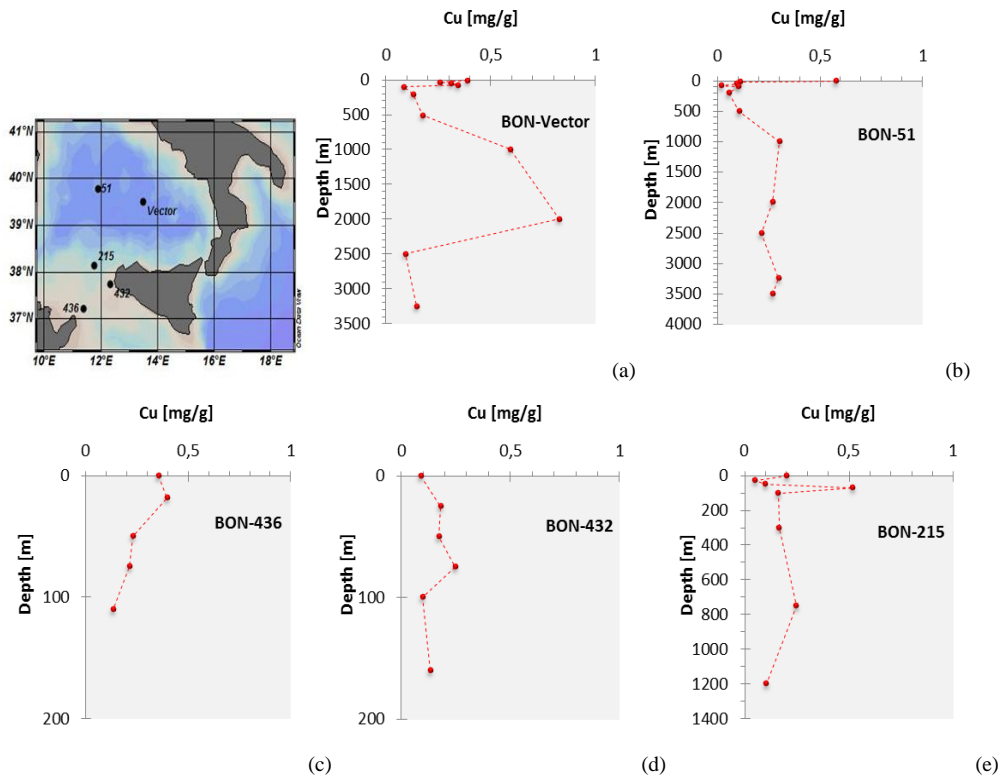
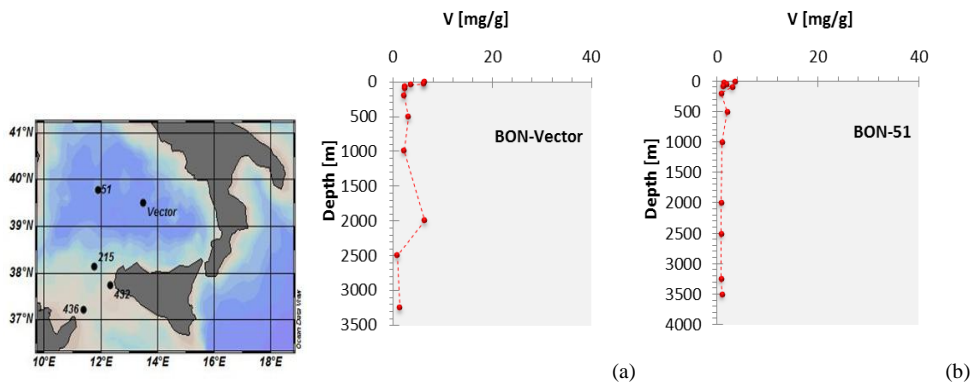


Figure 3.7 : Copper particulate collected during Bonifacio cruise.

3.2.5- Vanadium (V)

The distribution pattern of vanadium in the particulate $[V]_p$ shows a regular pattern of distribution along the water column in the sampled stations, except for station 436; the latter recorded a superficial value maximum of particulate vanadium equal to 30 mg/g.

The following figure shows the pattern of distribution along the water column in the sampled stations. The average concentrations in the Tyrrhenian stations amounted to 3.32 ± 2.02 and 1.53 ± 0.92 mg/g for the Vector station and the 51 station, respectively; the concentrations at the stations in the Sicily Channel amounted to 1.99 ± 0.43 - 6.04 ± 12.07 - 1.87 ± 1.26 mg/g for the stations 432, 436 and 215 respectively [Figures 3.8].



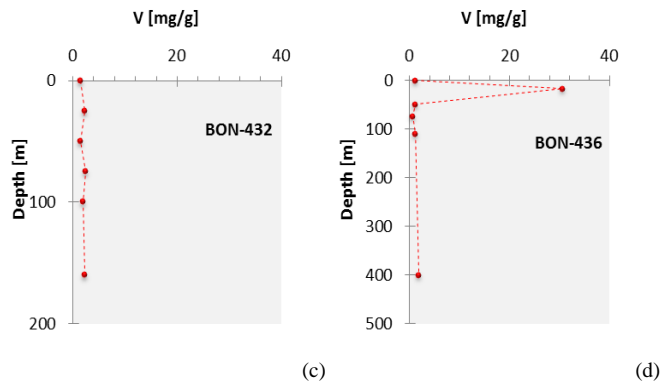


Figure 3.8 : Vanadium particulate collected during Bonifacio cruise.

3.2.6- Distribution of trace elements in particulate: comparison with literature information

Results of trace metals distribution in the particulate phase, collected during the oceanographic cruise Bonifacio have been here integrated with three other datasets collected from the oceanographic Sesame_2008, Transmed_2007 and Medsudmed_2008 cruises. For analytical purposes, the stations are grouped in distinctive regions/basins. [Figure 3.9; Table 3.1].

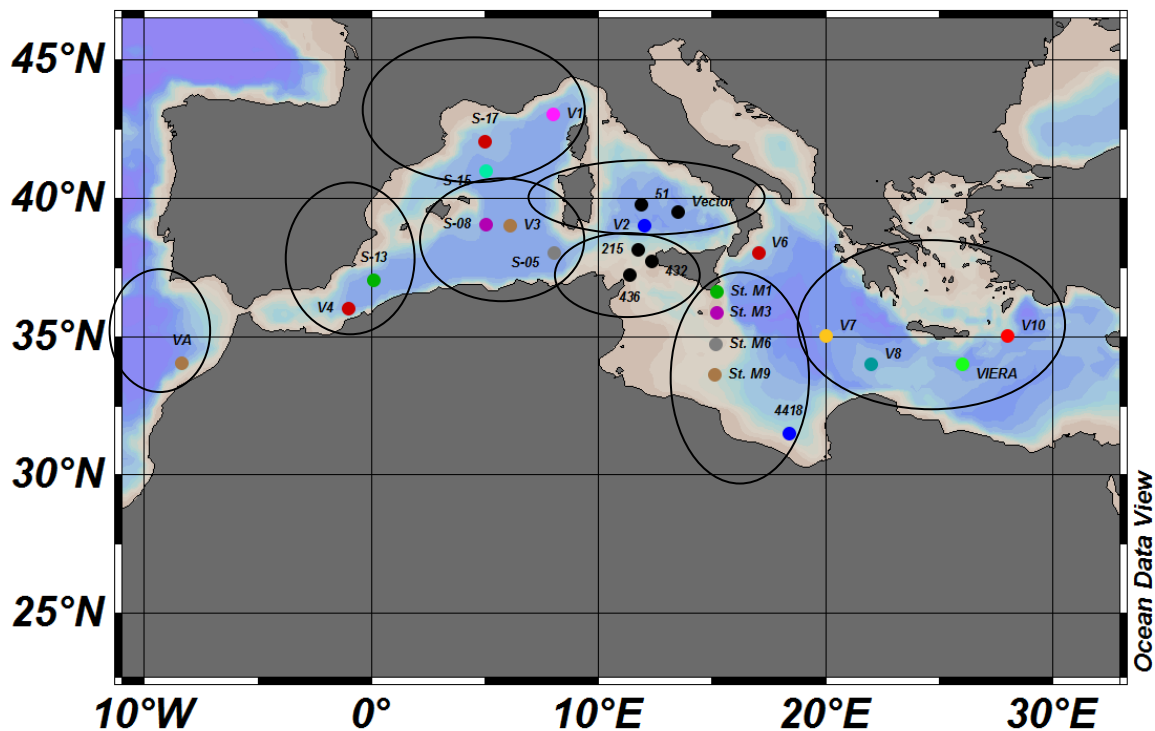


Figure 3.9: Map of particulate trace metals, black dots represent the station sampled during Bonifacio cruise collected in this work, the colored dots represent the datasets from other study.

STATION	BASIN	IDENTIFICATION CODE
VA *	Atlantic	ATL
V4*; S13*	Alboran	ALB
S15*; S17*; V1*	Gulf of Lion	GL
S08*; V3*; S05*	Western Mediterranean	MEDW
V2*; 51; VECTOR	Tyrrhenian	TYR
432; 436; 215	Sicily Channel 1	SIC CHAN 1
M1**; M3**; M6**; M9**44188**	Sicily Channel 2	SIC CHAN 2
V7*; V8*; VIERA*; V10*	Eastern Med	EAST

Table 3.1: Number of sampled stations collected in different basins [ref. Marianna Del Core*, Francesco Placenti**]

Compilation of the whole dataset provides a first synoptic image of distribution of trace elements in the marine particulate of the Mediterranean sea and an exciting opportunity to explore the potential role played by this component on the biogeochemical cycles of the basin.

The strategy used for the description of datasets related to trace metals in the particulate phase in the Mediterranean Sea provides the construction of Box whiskers plots allow to simultaneously synthesize the most important statistical parameters related to the analyzed trace elements and the subdivision of the concentrations of elements grouped by stations, identifying several basin areas. This approach allow to verify the distribution of trace metal in particulate, in the western and eastern of the Mediterranean sea.

Further the description of datasets related to trace metals in the particulate phase in the several basin provides a subdivision of the concentrations of elements grouped by depth range, identifying three water masses. Those ranging between 0-200 m of depth will be considered to refer to surface water mass, while the water layer between 200 -600 m is integrally considered as intermediate water (LIW). The water mass between > 600m is considered as Mediterranean Deep Water (MDW), (Eastern Mediterranean Deep Water EMDW - and Western Mediterranean Deep Water WMDW).

3.2.6.1- Distribution of particulate Aluminum

The median surface concentrations of $[Al]_p$ display the same order of magnitude in the different sub-basins, but moving toward the south-east values generally increase. In detail, the median surface concentrations recorded in the Sicily channel are close to 2 mg/g; moving toward the Tunisian coast the median surface concentrations increase of an order of magnitude [Figure 3.10]. The surface waters (0-200 meters) of the whole basin are characterized by higher concentrations of particulates with respect to intermediate and deep waters, possibly as direct response to impulsive events of the Sahara storms [Figure 3.10].

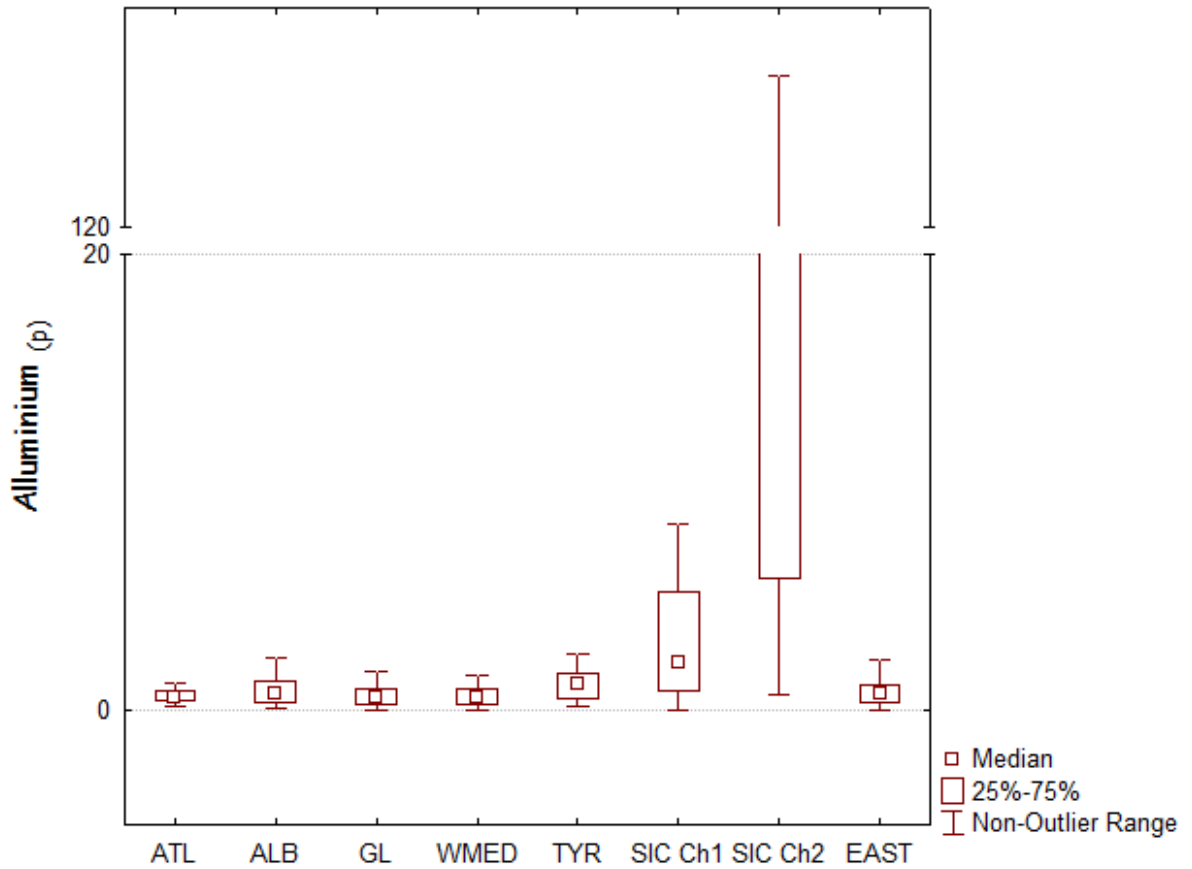
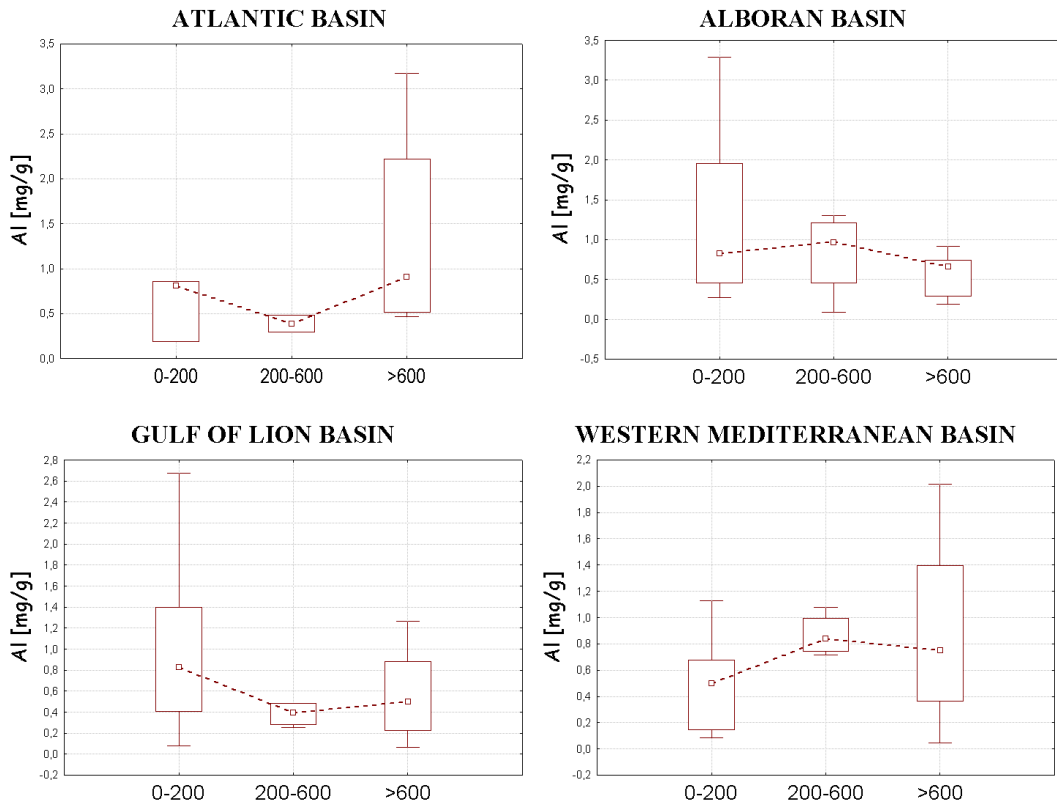


Figure 3.10 : Box whisker plot for Aluminum particulate concentrations in the different basins.



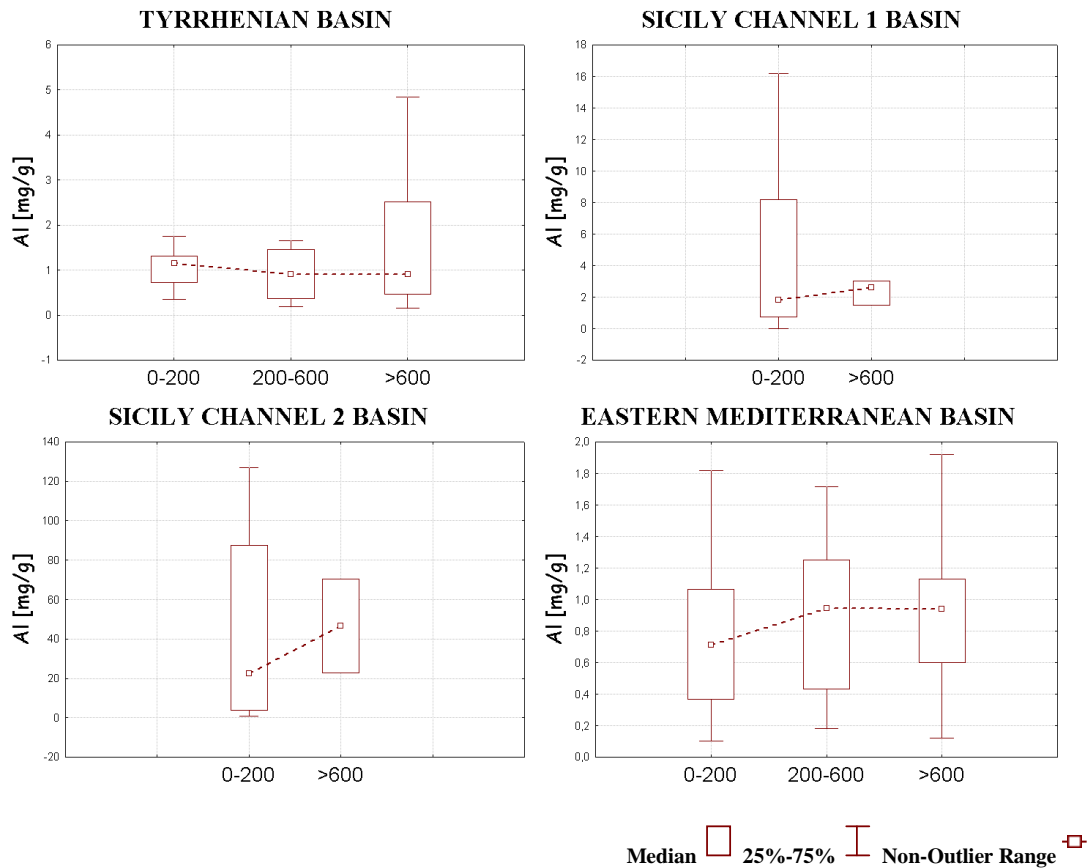


Figure 3.11: Box whiskers plot for Al particulate in surface (0-200), intermediate(200-600) and deep (>600) waters in the Mediterranean basins.

3.2.6.2- Distribution of particulate Iron

The Eastern basin show an increasing trend of Iron particulate Fe_p that appears significantly enriched with respect to the entire basin; this could suggest significant impact of the Sahara dust that affect particularly the SE area [Figure 3.12].

The Alboran, Tyrrhenian and Eastern basins recorded higher concentrations of particulate iron in the surface water (0-200 m), than in the intermediate and deep waters. Instead, in Sicily Channel 1, the intermediate layer appears particularly enriched, differently from deep waters that display values similar to the surface waters. In the Gulf of Lion basin the variability along the vertical axis is substantially reduced [Figure 3.13].

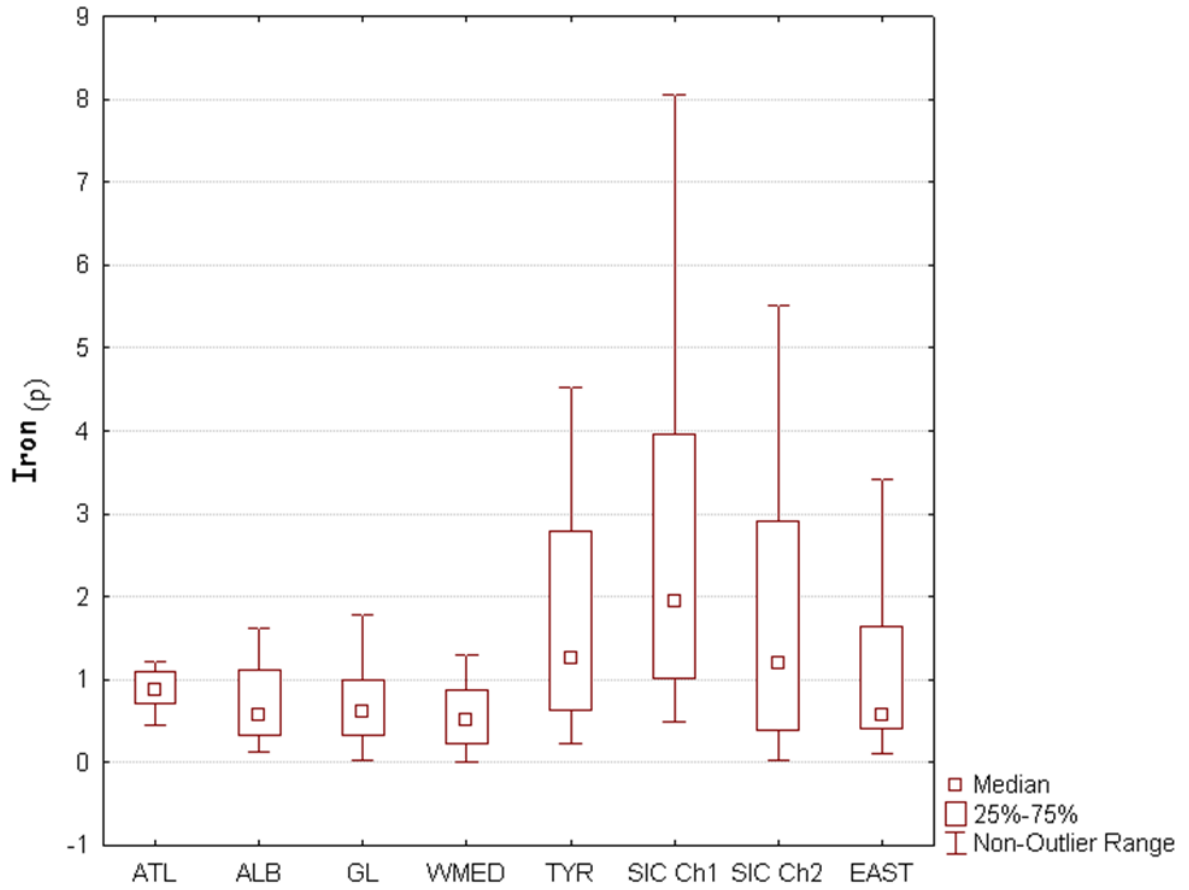
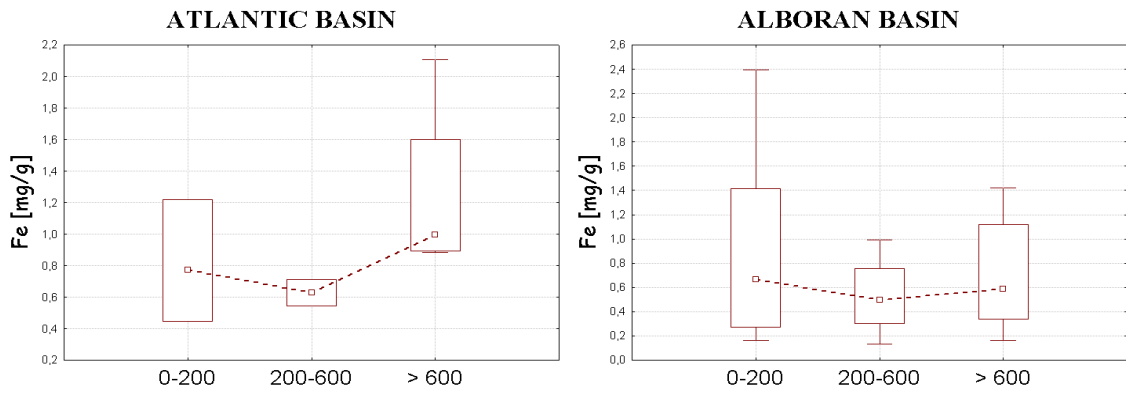


Figure 3.12 : Box whisker plot for Iron particulate concentrations in the different basins.



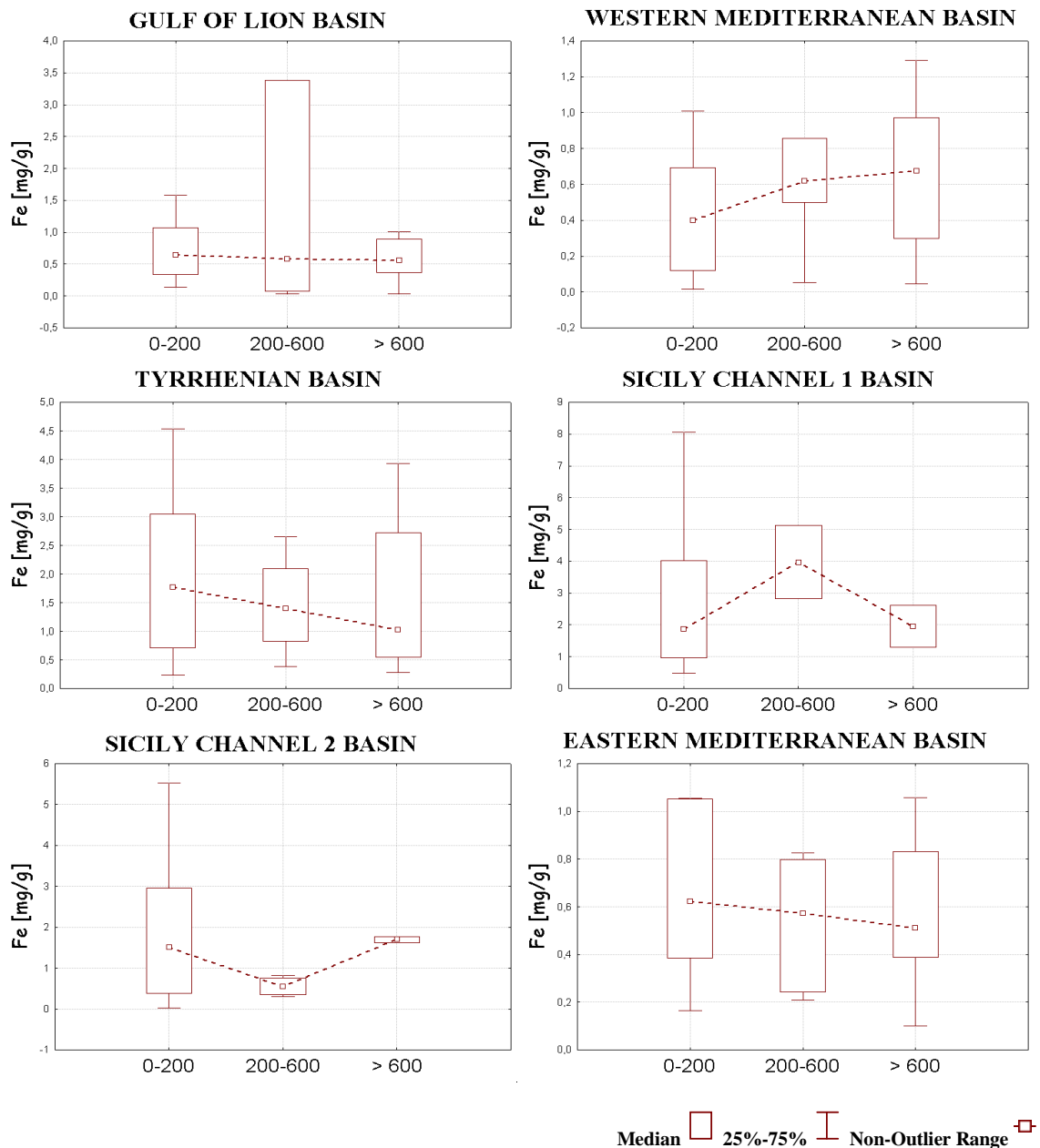


Figure 3.13: Box whiskers plot for Fe particulate in surface (0-200), intermediate(200-600) and deep (>600) waters in the Mediterranean basins.

3.2.6.3- Distribution of particulate Zinc

The distribution of zinc shows in the eastern Mediterranean values depleted with respect to the western basin, suggesting an probably impact of the more industrialized areas of the South Europe [Figure 3.14].

The distribution of particulate zinc presents highest median surface values with a decrease in the intermediate and deep layer. In contrast the western basin and the Channel of Sicily 2 basin show

low concentrations in the surface layer that increase in the deep layer. In Channel Sicily 1 the intermediate layer appears particularly enriched, differently from deep waters that record the same values as surface waters [Figure 3.15].

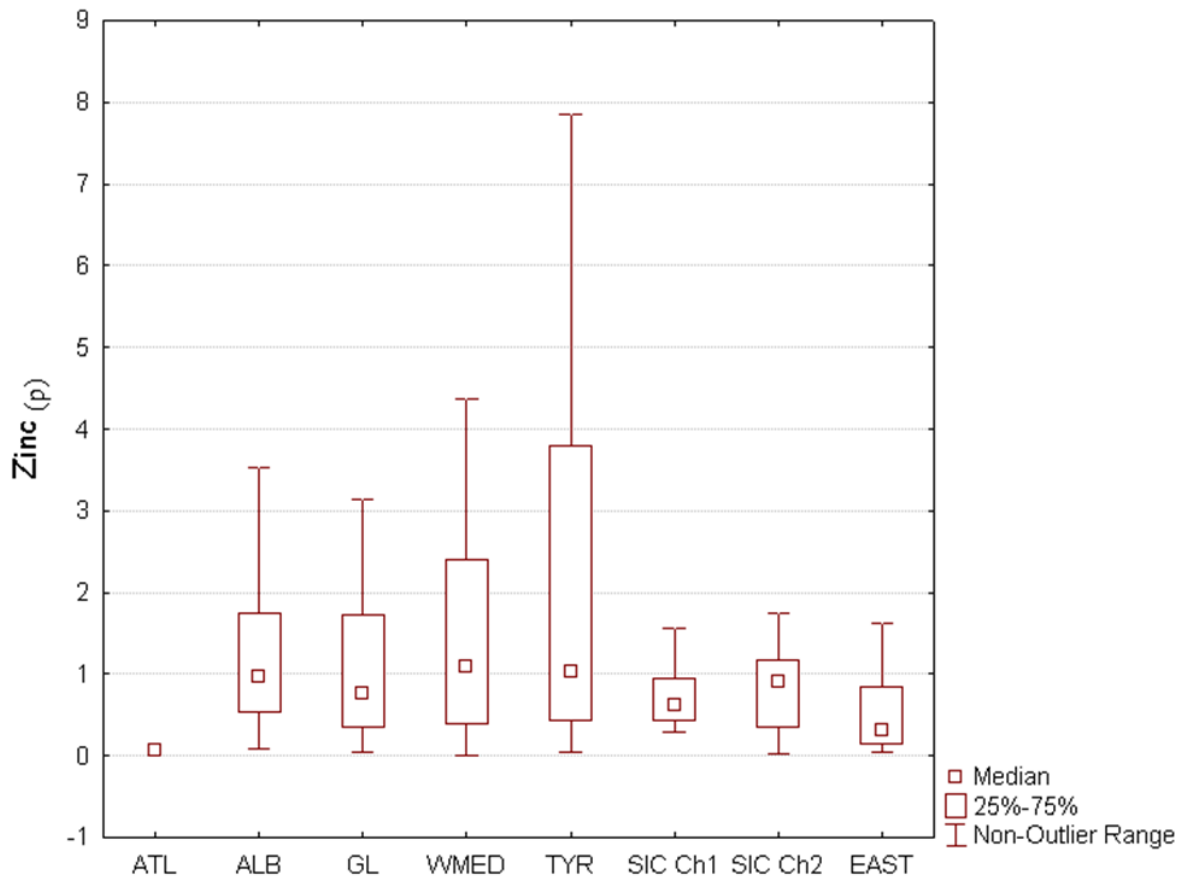
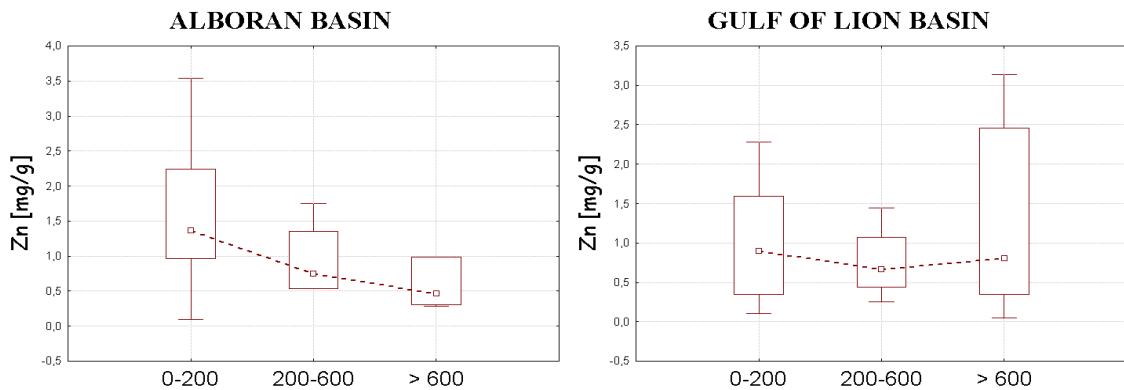


Figure 3.14: Box whisker plot for Zinc particulate concentrations in the different basins.



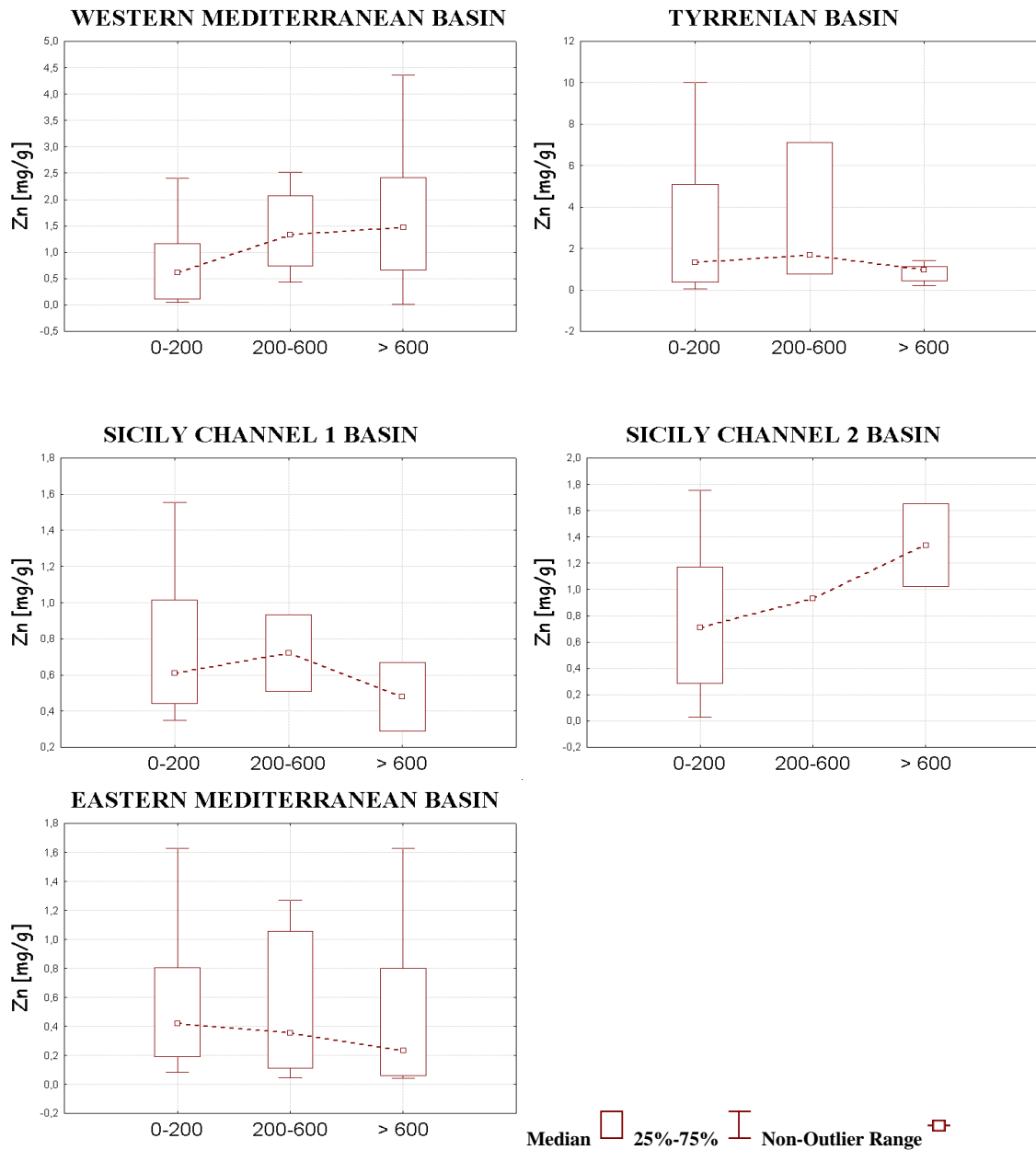


Figure 3.15 : Box whiskers plot for Zn particulate in surface (0-200), intermediate(200-600) and deep (>600) waters in the Mediterranean basins.

3.2.6.4- Distribution of particulate Copper

Low values of Cu particulate are evident in the western stations; instead in the eastern basin the scenario change profoundly. The distribution of copper, show an increase toward East, which could be due from crustal input [Figure 3.16].

The distribution of particulate copper in the surface layer appears particularly enriched. It shows a slight decrease in intermediate and deep waters for the Alboran, Gulf of Lion and Eastern basin

[Figure 3.17]; in contrast, low concentrations in surface water are recorded in the Tyrrhenian and Western basin and Sicily Channel 2.

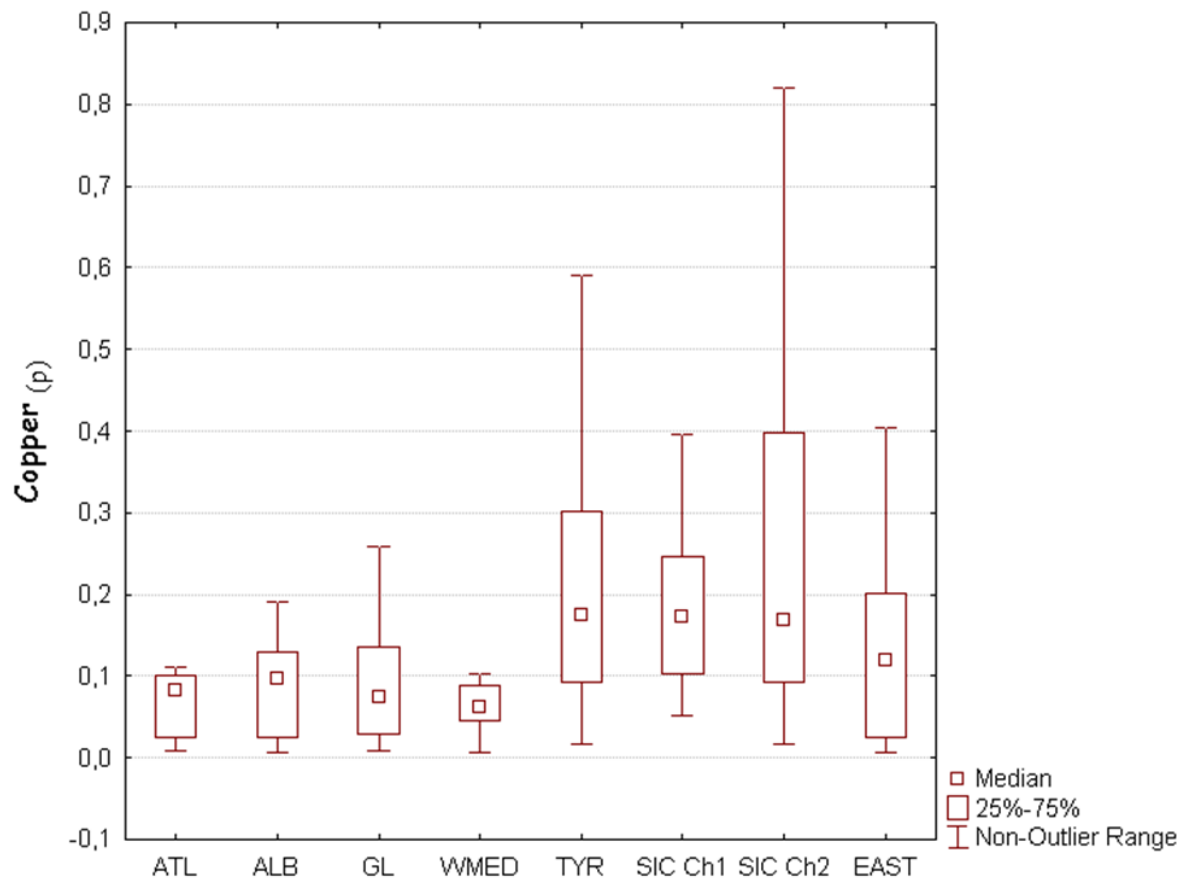
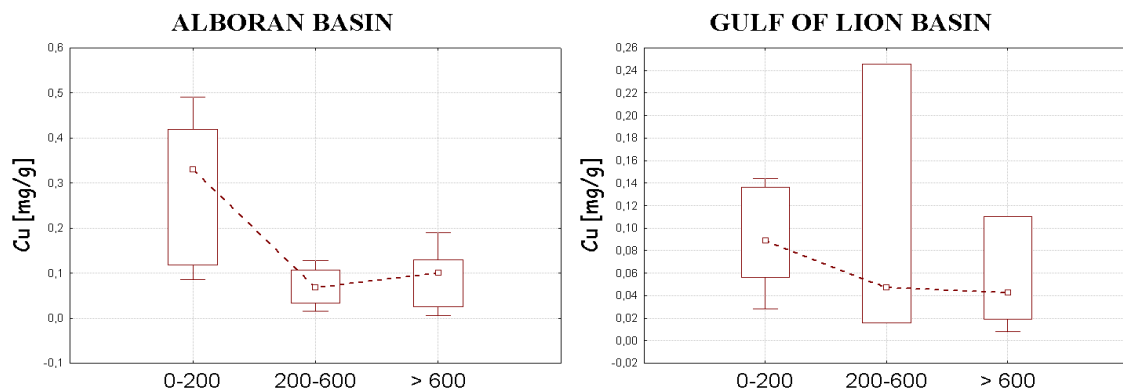


Table 3.16: Box wisher plot for Copper particulate concentrations in the different basins.



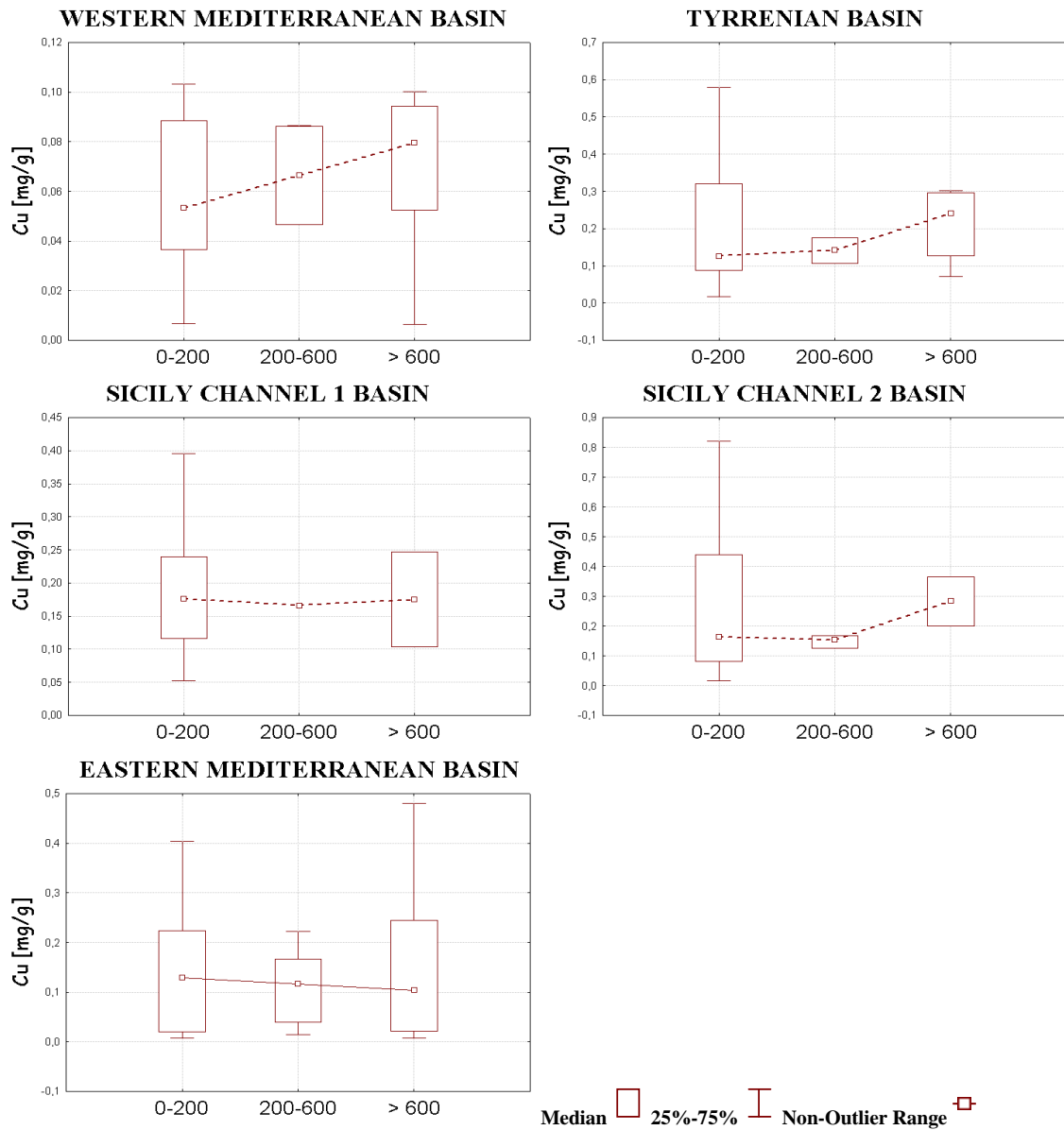


Figure 3.17: Box whiskers plot for Cu particulate in surface (0-200), intermediate(200-600) and deep (>600) waters in the Mediterranean basins.

3.2.6.5- Distribution of particulate Vanadium

The distribution of particulate Vanadium is shown only for the Tyrrhenian and Sicily Channel 1 basin; the Tyrrhenian basin has concentrations of particulates greater than the intermediate and deep waters, contrarily to the Sicily Channel 1 basin [Figure 3.18].

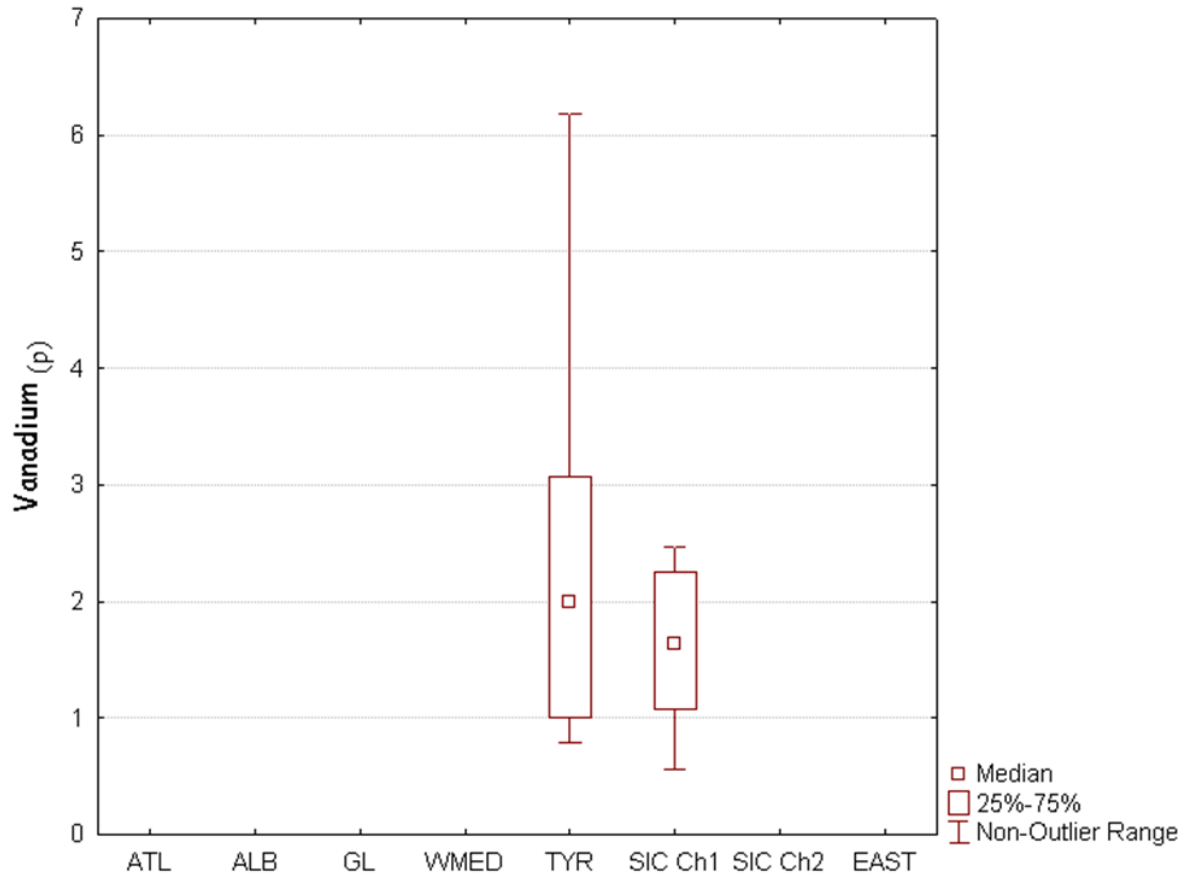


Figure 3.18: Box whisker plot for Vanadium particulate concentrations in the different basins.

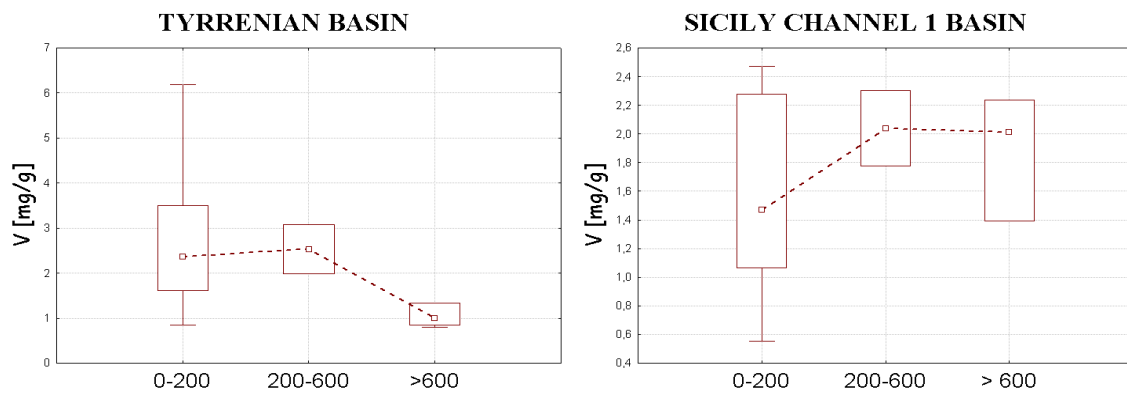


Figure 3.19 : Box whiskers plot for V particulate in surface (0-200), intermediate(200-600) and deep (>600) waters in the Mediterranean basins.

Chapter 4

DISCUSSION

Based on the recent literature, the Mediterranean sea appears characterized by a net deficit of silicon, more evident in the eastern basin. In particular, *Ribera d'Alcala' et al. (2003)* and *Lavezza (2010)* explored the flux of silicates at the Straits of Gibraltar and Sicily to synthetically capture the silicon dynamics at basin scale. The mass balance reported by *Ribera d'Alcala' et al. (2003)* shows a net loss of silicon in the eastern and western basins [Table A], including inputs of Si from ATI (ATI: Atmospheric and riverine inputs). Afterwards, *Lavezza (2010)*, based on a detailed compilation and interpretation of available data from a number of oceanographic cruises carried out in the period 1961 -2010 and at the light of more recent estimates of river inputs [*Ludwig et al., 2009, 2010*] provided evidence of Si accumulation in the western basin and net deficit in the eastern basin [Table B]. These results evidence a crucial difference in the biogeochemical dynamics of the two basins with the eastern one playing a key role and directly affecting the western part of the Mediterranean.

TABLE A	WMED		EMED	
	Si in/out Min	Si in/out Max	Si in/out Min	Si in/out Max
Atmospheric inputs	0,709	2,2	0,009	5,1
River inputs	11,5	39,2	12,2	78,7
Inputs (Tot)	12,2	42,1	12,8	83,8
Sicily strait	179	304	-179	-304
Gibraltar strait	-288	-424		
Input TOT	-109	-120	-179	-304
Deficit	-97	-77,9	-166	-220

Table A: Si budget in the Western and Eastern Mediterranean by Ribera d'Alcala' et al. (2003) [10^9 mol/y]

TABLE B	WMED		EMED	
	Si in/out Min	Si in/out Max	Si in/out Min	Si in/out Max
Atmospheric inputs	0,709	2,2	0,009	5,1
River inputs	11,7	13,1	21,2	23,5
Inputs (Tot)	12,4	15,3	21,2	28,8
Sicily strait	165	235	-165	-235
Gibraltar strait	-147	-199		
Input TOT	18	36	-165	-235
Deficit	30,4	51,3	-143,8	-206,4

Table B: Si budget in the Western and Eastern Mediterranean by Lavezza (2010) [10^9 mol/y]

The mass balance calculated by the two groups of authors did not consider the effects of atmospheric dust and particulate from river inputs as relevant inputs of dissolved Si in seawater, basically due to lack of reliable and basin scale information. The results from this research effort offer an opportunity to explore the potential role played by the atmospheric dust and particulate from river inputs, on the Si mass balance of the Mediterranean sea. Also, recent estimations of seawater fluxes at the Sicily strait provide new chance to calculate more accurate Si budget at Mediterranean scale and hereafter a new revision of 3D fluxes of silicon for the Mediterranean a sea is proposed.

In the following paragraphs I shall explore:

- the role played by the particulate in seawater (from atmosphere and rivers) on the dissolved Si budget of the Mediterranean sea;
- the relative contribution of anthropogenic and natural sources of atmospheric dust and particulate from river input to the seawater;
- a potential revision to the dissolved Si budget in the Mediterranean sea based on updated mass fluxes, specifically of deep waters, at the Sicily Strait.

4.1- Distribution of particulate in the Mediterranean sea

The Mediterranean sea is a geographical area significantly affected by inputs of particulate matter from the atmosphere and rivers, due to the presence of the Sahara desert, predominant NW wind trajectories that flow on the most important industrialized areas of North Europe and a number of relevant river inputs to the basin (particularly, Rhone, Po and Ebro).

The role played by the particulate in seawater, in terms of potential contribution to the marine chemistry of the Mediterranean sea, is driven by a large range of kinetic parameters regulating dissolution of trace elements in seawater and consequently bioavailability of metals in solution. The effects of particulate load and consequent dissolution in seawater, specifically in terms dissolved Si budget, have been only marginally explored, due to lack of reliable and basin scale datasets.

The Mediterranean is surrounded on the northern boundary by the European continent and on the southern side by the North Africa arid regions, with the big Saharan desert. Therefore, a combination of impacts on the seawater chemistry, by particulate transport and deposition, of the Mediterranean sea by anthropogenic and natural sources occur. Specifically, airflows from North Africa contain relatively highest concentrations of Al and Fe and generally lower contents of Cu Cd Ni Zn, while relatively high concentrations of Ni, Pb and V characterize airflows from Northern Europe with significant emissions of fuel burning [Chen 2008].

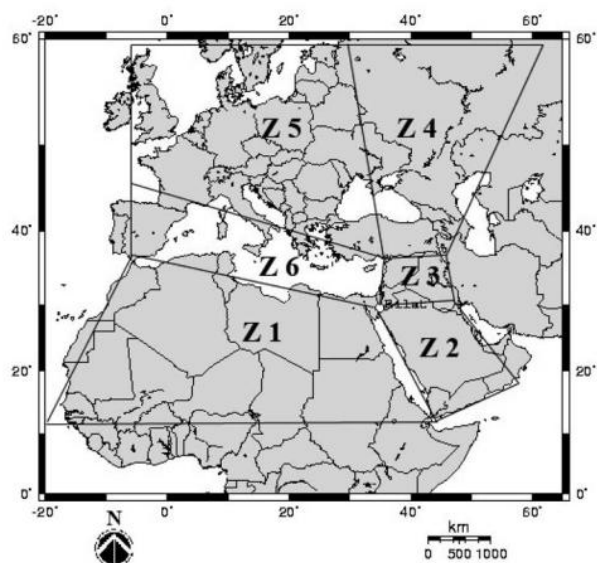
For most of metals, dry deposition appears to be the predominant removal and transport pathway, representing about 70% of particulate deposited on the sea surface. Manganese and Cu are essentially deposited by dry deposition, which represents 69% and 70% of the total atmospheric inputs, respectively. In contrast, Fe and Zn are removed from the atmosphere almost equally by wet and dry deposition. Finally 59–71% of V, Cd and Pb are deposited to the sea surface mainly through wet deposition, and particularly, V and Pb mainly occur in the insoluble form (68% and 64% of the total atmospheric deposition, respectively) and Cd in the soluble 60%. Manganese, Cu and Zn are mainly in soluble form in the total atmospheric deposition (61–70%) [Theodosi, 2010].

Basically, fluxes of trace elements from dry deposition are strongly variables and primarily depend on the sources of emissions and atmospheric trajectories.

A number of data on chemical composition of atmospheric dust from NW European countries and Saharan desert are available and provide crucial information on the sources of particulate in seawater [Dulac *et al.*, 1987; Bergametti *et al.*, 1989; Martin *et al.*, 1989; Chester *et al.*, 1996; Guerzoni *et al.*, 1997, 1999; Guieu *et al.*, 1997; Migon *et al.*, 1997]. Conversely, chemistry of atmospheric dust from the eastern Mediterranean appears relatively poorly studied and only a limited number of literature information are available [Kubilay and Saydam, 1995; Kubilay *et al.*, 1997; Gullu *et al.*, 1998].

Recently, Chen *et al.* (2008), provided geometric median concentrations of trace metals in aerosols and dust from the Mediterranean regions (normalized to aerosol masses), along with

Total Suspended Particulate concentrations covering several sectors, in particular North Africa, Western Europe and the Mediterranean Sea [Tab. 4.1].



	North Africa(z1)	Western Europe(z5)	Mediterranean sea(z6)
	n=19	n=37	n=47
	mg/g		
Al	37,7	24,9	24,6
Fe	23	15,6	15,7
	µg/g		
V	121	128	137
Cu	52	89,2	93,9
Zn	255	425	397

Table 4.1: Geometric median concentrations of TMS (mg/g; µg/g) in aerosol normalized to the aerosol masses (Chen et al, 2008)

However, concentration of Si in particulate in seawater is not considered a reliable proxy of silicates transport from dust and rivers. Actually, dissolution significantly affects Si in particulate and makes it difficult to extrapolate, in terms of original contents, atmospheric and dust river inputs. Actually, results of experiments on the dissolution kinetic reported in literature [e.g., *Desboeufs et al 2005*], show that the dissolution rates are more rapid in the earlier minutes of contact with seawater and that maximum of solubility is reached after about 20 min. Also Fe in particulate is affected by significant dissolution in seawater and cannot be used to properly calculate contents in atmospheric dust and/or to infer reliable information on the potential sources. *Duce and Tindale (1991)* definitively calculated that between 10 and 50% of the mineral Fe apparently dissolves when dust enters the ocean. Also, the fraction of Fe contained in the atmospheric dust is highly soluble in seawater being rapidly biologically up-taken once available to marine photosynthetic organisms. Iron, in surface seawater, undergoes further exchange

between the dissolved and particulate phases and can subsequently become partially available for uptake by plankton [*Baker 2010*].

Silicon and Al are the two most abundant elements of the atmospheric dust and particulate rivers. When entering the surface waters, Si dissolves while Al is essentially insoluble in seawater [*Tria 2007*]. Thus, Al can be considered a more conservative element than Si and a natural ideal tracer for quantifying the dust deposition in the surface ocean and inputs of particulate from rivers. For this reason, I used Al from the particulate fraction in seawater to conservatively calculate Si contribution from atmospheric dust and rivers particulate inputs to the sea. Aluminum is a major and relatively invariant component of continental materials [*Wedepohl, 1995*]. It is the third most common element in continental materials accounting for about 8% of crustal mass. The residence time of Al in the surface ocean is relatively short (6.5 years) [*Jickells et al., 1994*] which impedes important contribution and transport from the coastal areas to the open oceans. That means that the atmospheric input of Al to the surface ocean represents the main source of this element mainly for the remote areas of the sea. Also, the chemical dynamics of Al in seawater is comparable to that of Si, and partially Fe, because it is not involved in crucial and complex redox chemistry. By its nature Al is related to minerals that generally show lower dissolution kinetics and a conservative behavior in seawater [*Measures and Vink 2000; Han et al 2008*].

Thus, an appropriate knowledge of Si/Al ratios from different source areas represents an excellent way to calculate Si transported at the sea from different atmospheric particulates and then to infer more reliable budgets of Si from atmospheric and river inputs to the sea.

Data available from the literature, report Si/Al rather constant from the different source areas of atmospheric and rivers particulate. In particular, an average 2.2 value is reported for Si/Al from samples of African dust over southern Italy. Actually, recent information reported by Blanco et al. (2003) indicate Si/Al in samples collected across 20 dust events with a source region north western Sahara, ranging between 2 and 2.44, recording an average 2.2 value [**Tab. 4.2**].

Element	24-05-02	12-04-02	13-05-02	7-06-02	Average (min –max)
Si /Al	2	2.08	2.22	2.44	2.2

Table 4.2: Si/Al ratios in dust samples from the western Sahara as reported by Blanco et al. (2003)

On the other side, a number of information from the Netherlands Research Program on Particulate [Matter Hugo Denier van der Gon, Magdalena Jozwicka, Elise Hendriks, Mhtenkeni Gondwe and Martijn Schaap: BOP – WP2 – report Mineral Dust as a component of Particulate Matter], reported Si and Al concentrations from mineral dust of urban centers across Europe [Table 4.3]. Those data represent the best set of information to characterize chemistry of atmospheric dust coming from the Western European region. The calculated Si/Al ratio ranges between 1.95 and a maximum (recorded only from one site and considered a statistical outlier) of 5.46, with an average value of 2.6 from the whole North European system.

Country	Location	PM 2,5 [$\mu\text{g}/\text{m}^3$]	Al [ng/m^3]	Si [ng/m^3]	Si/Al
ITA	Pavia	35.3	228	539	2.36
ITA	Veron	41.5	336	759	2.26
ITA	Turin	44.9	380	744	1.95
FRA	Grenoble	19	257	1404	5.46
FRA	Paris	17.8	141	321	2.27
BEL	Antwerp South	20.08	128	263	2.05
DEU	Erfurt	16.3	148	313	2.11
Average	-	-	231 \pm 99.6	620 \pm 401.4	2.6

Table 4.3: Average annual concentrations of PM 2,5 and Aluminum and Silicon metals (data from Götschi et al., 2005)

On the other side, the Rhone river constitutes almost two-third of the total river discharge in the western Mediterranean Sea, and it is considered the most important of the basin. Olivier et al. (2011) reported concentrations of trace metals in the suspended particulate matter of the Rhône River during the years 2001–2003 with average Si /Al ratio equal to 2.9 [Table 4.4. see Appendix IV].

Location	Al [mol/kg]	Si [mol/kg]	Si/Al
Rhone River	2.30±0.53	6.73±0.77	2.9

Table 4.4: Silicon and Aluminum in the suspended particulate matter of the Rhone river (by Ollivier 2011)

Data on particulate chemistry from other Mediterranean rivers, specifically related to distribution of Si and Al, are presently not available and thus, we assume that Si/Al ratios variability could be reliably constrained in the range of the existing information, specifically those from the Rhone river.

Summarizing, the range of variability of Si/Al ratios from different sources (atmosphere and/or rivers) appear constrained in the non-outliers maximum-minimum 2.2-2.9 range of variability. This range of Si/Al variability will be used to constrain the potential of Si dissolution from atmospheric and river particulate in seawater.

4.2- Estimation of dust deposition at basin scale

The aerosol deposition over the sea is much more difficult to map over time with direct and synoptic measurements. In literature there are measurements obtained during cruises that measure mostly aerosol in air although lack information about modes and times of particulate deposition [*Querol et al., 2009; Markaki et al., 2010*].

Dust aerosol has a high spatial and temporal variability; dust is deposited on the sea surface with a high seasonal variability and directly depends on highly variable wind trajectories. The only way to reliably constraint dust input to the seawater is to combine experimental observations with modeling approaches, in order to improve accuracy and predictability of the estimates.

In order to estimate atmospheric dust inputs, integrated on yearly scale, to the Mediterranean basin we explored the outcomes of the BSC-DREAM8b model (Dust Regional Atmospheric Model), reported by the Barcelona Supercomputing Center, whose estimates of global dust input are based on ground, satellite observations and modeling studies [*Perez 2009*]. A crucial component of the model is related to an efficient and apparently reliable capability to simulate and/or predict atmospheric flow and associated mineral dust aerosol. The model also provides parameters for simulating dry particle deposition taking into account a number of key

parameters: diffusion, gravitational settlement associated to different grain size, interception and impaction on surface roughness objects, etc. Also, parameters for analysis and impact of wet deposition is based on a simple below-cloud scavenging effects by precipitation. The models predicts the atmospheric life cycle of the eroded desert dust, which is essential to understand the dust processes and its impact on deposition of particulate in seawater surface, and provides forecast images with boundary conditions update every 6 hour.

Analysis of the model outcomes on wet and dry deposition, allowed me to extract average daily and annual cumulative dust deposition on the seaware at Mediterranean basin scale. In particular, I selected the entire available investigated time interval (years 2002-2005), to analyse inter-annual dust deposition for the Mediterranean sea. These values reported in **Table 4.5**, express the total quantity of dry and wet annual dust deposition on the sea surface of the Mediterranean sea.

YEAR	CUMULATIVE [Tg]		AVERAGE [Tg]	
	DRY	WET	DRY	WET
2002	17.56	19.3	0.08	0.08
2003	4.93	9.19	0.02	0.03
2004	2.85	24.26	0.01	0.07
2005	1.89	9.18	0.01	0.03

Table 4.5: Estimated values of the dry deposition in Teragrams [Tg]

Thus, considering the concentrations of Al measured in the most superficial (50 m of depth) seawater particulate, as expression of an equivalent temporal horizon for the Mediterranean sea we calculated the amount of aluminum transported and deposited by dust and rivers particulate at the sea. The aim of our mass balance is the basin scale and therefore, we considered the median values of dry and wet deposition for the available four years calculated by the model. On the other side, the concentrations of Al in the surface seawater layer (0-50 m) were calculated from each sampling site considering the first and third quartiles as the best index of variability associated to the single measurement.

The **Table 4.6** reports the results, in the surface layer, of the total particulate aluminum (mg) coming from dust deposition (median, first and third quartile). A highly variability is evident and definitively reflects strong differences in Al deposition patterns at basin scale.

Layer 0-50 m	
Al Median	Al TOT
1.1	10.70
Al Q1	Al TOT
0.55	5.35
Al Q3	Al TOT
2.4	23.34

Table 4.6:Total particulate aluminum (mg) coming from dust deposition

Assuming the above discussed robust range of variability of Si/Al ratios of 2.2-2.9, it has been possible to constrain silicon concentration in particulate from Al distribution in the same matrix. Then, based on the available literature information on range of Si dissolution in seawater, I approximated the contribution of dissolved silicon in seawater from atmospheric dust and rivers particulate input.

In particular, few studies combined field and laboratory for accurate measurements of silicon solubility in seawater (*Durr et al. 2011*). The percentage of particulate Si that dissolves in seawater primarily depends on mineral composition and size of particulate. Tréguer et al. (1995) assume that 5–10 percent of the Si transported to the ocean surface by aeolian dust dissolves in the surface water; on the other side, Guerzoni et al. (1999) report 1 percent solubility for Si from Saharan dust samples collected in the sampling fixed station located in Sardinia. Finally, Gehlen et al. (2003) assume a 3% solubility of aluminosilicates in seawater in their kinetic models.

I assumed, as the most conservative hypothesis three different scenarios from Si solubility in seawater in the 1-10%, covering the entire spectrum of variability available from literature data [Table 4.7].

	1% Si		5% Si		10% Si	
	min	Max	min	Max	min	Max
Si (Al Q1)	0,12	0,16	0,59	0,78	1,18	1,55
Si (Al median)	0,24	0,31	1,18	1,55	2,35	3,10
Si (Al Q3)	0,51	0,68	2,57	3,38	5,13	6,77

Table 4.7:Conservative hypothesis of the Si solubility in seawater

The Tab. 4.8 synthesizes the contribution of Si to the dissolved budget of the Mediterranean sea coming from atmospheric dust and river particulate. The range of variability takes into account the complete range of the different estimates and therefore can be considered a reliable projection of data estimate for a Si balance at basin scale.

Compared to the river inputs and/or the final deficit of Si calculated for the Mediterranean sea, the contribution from particulate of atmospheric and river origin represents a wide range of variability, from a trivial ~ 1 to a more significant the ~ 10% of the dissolved budget.

EASTERN MEDITERRANEAN

	Si		Si		Si	
	in/out	Si in/out	Si in/out	Si in/out	Si in/out	Si in/out
	min	Max	min	Max	min	Max
Atmospheric input* (%)	(1%) 0,24	(1%) 0,31	(5%) 1,18	(5%) 1,55	(10%) 2,35	(10%) 3,10
Rivers input**	21,32	23,54	21,32	23,54	21,32	23,54
Input (Tot)	21,56	23,85	22,5	25,09	23,67	26,64
Inflow***	88,98	88,98	88,98	88,98	88,98	88,98
Outflow***	138	138	138	138	138	138
Transport Strait of Sicily	-49,02	-49,02	-49,02	-49,02	-49,02	-49,02
Deficit	-27,46	-25,17	-26,52	-23,93	-25,35	-22,38

Table 4.8: Silicon Budget in the Eastern Mediterranean (10^9 mol/a)- (*) % of dissolve Silicon contribution from atmospheric and river particulates [This study]; (**) [Ludwig 2009]; (***) Silicon concentrations and Transport (infow –outflow) at Strait of Sicily [Schroeder et al; 2008]

Noteworthy, the range of dissolved Si contribution from atmospheric and river particulates takes into account an enormous amount of parameters with associated highly variable and extremely sensible forcing acting at different spatial and temporal scale. Atmospheric variability in trajectories and potential source areas, variability in river inputs, different sources areas with different mineral composition, represent only a very small part if potential impact on the contribution of dissolved Si budget to the Mediterranean sea from atmospheric dust and rivers particulate. Therefore, I consider the presented results only a first step for a deeper understanding of the potential role played by particulate in seawater as actor of a more complex and intriguing story of silicon in the Mediterranean sea. A number of experiments and theoretical approaches are needed to better constrain kinetic and dynamic parameters controlling and driving the effects of Si dissolved from particulate in seawater. Also, finalized combination of synoptic measurements from satellite and more specific data collection of particulate in seawater could better contribute to specifying the role of particulate in the Si budget of the basin.

Therefore, this is only a first milestone to better understand the impact of atmosphere and river inputs on the mass balance of a key nutrient in seawater. Global warming and more generally global changes will affect atmospheric circulation and E-P budget at Mediterranean scale, thus directly contributing to significant variations in chemical and physical parameters which control

dynamics of Si dissolution of particulate in seawater. These results therefore provide a first order of estimates to better constrain and evaluate potential effects of climate changes on Si mass balance at basin scale with specific contribution from atmospheric dust and rivers particulate.

4.3 - Hydrographic characteristics at the Strait of Sicily: new observations for the silicon balance

The connection between the eastern and the western basins is through the Sicily Strait, a topographically complex region; dynamically, the channel is a two-layer system: the upper layer (about 200 m thick) is occupied by the AW and flows eastward, while the deeper layer is composed mainly of LIW and upper EMDW, flowing from east to west.

Hydrographic measurements in the Sicily Channel and in the southern Tyrrhenian Sea show that the water outflowing from the Eastern Mediterranean Basin enters the Tyrrhenian Sea directly, close to the Sicily coast. Two water types have been distinguished: the upper part constituted by the Levantine Intermediate Water LIW, and the transitional Eastern Mediterranean Deep Water EMDW below.

The well-known Levantine Intermediate Water (LIW) is characterized by a relative maximum in temperature, and an absolute maximum in salinity ($T=13.85$, $S=38.75$). The second water mass is generally colder and denser and flows close to the bottom of the Tunisian side of the Strait. That is composed by waters that originate from the upper deep layer of the Ionian sea, and is identified as a transitional Eastern Mediterranean Deep Water (*tEMDW*) ($T=13.65$, $S=38.73$). A significant part of the Eastern Mediterranean outflow is denser than the resident Tyrrhenian water. Consequently, it sinks along the bottom slope after entering the basin, reaching a new equilibrium at very deep levels down to 1800 m. During the sinking, the dense water mixes with entrained ambient water, and its salinity and temperature are modified; therefore *tEMDW* passes through the Sicily Strait, below the LIW, and sinks to a depth of 1850 m in the Tyrrhenian Sea [Sparnocchia *et al.*, 1999].

Following Pollak (1951), several authors [Sparnocchia, Gasparini, Astraldi, Borghini and Pistek (1999)] recognized it as a transitional water mass, produced by mixing of LIW and EMDW. Once it enters the Sicily Channel over the Maltese sill, this colder water sinks because it is of higher density than the resident waters, and from there it flows along the bottom of the Sicily Channel, displaying lower temperatures and salinities than the LIW [Figure 4.9].

The transport of transitional EMDW through the Sicily Channel is estimated to be about 0.2–0.3 Sv [Sparnocchia *et al* 1999].

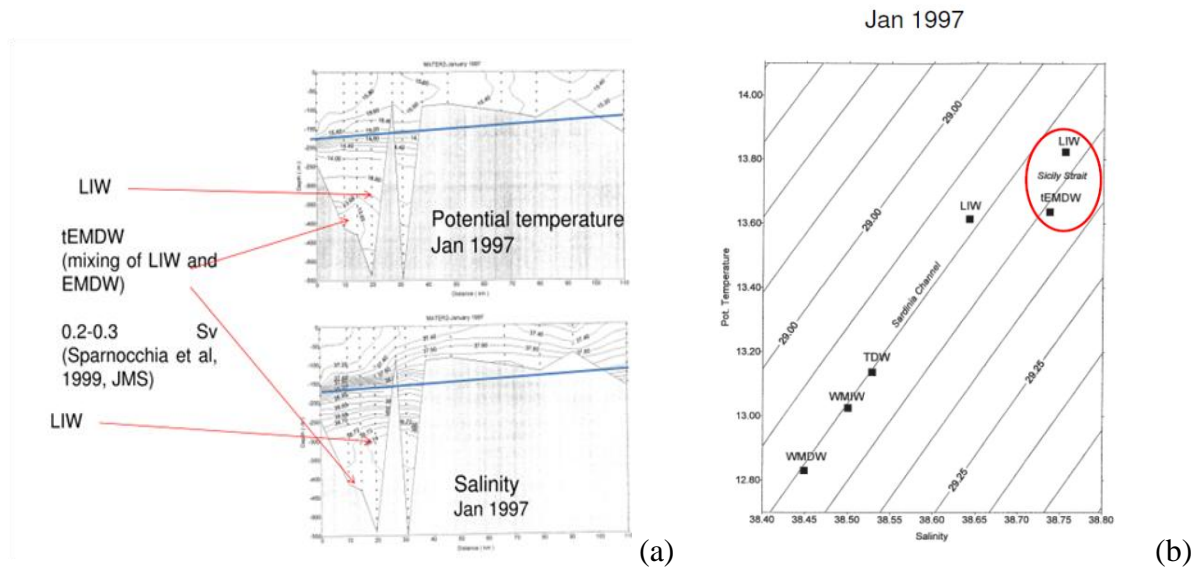


Figure 4.9: Vertical distribution of the potential temperature and salinity in the Sicily Strait in January 1997 (by Astraldi 1999)(a) ; diagramm relative to the intermediate and deep water in the Sicily Channel (by Astraldi 1999 (b))

The Coriolis effect induces the upper layer of the EMDW (indicated in the following as transitional EMDW, or tEMDW) to cross the channel mainly on the Tunisian side [Millot, 1999], while Astraldi *et al.* (2001) pointed out that the significant Bernoulli effect associated with the high LIW velocity further favours the tEMDW outflow to reach the western basin. The inflow of transitional EMDW in the Tyrrhenian sea has an important role in the deep salt budget of this basin. Besides the along-slope current may also have implications on the transport and dispersion of material in the particulate and dissolved phases.

Considering a contribution of tEMDW of about 0.2–0.3 Sv, as reported by Sparnocchia *et al.* (1997) to the western basin, associated to a range of dissolved Si variability of 3.85–7.43 $\mu\text{mol/l}$, according to the vertical profile of Lavezza [Figure 4.10], it is possible to estimate an extra contribution of Si of about $36 \cdot 10^9$ mol/year.

This extra contribution, previously not considered in the mass balances at basin scale, provides a new scenario for dissolved Si in the Mediterranean sea. In particular, the eastern basin now shows an accumulation of silicon and is a net provider of Si for the western basin and for the Atlantic ocean.

The silicon budget obtained for the eastern Mediterranean basin, allows us to formulate a new hypothesis concerning dynamic behavior of silicon. The deficit of silicon could be linked to the slow dissolution of the silicon and to a release from the reservoir through the deep waters [Table 4.11].

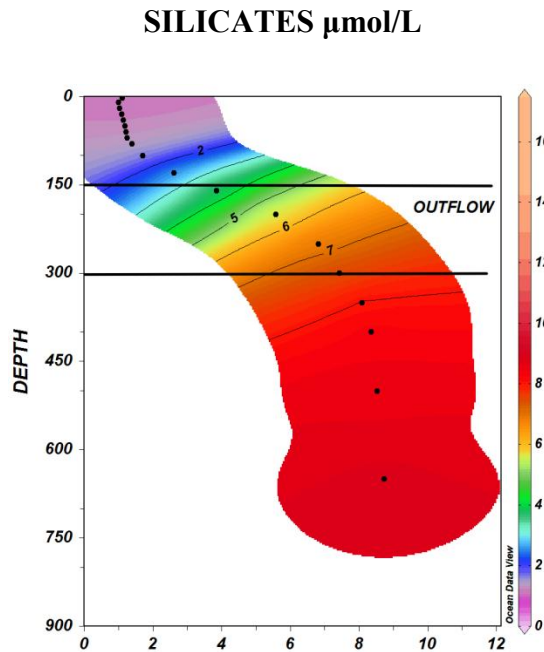


Figure 4.10: Vertical profile (by Lavezza 2010).

EASTERN MEDITERRANEAN

	Si in/out min	Si in/out Max	Si in/out min	Si in/out Max	Si in/out min	Si in/out Max
Atmospheric input* (%)	(1%) 0,24	(1%) 0,31	(5%) 1,18	(5%) 1,55	(10%) 2,35	(10%) 3,10
Rivers input**	21,32	23,54	21,32	23,54	21,32	23,54
Input (Tot)	21,56	23,85	22,5	25,09	23,67	26,64
Inflow***	88,98	88,98	88,98	88,98	88,98	88,98
Outflow***	102	102	102	102	102	102
Transport Strait of Sicily	-13,02	-13,02	-13,02	-13,02	-13,02	-13,02
Deficit	8,54	10,83	9,48	12,07	10,6	13,62

Table 4.11: Silicon Budget in the Eastern Mediterranean (10^9 mol/a)- (*) % of dissolve Silicon contribution from atmospheric and river particulates [This study]; (**) [Ludwig 2009]; (***) Silicon concentrations and Transport (inflow –outflow) at Strait of Sicily [Schroeder et al; 2008] [Sparnocchia et al 1999]

4.4- Particulate chemistry and source areas

Analysis of trace elements chemistry in the seawater particulate provides a good chance to discriminate natural and anthropogenic sources influencing different areas of the Mediterranean basin. Contribution to the seawater chemistry from particulate is clearly evidenced by the relatively high concentration of many trace elements (Cd, Mo, Pb, etc.) recorded in the Mediterranean sea once compared to the open ocean [Heidenburger, 2011]. However, many problems limit our ability to extrapolate from particulate chemistry potential effects on the elements distribution in the dissolved phase: kinetics parameters, thermodynamics at the surface/seawater interface, effects of chemical interactions with particulate in dry or wet deposition, etc. Also, the ensemble of these limiting factors permits only a semi-quantitative investigation of the particulate chemistry as proxy of sources areas.

In this chapter, I will explore the distribution patterns of trace elements in seawater particulate here analysed and compiled with data reported from the five oceanographic cruises SESAME_2008, TRASMED_2007, MEDSUDMED_2008, and BONIFACIO_2010.

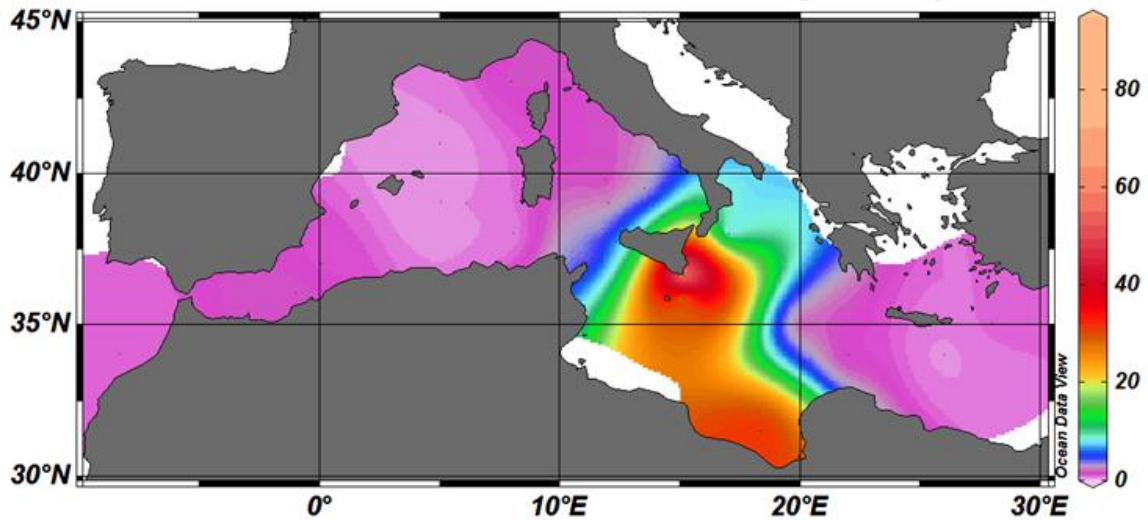
Main aim of this research activity is the possibility to discriminate basin areas affected by input of particulate from specific land regions. Accordingly, a careful examination of distribution maps of chemical in particulate will be provided along with calculation of enrichment factors with respect to i) average shale contents in upper crust continental reported *Taylor and McLennan (1995)* ii) other crustal compositions (Sahara desert, soils from NW Europe, etc.). Interpolation of spatial maps, although possibly affected by errors due to the limited number of studied sampling stations, offers a rudimentary vision of the macroscopic patterns which characterise distribution pattern and features of particulate chemistry in seawater and at the basin scale.

The maps of trace elements concentration in particulate, based on the available 25 sampling stations, were produced for Al, Fe, Cu, Zn, Ni, Pb, Cd, and Ag for the first 100 m of the water column.

The distribution of $[Al]_p$ reported in [Figure 4.12 (a)], clearly evidence an asymmetric surface pattern between eastern and western basin with the higher values measured in the east part. In particular, the SE area appear characterized by the highest Al particulate concentration that testify a crucial impact of the Saharan dust on the distribution modes of this element in the Mediterranean seawater.

$[Al]_p$ (mg/g) [0-100m]

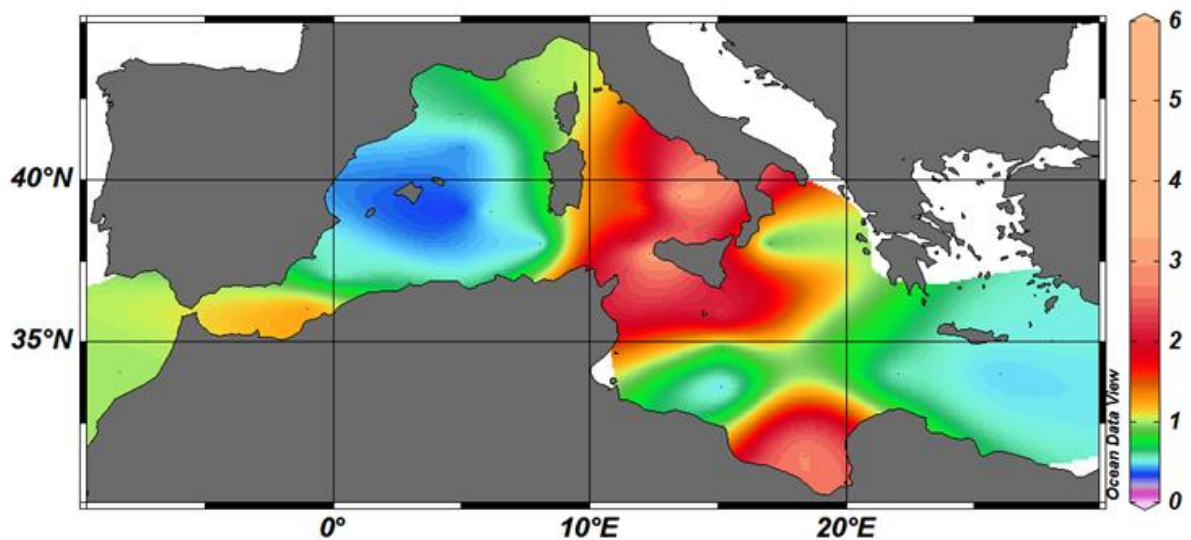
(a)



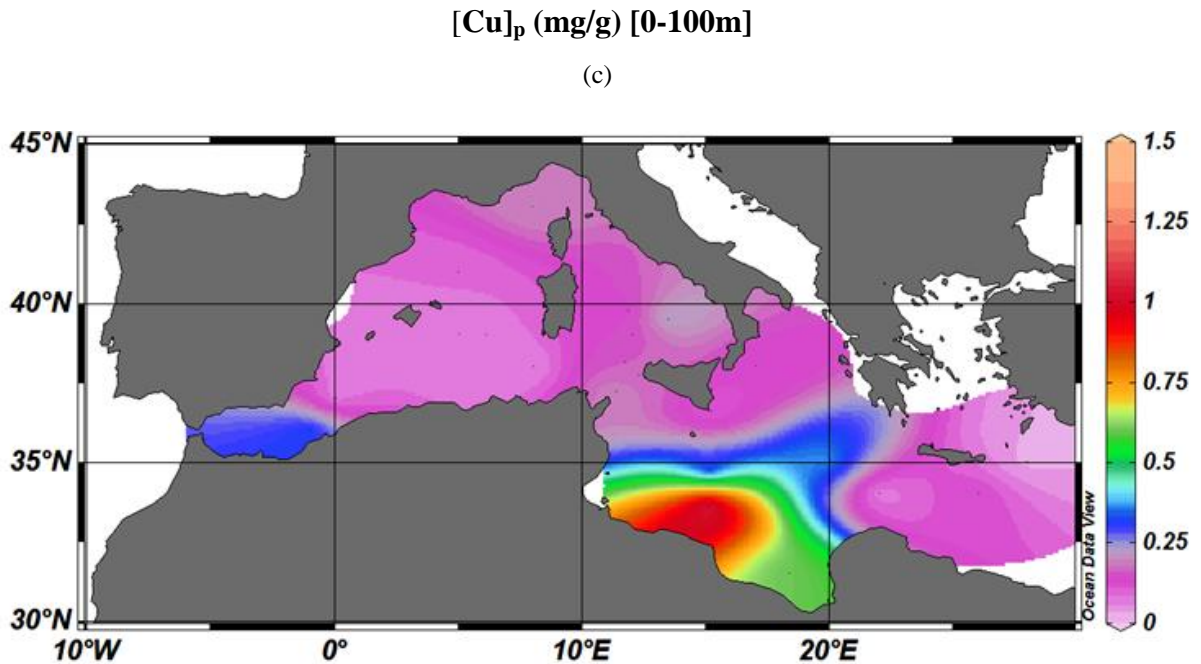
The major source of iron to the open ocean is generally related to the atmospheric inputs. The mean concentrations of iron in the airflows from the north Africa sector [Chen *et al.*, 2008] are significantly higher than the other sectors. Evidence of the impact of atmosphere inputs of particulate in the Mediterranean sea, were clearly reported by Dulac *et al.* (1996) with evident maxima recorded in the surface waters of the Ligurian sea after a number of major storms of Sahara dust. Distribution of $[Fe]_p$ here reported show evident enrichments in the surface waters of the Sicily and Libya coast [Figure 4.12 (b)] definitively confirming a crucial impact of the African desert as primary provider of iron to the Mediterranean seawaters.

 $[Fe]_p$ (mg/g) [0-100m]

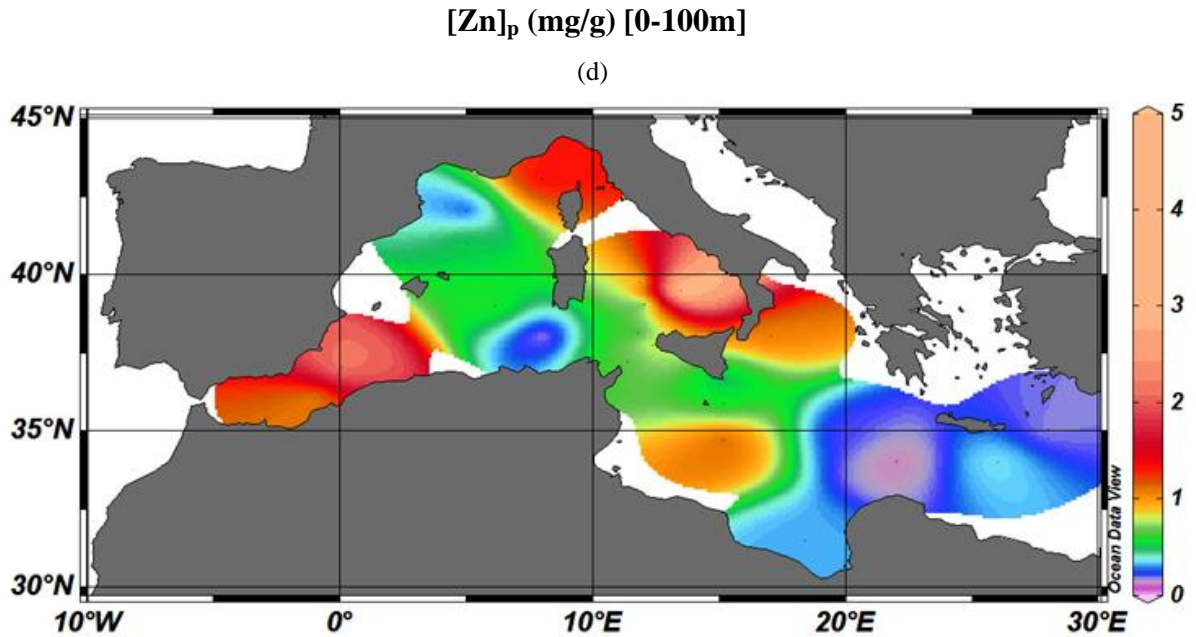
(b)



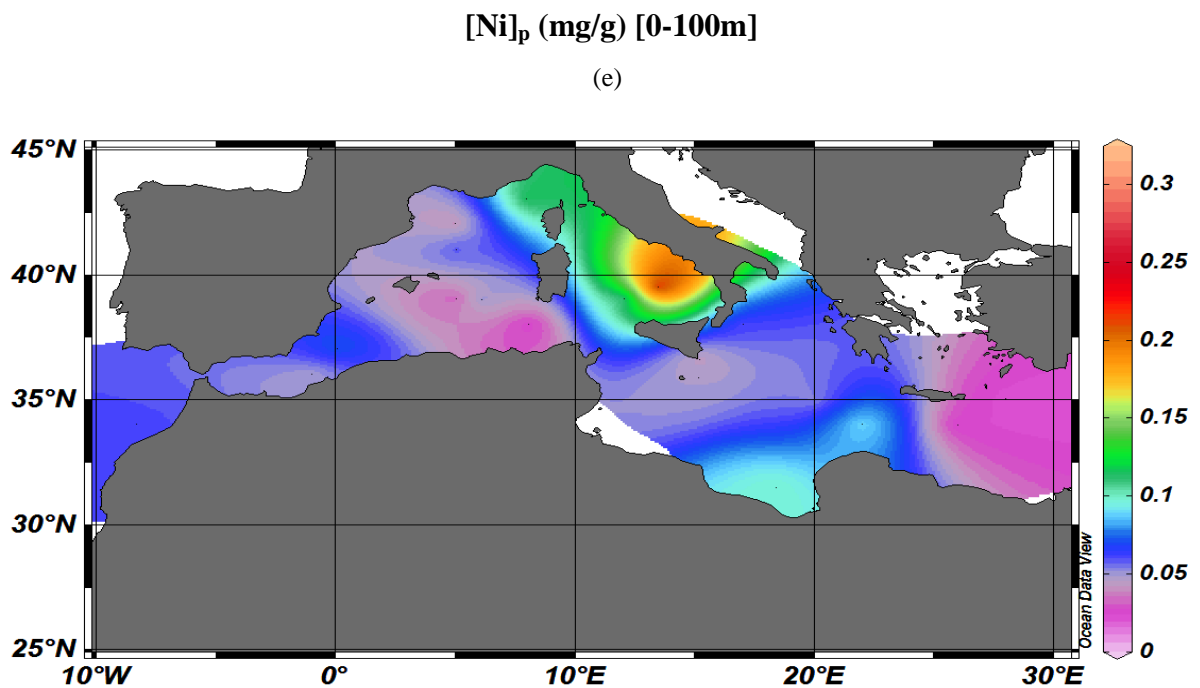
The concentrations of Cu_p [Figure 4.12 (c)] show higher values near the Libya coast suggesting a dominant mineral dust probably to correlate with inputs from the Libya coast which are considered the most important source of anthropic Cu to the Mediterranean seawater [Pirrone *et al.*, 1999].



The concentrations of Zn_p appear higher in the Tyrrhenian basin and in the Liguria sea; this primarily suggests a dominant anthropogenic influence on the distribution modes of this element at basin scale. Actually, the Ligurian Sea is subject to important emission from the large urbanised area between Toulon and Genoa. Zinc is generally associated to emission of waste incinerations [Huang *et al* 2001] particularly by effects of incineration of waste residual muds [Figure 4.12 (d)].

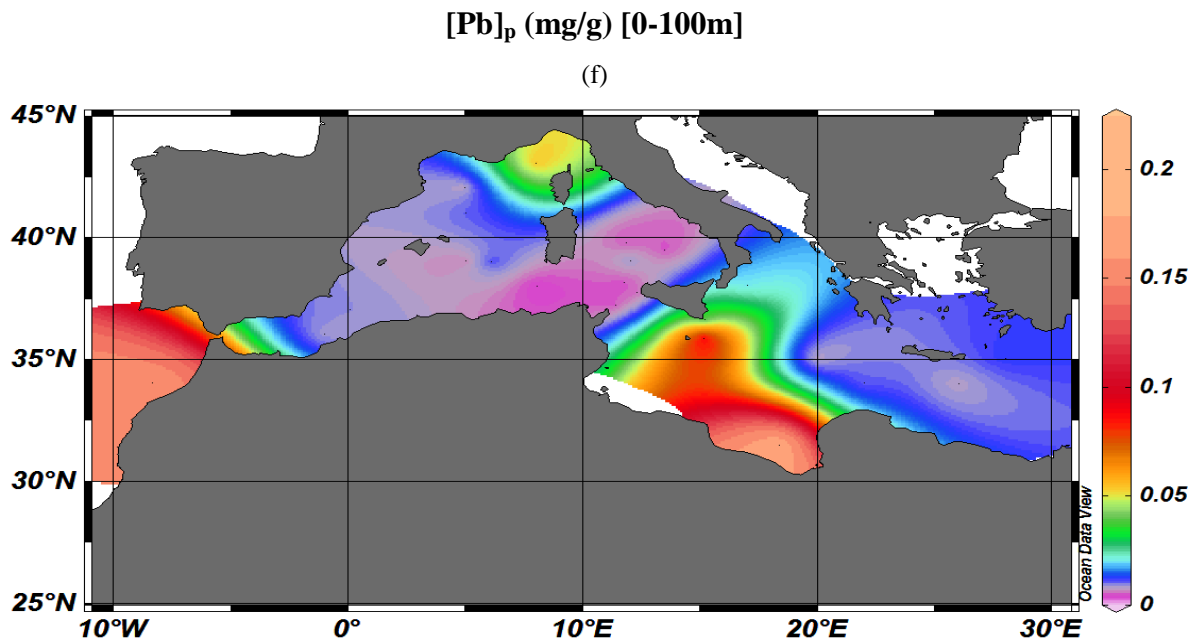


The most enriched surface areas of Nickel particulate are in the Tyrrhenian sea and in the North Western Mediterranean. Once again, it is reasonable to suppose a significant anthropogenic inputs for this element in two key areas of the basin where important industrialized impact occurs (*Barnaba and Gobbi*) [Figure 4.12 (e)].



Distribution maps of Pb_p shows relative high values in three main areas of the Mediterranean sea, the Alboran sea, the Gulf of Lyon and the SE area of the basin. Inputs of Pb_p can be associated to a different typologies of industrial activities. Thus, the SE area of the Mediterranean, could be mostly influenced by activities industrial of Arabian Peninsula, according to Chen et al. (2008) whot show airflows significantly enriched of Pb in the local and

Arabian peninsula. The particulate of Pb in the Gulf of Genoa and in the Alboran sea could be reasonably associated with the possible inputs from Rhone river and Saguaro river [Figure 4.12 (f)].



The marine biogeochemistry of silver is not well known, yet. High [Ag_p] occur in the area of the gulf of Genoa where shipyard activities mainly with important industrial activities (in particular associated to galvanic processes) could deliver important amount of Ag at sea.

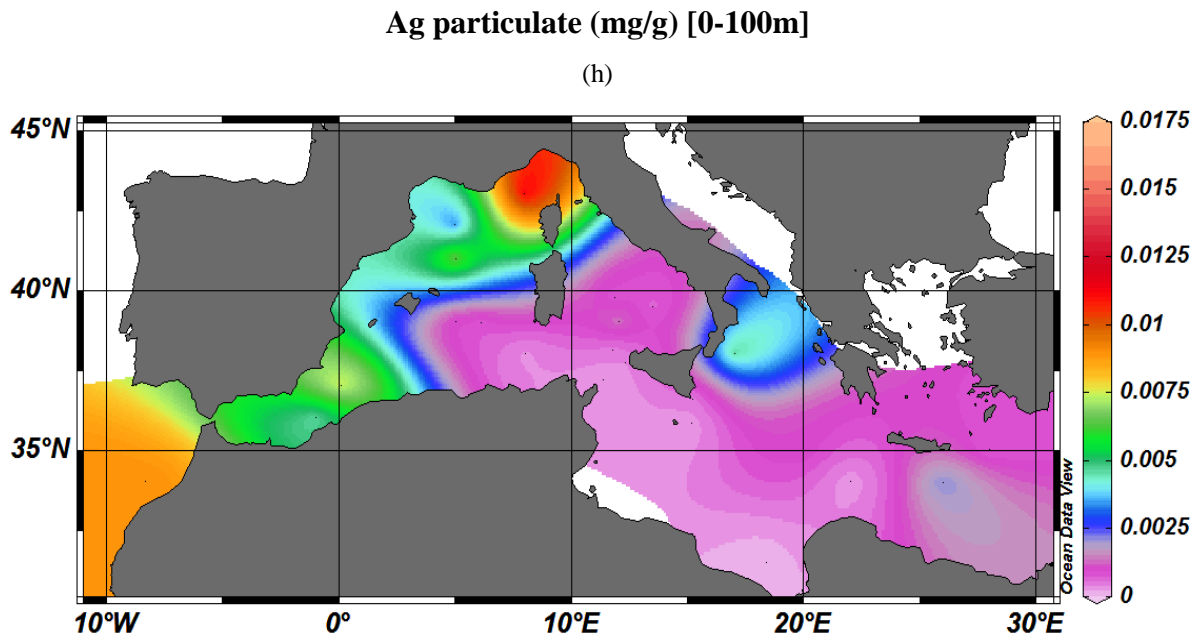


Figure 4.12 : Surface distribution of Al (a), Fe (b), Cu (c) Zn (d) Ni (e) Pb (f) Cd (g) Ag (h) in seawater particulate (mg/g)

4.5- Enrichment factors

Elements concentrations (TM) were normalized to Al in order to standardize metal contents to changes in mineralogical composition and grain-size [Loring,1990, Salomons and Forstner, 1984]. Actually, Al is usually selected as the crustal reference element for normalization, being a major crustal component and minimally affected by diagenesis [Brumsack, 1986]. Subsequently, the obtained TM/Al values were compared to the average shales composition and Sahara dust composition. Thus, if EF_{TM} is greater than 1, the trace metal (TM) is enriched in the samples relatively to the reference values; accordingly, if the $EFTM$ is less than 1, the element is depleted. I calculated the Enrichment factors following the equation:

$$EF = \frac{(Ei/Al)_{\text{Particulate}}}{(Ei/Al)_{\text{reference background}}}$$

where $(Ei/Al)_{\text{part}}$ is the concentration ratio of the single trace elements to Al in the particulate phase of collected seawater samples and $(Ei/Al)_{\text{reference background}}$ is the estimated average element to Al ratio estimated for the upper continental crust (Taylor and McLennan 1985) and selected Saharan source dusts (Tomadin et al. 1984; Eltajeb et al. 2001) [Table 4.13].

Upper crust Taylor & McLennan 1985		Sahara Dust Tomadin et al 1984		Sahara Sand Eltajeb et al 2001	
Cu/Al	3,1	Cu/Al	18	Cu/Al	3,4
Fe/Al	0,44	Fe/Al	0,55	Fe/Al	0,79
Zn/Al	8,8	Zn/Al	-	Zn/Al	26
Ni/Al	2,5	Ni/Al	30	Ni/Al	-
Cd/Al	0,012	Cd/Al	-	Cd/Al	-
Pb/Al	2,5	Pb/Al	-	Pb/Al	3,4
Ag/Al	6,21	Ag/Al	-	Ag/Al	-

Table 4.13: Element to Al ratios in the Upper Crust and Sahara Dust (Taylor & McLennan 1985; Tomadin 1984; Eltajeb 2001)

Calculated box whiskers plots allow to simultaneously synthesize variations of EF values estimated against the chemistry of the two source areas for the particulate sampled in seawater.

The **Figures 4.14** show the calculated EF values for the different elements. Specifically, EFs calculated for Fe show a clear imprint of Saharan dust on the distribution patterns of this element in most of the studied area of the Mediterranean sea.

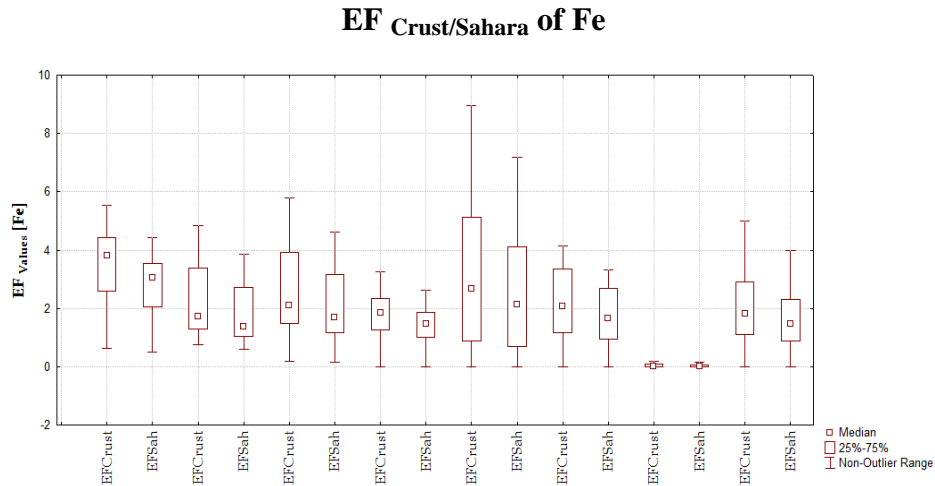


Figure 4.14: Box plots of EF Fe_{Crust} and EF Fe_{Sahara} in the basins of the Mediterranean sea.

EFs calculated for Cu, Ni, Zn and Pb [Figures 4.15-4.16-4.17-4.18] show very low values that reflect a significant effect of dissolution of the different trace elements in seawater with respect to the more conservative Al. This definitively erases a primary signature of the trace elements in the particulate and makes it difficult to explore potential source areas for the particulate on the basis of these metals.

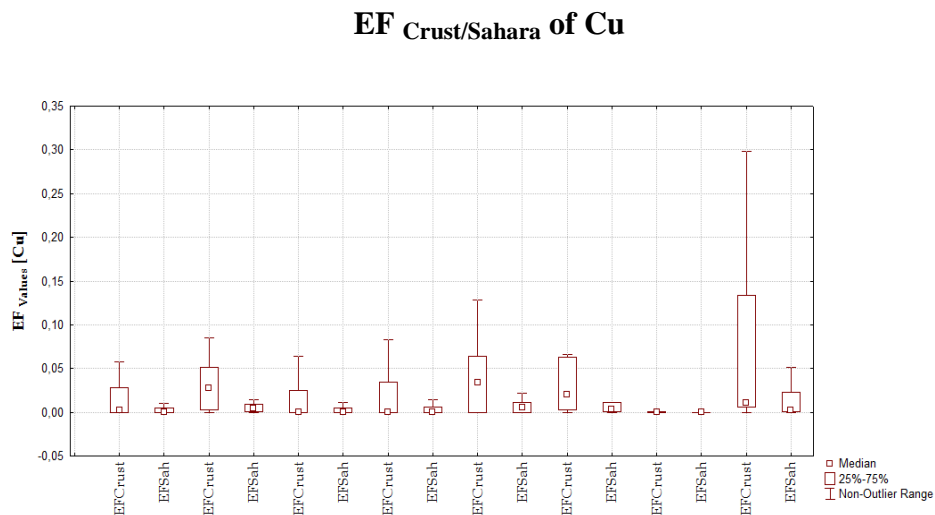


Figure 4.15: Box plots of EF Cu_{Crust} and EF Cu_{Sahara} in the basins of the Mediterranean sea.

EF Crust/Sahara of Zn

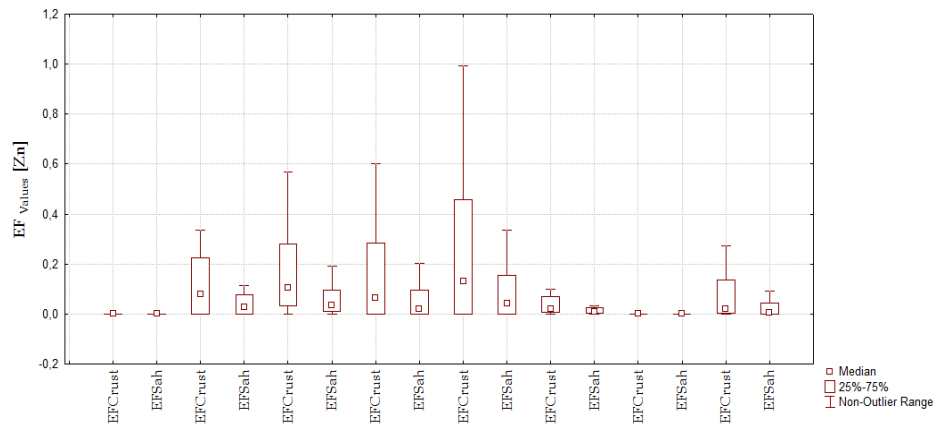


Figure 4.16: Box plots of EF Zn_{Crust} and EF Zn_{Sahara} in the basins of the Mediterranean sea.

EF Crust/Sahara of Ni

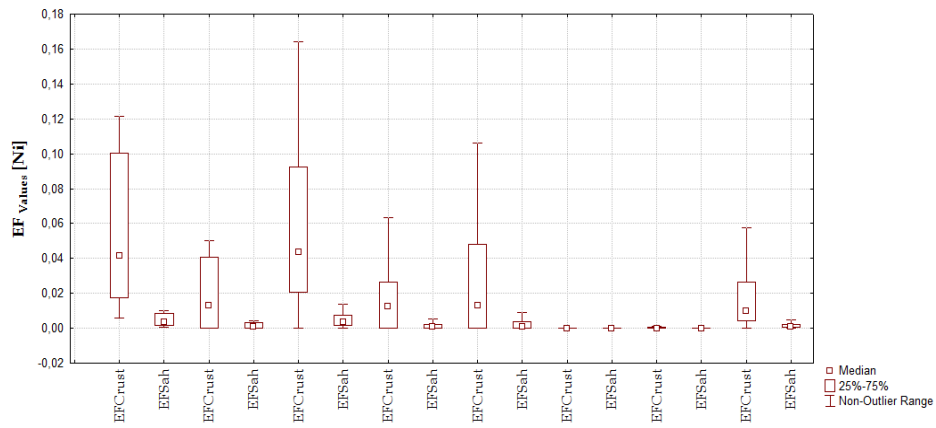


Figure 4.17: Box plots of EF Ni_{Crust} and EF Ni_{Sahara} in the basins of the Mediterranean sea.

EF Crust/Sahara of Pb

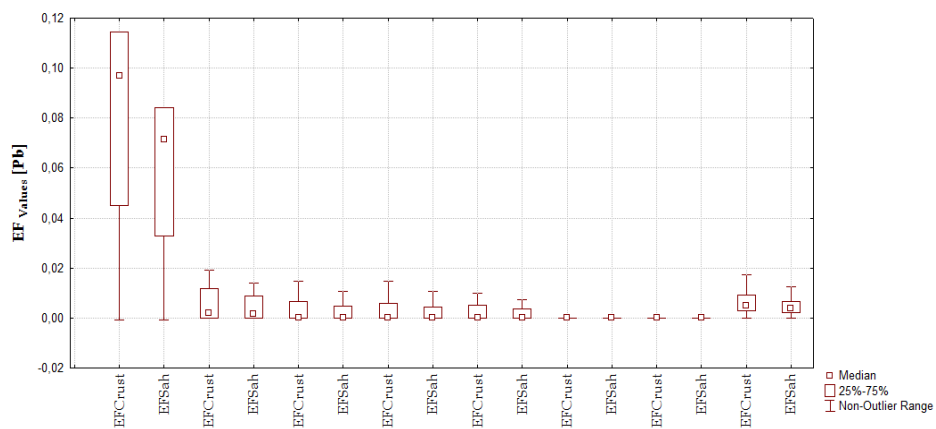


Figure 4.18: Box plots of EF Pb_{Crust} and EF Pb_{Sahara} in the basins of the Mediterranean sea.

Chapter 5

CONCLUSIONS

This research work provided an unprecedented compiled dataset of particulate chemistry in seawater of the Mediterranean sea. A number of exploratory strategies were used to investigate the potential role played from this specific component in seawater in terms of silicon budget to basin scale. Actually very few information report direct measurements of potential impact of silicon dissolved from particulate as potential sources of this element in seawater. Also, a deep exploration of the potential sources of particulate collected in seawater has been carried out by means analysis of spatial maps, enrichment factors calculated with respect to different reference backgrounds.

The most important results achieved by this research job can be summarized in the following points:

- ✓ The role of particulate in releasing dissolved silicon in seawater appears extremely limited with a range of variability estimated in a range of 1-10% of the entire budget. This estimates shows crucial uncertainties related to a very reduced information about kinetics of dissolution of different minerals (present in the particulate) in seawater, trajectories and fluxes of atmospheric dust on the basin. However, this research presents a first order information and dataset useful for future scientific programs focused to better constrain the role of atmospheric dust at Mediterranean scale, in an area strongly affected by inputs from the near Saharan desert.
- ✓ Incorporation of dissolved Si from deep water masses, specifically the transitional Eastern Mediterranean Deep Water, previously not considered in the available basin scale mass balance, appears of key importance. Particularly, Si transport at yearly scale of the extra 0.2-0.3Sv of tEMDW to the western basin definitively re-equilibrate the budget of Si at basin scale and evidence the importance of the large inventory of Si present in the

deep and bottom waters of the eastern Mediterranean sea to balance fluxes and mass of this element at basin scale.

- ✓ Exploration of trace elements chemistry of particulate collected clearly highlighted the role played by the Saharan on dust transport and deposition in most of the basin. Also, influxes of atmospheric inputs from highly anthropised areas of the western basin are clearly reflected in signatures of Zn , Cd, Pb and Ag measured in particulate collected in the Mediterranean seawater.

References

- Adjou M., Treguer P., Dumousseaud C., Corvaisier R, Brzezinski, Mark A. David M. Nelson (2011). Particulate silica and Si recycling in the surface waters of the Eastern Equatorial Pacific. *Deep-Sea Research II* 58, 449-461.
- Aldeanueva F., Criado, F., Javier Soto-Navarro and Jes'us Garcia Lafuente (2010). Seasonal and interannual variability of surface heat and freshwater fluxes in the Mediterranean Sea: budgets and exchange through the Strait of Gibraltar. *International Journal of Climatology*.
- Alpert P., and B. Ziv, (1989). The Sharav cyclone, observations and some theoretical considerations, *J. Geophys. Res.*, 94, 18495-18514.
- Artale V., Provenzale A., Santoleri R (1989). Analysis of internal temperature oscillations of tidal period on the Sicilian continental shelf; *Continental Shelf Res.*, 9, 867-888.
- Astraldi M., Gasparini, G.P., Sparnocchia, S., Moretti, M., Sansone, E., (1996). The characteristics of the water masses and the water transport in the Sicily Strait at long time scales. In: (ed.), Bulletin del l'Institut Océanographique, Monaco, no spécial 17, CIESM Science Series no 2, 95-115.
- Astraldi M., Balopoulos E., Candela J., Font J., Gacic M., Gasparini G. P., Manca B., Theocharis A., Tintore J., (1999). The role of straits and channels in understanding the characteristics of Mediterranean circulation. *Prog. in Oceanogr.* 44, 65-108.
- Astraldi M., Gasparini G.P., Vetrano A., S. Vignudelli (2002). Hydrographic characteristics and interannual variability of water masses in the central Mediterranean: a sensitivity test for long-term changes in the Mediterranean Sea. *Deep-Sea Research I* 49 ,661–680.
- Astraldi M., Gasparini G.P. , and Gervasio L.(2001). Dense Water Dynamics along the Strait of Sicily (Mediterranean Sea)
- Balboni V., P. Giordani, S. Miserocchi, and G. Montanari, (1999). Hydrological and biogeochemical properties of northwestern adriatic coastal waters south of Po delta. In: Hopkins TS, Artegiani A, Cauwet G, Degobbi D, Malej A (ed) *The Adriatic Sea – Proceedings of the Workshop 'Physical and Biogeochemical Processes in the Adriatic Sea', Ecosystem Research Report No. 32, Portonovo (Ancona), Italy 23 to 27 April 1996, Office for Official Publications of the European Community, Luxembourg*, pp 39–57.
- Baker A.R., Jickells TD, Witt M, Linge KL. (2006). Trends in the solubility of iron, aluminium, manganese and phosphorus in aerosol collected over the Atlantic Ocean. *Geophys. Res. Lett.* 33:L07805
- Baker A.R., Croot P.L. (2010). Atmospheric and marine controls on aerosol iron solubility in seawater. *Marine Chemistry* 120 4–13.
- Barnaba F. and Gobbi G.P. (2004). Aerosol seasonal variability over the Mediterranean region and relative impact of maritime, continental and Saharan dust particles over the basin from MODIS data in the year 2001. *Atmos. Chem. Phys.*, 4, 2367-2391.
- Benoit et al., (1994). Partitioning of Cu, Pb, Ag, Zn, Fe, Al and Mn between filter retained particles, colloids and solution in six Texas estuaries. *Mar. Chem.* 45, 307–336.
- Bergametti G., A. L. Dutot, P. Buat-Me'nard, R. Losno, and E. Remoudaki (1989a), Seasonal variability of the elemental composition of atmospheric aerosol particles over the northwestern Mediterranean, *Tellus B.*, 41B, 353– 361.
- Bethoux J.P.,(1980). Mean water fluxes across sections in the Mediterranean Sea, evaluated on the basis of water and salt budget and of observed salinities. *Oceanol. Acta*, 3-79-88.
- Bethoux J.P, P. Morin, C. Chaumery, O. Connan, B. Gentili ,D. Ruiz-Pino (1998). Nutrients in the Mediterranean Sea, mass balance and statistical analysis of concentrations with respect to environmental change. *Mar Chem.* 63,155-169.

- Béthoux et al., (1990) Trace metal pollution in the Mediterranean Sea, *Oceanologica Acta* **13** (4) (1990). pp. 481–488.
- Béthoux J.P. and Gentili, B., (1996). The Mediterranean Sea, coastal and deep-sea signatures of climatic and environmental changes. *J. Mar. Syst.* **7**, pp. 383–394.
- Béthoux J.P. and Gentili (1999). Functioning of the Mediterranean Sea: past and present changes related to freshwater input and climate changes, *J. Mar. Syst.* **20** pp. 33–47.
- Béthoux J.P. Morin P., Diana P. Ruiz-Pino (2002). Temporal trends in nutrient ratios: chemical evidence of Mediterranean ecosystem changes driven by human activity. *Deep-Sea Research II* **49** 2007–2016.
- Blanco A. De Tomasi F., E. Filippo, D. Manno, M. R. Perrone, A. Serra, A. M. Tafuro, and A. Tepore (2003). Characterization of African dust over southern Italy. *Atmos Chem. Phys.*, **3**, 2147–2159.
- Bruland and Loan., (2004). - Controls of trace metals in seawater Chapter 2 in *The Oceans and Marine Geochemistry*, Vol. 6 (Ed. Harry Elderfield) in *Treatise on Geochemistry* (Eds. H.D. Holland and K.K. Turekian).
- Censi et al., (2006). Heavy metals in coastal water systems. A case study from the north western Gulf of Thailand. *Chemosphere* **64** 1167–1176.
- Chen Y., Street J., Golan D, Post A., and. Paytan A (2007). Estimate of atmospheric dry deposition and associated input of nutrients to the Gulf of Aqaba seawater, *J. Geophys. Res.*, **112**, D04309.
- Chen Y., Adina P., Chase Z, Measures Christopher, Beck Aaron J., Sanudo-Wilhelmy Sergio A, and. Post Anton F (2008). Sources and fluxes of atmospheric trace elements to the Gulf of Aqaba, Red Sea. *Journal of Geophysical Research*, vol. **113**, D05306..
- Chester et al., (1989). Atmospheric inputs of trace metals, trace organics and nutrients to the western Mediterranean—The EROS 2000 Programme. In: J.M. Martin and H. Barth, Editors, *Water Pollut. Repts* Vol. 13, Commission of the European Communities, pp. 357–367.
- Chester et al., (1993). Factors controlling the solubilities of trace metals from non-remote aerosols deposited to the sea surface by the dry deposition mode. *Mar Chem* **42**:107.
- Chester, R., Nimmo, M., Corcoran, P.A., (1997). Rain water-aero- sol trace metal relationships at Cap Ferrat: a coastal site in the Western Mediterranean. *Mar. Chem.* **58**, 212–293.
- Conley D.J., Schelske, C.L., Stoermer, E.F., (1993). Modification of the biogeochemical cycle of silica with eutrophication. *Marine Ecology Progress Series* **101**, 179-192.
- Conley D.J., (1997). Riverine contribution of biogenic silica to the oceanic silica budget. *Limnol Oceanogr* **42**, 774-777.
- Conley D.J. and Schelske, C. L. (2001). Biogenic silica, in: *Tracking Environmental Change Using Lake Sediments: Biological Methods and Indicators*, edited by: Smol, J. P., Birks, H. J. B., and Last, W. M., *Kluwer Academic Press*, 281–293.
- Correns C.W. (1949) *Einführung in die Mineralogie* : Springer, Berlin, 414 pp.
- Cruzado A., Velásquez, Z., Pérez, M. C., Bahamón, N., Grimaldo, N. S., and Ridolfi, F.: (2002). Nutrient fluxes from the Ebro River and subsequent across-shelf dispersion, *Cont. Shelf Res.*, **22**, 349–360.
- Degobbi D., and M. Gilmartin, (1990). Nitrogen, phosphorus, and biogenic silicon budgets for the northern Adriatic Sea, *Oceanol. Acta*, **13**, 31–45,.
- Desboeufs K.V., Sofikitis, A., Losno, R., Colin, J.L., Ausset, P., 2005. Dissolution and solubility of trace metals from natural and anthropogenic aerosol particulate matter. *Chemosphere* **58**, 195–203.
- Duce R C. , Tindale N W. (1991). The atmospheric transport of iron and its deposition In the ocean. *Limnology and Oceanography*, **36**, 1715-1726.

- Dugdale R.C., (1976). Nutrient cycles, in: *The ecology of the sea*, edited by: Cushing, D. H., Blackwell.
- Dugdale R.C., Wilkerson, F.P., Minas, H.J., (1995). The role of a silicate pump in driving new production. *Deep-Sea Res.* 42, 697–719.
- Dulac F., Buat M nard P., Ezat U, (1987) Atmospheric input of trace metals to the western Mediterranean sea: 1. Factors controlling the variability of atmospheric concentration. *Journal of geophysical Research*, 92, 8437-8453
- Dulac F., Moulin, C., Lambert, C. E., Guillard, F., Poitou, J., Guelle, W., Que tel, C., Schneider, X., & Ezat, U. (1996). Quantitative remote sensing of African dust transport to the Mediterranean. In: Guerzoni, S., Chester, R. (Eds.), *The Impact of African Dust Across the Mediterranean*. Kluwer Academic Publishers, Norwell, MA, pp. 25}49.
- D'urr H. H., Meybeck, M., Hartmann, J., Laruelle, G. G., and Roubeix, V. (2011). Global spatial distribution of natural riverine silica inputs to the coastal zone, *Biogeosciences*, 8, 597–620.
- Eshel G., and B. F. Farrel, (2000). Mechanisms of Eastern Mediterranean rainfall variability. *J. Atmos. Sci.*, 57, 3219–3232.
- Garnier J., Billen, G., Coste, M., (1995). Seasonal succession of diatoms and chlorophyceae in the drainage network of the River Seine: observations and modeling. *Limnology and Oceanography* 40, 750-765
- Garett C. (1996): The role of the Strait of Gibraltar in the evolution of the Mediterranean water properties and circulation. In F. Briand *Dynamics of Mediterranean straits and channels, CIESM Science series.*
- Gehlen M., L. Beck, G. Calas, A.-M. Flank, J. A. van Bennekom, and J. E. E. van Beusekom, (2002). Unraveling the atomic structure of biogenic silica: Evidence of the structural association of Al and Si in diatom frustules, *Geochim. Cosmochim. Acta*, 66, 1601– 1609.
- Gehlen et al; (2003). Coupled Al-Si geochemistry in an ocean general circulation model: A tool for the validation of oceanic dust deposition fields? *GLOBAL BIOGEOCHEMICAL CYCLES*, VOL. 17, NO. 1, 1028.
- Gilman C., Garret C (1994). Heat flux parameterizations for the Mediterranean Sea: the role of atmospheric aerosols and constraints from the water budget. *J Geophys Res* 99:5119–5134.
- Grim R. E., Dietz, R. S. and Bradley, W. F. (1949). Clay mineral composition of some sediments from the Pacific Ocean off the California coast and the Gulf of California: *Bull. Geol. Soc. Amer.*, v. 60, pp. 1785-1808.
- Grim R. E., and Johns, W. D. (1954) .Clay mineral investigation of sediments in the northern Gulf of Mexico : in *Clays and Clay Minerals*, Natl. Acad. Sci.--Natl. Res. Council, pub. 327, pp. 81-103
- Gullu G.H., Olmez, I., Aygun, S., Tuncel, G., (1998). Atmospheric trace element concentration over the eastern Mediterranean Sea: factors affecting temporal variability. *Journal of Geo-physical Research* 103, 21943 21954.
- Guerzoni, & R. Chester, (1996). *The impact of desert dust across the Mediterranean* (pp. 25–49). Kluwer Academic Publishers.
- Guerzoni, Landuzzi, Lenaz, Quarantotto, Rampazzo, Molinaroli et al., (1993). Fluxes of soluble and insoluble metals and nutrients from the atmosphere to the Central Mediterranean Sea. *Water Poll. Res. Rep.* 30 , pp. 438–493.
- Guerzoni, S., Molinaroli, E. and Chester, R., (1997). Saharan dust inputs to the western Mediterranean Sea: depositional patterns, geochemistry and sedimentological implications. *Deep-Sea Research I* 44, pp. 631–654.
- Guerzoni, Molinaroli E., Rossigni (1999). The role of atmospheric deposition in the biogeochemistry of the Mediterranean Sea. *Progress in Oceanography*, vol. 44, 147¹90.

- Guieu C., Martin JM, Thomas AJ, Elbaz-Poulichet F (1991). Atmospheric versus river inputs of metals to the Gulf of Lions. Total concentrations, partitioning and fluxes. *Mar Pollut Bull* 22:176.
- Guieu C., (1996). Atmospheric input of dissolved and particulate metals to the north western Mediterranean. *Deep-Sea Research II*, 44, 655–674.
- Han Q., Moore, J.K., Zender, C., Measures, C., Hydes, D., (2008). Constraining oceanic dust deposition using surface ocean dissolved Al. *Global Biogeochemical Cycles*, Volume22, Issue 2.
- Heimbürger Lars-Eric, Christophe Migon, Daniel Cossa (2011). Impact of atmospheric deposition of anthropogenic and natural trace metals on Northwestern Mediterranean surface waters: A box model assessment. *Environmental Pollution* Volume 159, Issue 6, Pages 1629–1634.
- Herman J. R., P. K. Bhartia, O. Torres, C. Hsu, C. Seftor, and E. Celarier. (1997). Global distribution of UV-absorbing aerosols from Nimbus 7/TOMS data. *Journal of Geophysical Research* 102:16,911–16,922.
- Herut B., and M. Krom, (1996). Atmospheric input of nutrients and dust to the SE Mediterranean, in *The Impact of Desert Dust Across the Mediterranean*, edited by S. Guerzoni and R. Chester, pp. 349 – 358, Kluwer Acad., Norwell, Mass.
- Hydes D. J., De Lange G. T., and De Baar H. J. W. (1988) Dissolved aluminium in the Mediterranean. *Geochim. Cosmochim. Acta* 52, 2107–2114.
- Humborg C, Conley DJ, Rahm L, Wulff F, Cociasu A, Ittekkot V. (2000). Silicon retention in river basins: far-reaching effects on biogeochemistry and aquatic food webs in coastal marine environments. *Ambio* 29:45–50.
- Jickells T. D. (1995), Atmospheric inputs of metals and nutrients to the oceans: Their magnitude and effects, *Mar. Chem.*, 48, 199 – 214.
- Israelevich, P. L., Z. Levin, J. H. Joseph, and E. Ganor (2002), Desert aerosol transport in the Mediterranean region as inferred from the TOMS aerosol index, *J. Geophys. Res.*, Vol 107(D21), 4572.
- Kallos G., Astitha M, Katsafados P, and Spyrou C (2006), Long-Range Transport of Anthropogenically and Naturally Produced Particulate Matter in the Mediterranean and North Atlantic: Current State of Knowledge. *Journal of Applied Meteorology and Climatology*, Vol 64.
- Kamatani A., (1982) Dissolution rates of silica from diatoms decomposing at various temperatures. *Mar. Biol.* 68, 91–96.
- Klein B., W. Roether, B.B. Manca, D. Bregant, V. Beitzel, V. Kovacevic and A. Luchetta. (1999). The large deep water transient in the Eastern Mediterranean, *Deep-Sea Res. I* 46 (1999), pp. 371–414.
- Kocak M., Nimmo, M., Kubilay, N., and Herut, B. (2004). Spatial and temporal aerosol trace metal concentrations in the Levantine Basin of the Eastern Mediterranean. *Atmospheric Environment*, 38, 2133-2144.
- Krauskopf K. B. (1956). Dissolution and precipitation of silica at low temperatures : *Geochemist. Cosmochim. Acta*, v. 10, pp. 1-26.
- Krom M.D., Herut, B., Mantoura, F., (2004). Nutrient budget for the Eastern Mediterranean, implications for P limitation. *Limnol. Oceanogr.* 49, 1582–1592.
- Kubilay N., and C.Saydam (1995) Trace elements in atmospheric particulates over the Eastern Mediterranean; Concentrations, sources, and temporal variability. *Atmospheric Environment.*, 29: 2289-2300.
- Kubilay N., (1996). The Composition of Atmospheric Aerosol Over The Eastern Mediterranean; The coupling of geochemical and meteorological parameters. *Ph.D. Dissertation*, pp.219, Institute of Marine Sciences, METU, Erdemli-Turkey.

- Lascaratos A., Roether, W., Nittis, K., Klein, B., (1999). Recent changes in deep water formation and spreading in the eastern Mediterranean Sea: *a review*. *Prog. Oceanogr.* 44, 5–36.
- Lavezza R.(2010). Dinamica dei nutrienti nel Mediterraneo con particolare riguardo a quella del Silicio. Tesi di laurea.
- Lawson D. S., Hurd D. C., and Pankratz H. S. (1978) Silica dissolution rates of decomposing phytoplankton assemblages at various temperatures. *Am. J. Sci.* 278, 1373–1393.
- Lewin J. C. , (1961) The dissolution of silica from diatom walls. *Geochim. Cosmochim. Acta* 21, 182-198.
- Lionello P., Malanotte-Rizzoli, P. and R. Boscolo (2006). Mediterranean Climate Variability, *Elsevier Science*, pp 438.
- Lolis C.J., A Bartzokas, and B.D. Katsoulis (2002), Spatial and Temporal 850 hPa air temperature and sea-surface temperature covariances in the Mediterranean region and their connection to atmospheric circulation, *International Journal of Climatology*, Vol.22, 663-676.
- Ludwig W., Dumont, E., Meybeck, M., Heussner, S., (2009). River discharges of water and nutrients to the Mediterranean and Black Sea: major drivers for ecosystem changes during past and future decades? *Progress in Oceanography* 80, 199–217.
- Maheras P., E. Xoplaki, T. Davies, J. V. Vede, M. Bariendos, and M. Alcoforado, (1999). Warm and cold monthly anomalies across the Mediterranean basin and their relationship with circulation; 1860–1990. *Int. J. Climatol.*, 19, 1697–1715.
- Malanotte-Rizzoli et al., (1997). A synthesis of the Ionian Sea hydrography, circulation and water mass pathways during POEM-Phase I. *Prog. Oceanog.* Vol. 39, pp. 153-204.
- Manzella G.M.R., Gasparini, G. P., and Astraldi M., (1988). Water Exchange between the eastern and western Mediterranean through the Strait of Sicily, *Deep-Sea Res. Pt. I*, 35(6), 1021–1035.
- Markaki Z., K. Oikonomu, M. Kocak, G. Kouvarakis, A. Chaniotaki, N. Kubilay, and N. Mihalopoulos (2003), Atmospheric deposition of inorganic phosphorus in the Levantine Basin, eastern Mediterranean: Spatial and temporal variability and its role in seawater productivity, *Limnol. Oceanogr.*, 48(4), 1557– 1568.
- Markaki Z., Loÿe-Pilot M.D., Violaki K., Benyahya L., Mihalopoulos N. (2010). Variability of atmospheric deposition of dissolved nitrogen and phosphorus in the Mediterranean and possible link to the anomalous seawater N/P ratio. *Marine Chemistry*, MARCHE-02648; No of Pages 8.
- Martin J.M., Elbaz-Poulichet, F., Guieu, C., Looye-Pilot, M.D., Han, G., (1989). River versus atmospheric input of material to the Mediterranean Sea: an overview. *Marine Chemistry* 28, 159–182.
- Measures C.I., (1999). The role of entrained sediments and sea ice in the distribution of aluminum and iron in the surface waters of the Arctic Ocean. *Marine Chemistry*, 68, 59-70.
- Meybeck M.-H., (1994). Studies on geophysics – material fluxes on the surface of the Earth – origin and variable composition of present day riverborne material. National Academy Press, *Washington Press* 4, 61-73.
- Meybeck M., D'ur H., Roussennac, S., and Ludwig W., (2007). Regional seas and their interception of riverine fluxes to oceans, *Mar. Chem.*, 106, 301–325.
- Migon C., Morelli, J., Nicolas, E., & Copin-Montegut, G. (1991). Evaluation of total atmospheric deposition of Pb, Cd, Cu and Zn to the Ligurian Sea. *The Science of the Total Environment*, 105, 135–148.
- Migon C., Journel, B., & Nicolas, E. (1997). Measurement of trace metal wet, dry and total atmospheric fluxes over the Ligurian Sea. *Atmospheric Environment*, 31, 889–896.
- Migon C., Nicolas, E., (1998). The trace metal recycling component in the north-western Mediterranean. *Marine Pollution Bulletin* 36 (4), 273–277.

- Millot C., (1995). PRIMO-0 and related experiments. *Oceanol. Acta* 18 (2), 137– 138.
- Millot C., (1999). Circulation in the Western Mediterranean Sea, *J. Mar. Syst.*, 20(1–4), 423–442,
- Moutin T., Raimbault, P., Golterman, H.L., Coste, B., (1998). The input of nutrients by the Rhone River into the Mediterranean Sea: recent observations and comparison with earlier data. *Hydrobiologia* 373/374, 237–246.
- Mukherjee J. N., Chatterjee, B. and Ray, A. (1948) Liberation of I-I+, Al+a, and Fo +3 ions from pure clay minerals on repeated salt treatment and desaturations : *J. Colloid Sc.*, Vol.3, pp. 437-446.
- Nixon S.W., (2003). Replacing the Nile: Are Anthropogenic Nutrients Providing the Fertility Once Brought to the Mediterranean by a Great River? *Ambio* 32, 30–39.
- Perez C., Nickovic S., , Baldasano J., M., Sicard M., , Rocadenbosch F., and Cachorro V.E: (2006a). A long Saharan dust event over the western Mediterranean: Lidar, Sun photometer observations, and regional dust modeling, *J. Geophys. Res.-Atmos.*, 111, D15214, 25.
- Perez C. , Dust Modelling and Forecasting in the Barcelona Supercomputing Center: Activities and Developments. *Earth and Environmental Science* Vol.7.
- Pinardi N., Masetti E. (2000). Variability of the large scale general circulation of the Mediterranean Sea from observations and modelling: a review *Palaeogeography, Palaeoclimatology, Palaeoecology* 158, p153-173.
- Pirrone N., Ferrara R, Hedgecock IM, Kallos G, Mamane Y, Munth J, Pacyna JM, Pytharoulis I, Sprovieri F, Voudouri A, Wangberg I. (2003). Dynamic processes of mercury over the Mediterranean region: results from the Mediterranean Atmospheric Mercury Cycle System (MAMCS) project. *Atmos Environ*;37:S21-S39.
- Pollak M. I., (1951). The sources of deep water of the Eastern Mediterranean Sea. *Journal of Marine Research*, 10, 128–152.
- Prospero J.M.,(1996). Saharan dust transport over the North Atlantic Ocean and Mediterranean: An overview, in *The Impact of Desert Dust Across the Mediterranean*, edited by Guerzoni and R. Chester, Kluwer, Dordrecht.
- Prospero J.M., Lamb, P.J., (2003). African droughts and dust transport to the Caribbean: climate change implications. *Science* 302, 1024–1027.
- Queroll et al., (2009). Data files directly obtained from Xavier Querol (personal Communication, Ragueneau O. et al., (2005). A new method for the measurement of biogenic silica in suspended matter of coastal waters: using Si:Al ratios to correct for the mineral interference. *In continental Shelf Research* 25, p 697-710.
- Ribera M. d'Alcala`, G. Civitarese, F. Conversano and R. Lavezza, (2003). Nutrient ratios and fluxes hint at overlooked processes in the Mediterranean Sea. *Journal of Geophysical Research* , Vol. 108, NO C9, 8106.
- Robinson A.R., Leslie W. G., Theocharis A., Lascaratos A. (2001). Mediterranean Sea Circulation. In: *Ocean Currents Indira Ed. Academic Press*. pp. 1'9.
- Rodwell M.J ., and B.J. Hoskins (1996). Monsoons and the dynamics of desert, *The Quarterly Journal of the Royal Metereological Society*, 122, 1385-1404.
- Roether W., B. Manca, B. Klein, D. Bregant, D. Georgopoulos and V. Beitzel *et al.*, (1996). Recent changes in the eastern Mediterranean deep waters. *Science* 271 Sadiq M. Toxic Metal Chemistry in Marine Environments. , Marcel Dekker, New York, pp. 333–335.
- Roether W., and J. E. Lupton (2011). Tracers confirm downward mixing of Tyrrhenian Sea upper waters associated with the Eastern Mediterranean Transient. *Ocean Sci.*, 7,91 99.
- Rohling E.J., and H. Bryden, (1992). Man-induced salinity and temperature increase in the western Mediterranean deep water. *J. Geophys. Res.*, 97, NO. C7, 11191-11198.

- Sandroni V., Raimbault, P., Migon, C., Garcia, N., and Gouze, E.: (2007). Dry atmospheric deposition and diazotrophy as sources of new nitrogen to northwestern Mediterranean oligotrophic surface waters. *Deep-Sea Res. Pt. I* 54, 1859–1870.
- Schink D. R., N. L. Guinasso J., and Fanning K. A. (1975). Processes Affecting the Concentration of Silica at the Sediment-Water Interface of the Atlantic Ocean. *J. Geophys. Res.* 80 (21), 3013-3031.
- Schroeder K. , Taillandier V., Vetrano A., G.P. Gasparini (2008) .The circulation of the western Mediterranean Sea in spring 2005 as inferred from observations and from model outputs. *Deep-Sea Research I* 55 947– 965.
- Sciarra R. , G. Volpe, and R. Santoleri (2003). Complete catalogue of the Saharan dust events and polluted aerosols from historical SeaWiFS data, *ADIOS Project Deliverable 32*, 21 pp., Cent. Natl. de la Rech. Sci., Perpignan, France.
- Scrivner A., D. Vance, and E. J. Rholing (2004). New neodymium isotope data quantify Nile involvement in Mediterranean anoxic episodes, *Geology*, 32, 565-568.
- Sferratore A., Garnier, J., Billen, G., Conley, D. J., and Pinault, S.: Diffuse and point sources of silica in the Seine River watershed, *Environ. Sci. Technol.*, 40, 6630–6635, 2006
- Skliris S. and A. Lascaratos,(2004). Impacts of the Nile River damming on the thermohaline circulation and water mass characteristics of the Mediterranean Sea, *J. Mar. Syst.* 52 , pp. 121–143.
- Skliris S. Sofianos and A. Lascaratos, (2006). Hydrological changes in the Mediterranean Sea in relation to changes in the freshwater budget: A numerical modelling study. *J. of Marine System*, 65, 400-416.
- Skoulikidis N. T., and Gritzalis, K. (1998).Greek river inputs in the Mediterranean. Their intra-annual and inter-annual variations, *Fresenius Environ. Bull.*, 7, 90–95,
- Sparnocchia S., Gasparini, G.P., Astraldi, M., Borghini, M., Pistek, P., (1999). Dynamics and mixing of the Eastern Mediterranean outflow in the Tyrrhenian basin. *Journal of Marine Systems* 20, 301–317.
- Stumm W., and Morgan J. (1970). *Aquatic Chemistry Wiley Interscience publication*, Vol.1, pp.583.
- Taylor Mc Lennan, (1985), *The Geochemical Evolution of the Continental Crust*, Blackwells, Oxford, England, 312 pp.
- Theocharis A., Nittis K., Kontoyiannis H., Papageorgiu E, Balopoulos E., (1999). Climatic changes in the Aegean influence the eastern Mediterranean thermoaline circulation (1986-1997). *Geophys Res Let* 26. 1617-1620.
- Theocharis A., Lascaratos, A. and Sofianos, S., (2002). Variability of sea water properties in the Ionian, Cretan and Levantine seas during the last century. *CIESM Workshop Ser.* 16, pp. 71–74.
- Theodosi C., Markaki Z., Tselepides A., Mihalopoulos N. (2010). The significance of atmospheric inputs of soluble and particulate major and trace metals to the eastern Mediterranean seawater. *Marine Chemistry* 120 154–163.
- Tegen I., and Kohfeld Karen E. Atmospheric Transport of Silicon (2006). In: *The silicon cycle Human perturbations and impacts on aquatic systems*. Island Press, Island, (Scope 66)
- Treguer P. , Nelson DM, van Bennekom AJ, DeMaster DJ, Leynaert A, Qu'éguiner B. (1995). The balance of silica in the world ocean: a re-estimate. *Science* 268:375–79.
- Tria et al; (2007). Determination of aluminium in natural water samples. *Elsevier Analytica Chimica Acta* 588, 153–165.
- Van Bennekon A. , J., Berges G. W., van der Gaast S. J., and de Vries R. T. P. (1988). Primary productivity and the silica cycle in the Southern Ocean (Atlantic sector). *Paleoecology* 67, 19-30.

- Van Bennekom A. J., Buma A. G. J., and Nolting R. F. (1991). Dissolved aluminum in the Weddell-Scotia confluence and effect of Al on the dissolution kinetics of biogenic silica. *Mar. Chem.* 35, 423–434.
- Volpe G., Viva F., Banzon, Robert H. Evans, Rosalia Santoleri, Arthur J. Mariano, and Roberto Sciarra (2009). Satellite observations of the impact of dust in a low-nutrient, low-chlorophyll region: Fertilization or artifact? *Global Biogeochemical Cycle*, Vol 23.
- Ziv B., H. Saaroni, and P. Alpert (2004). The factors governing the summer regime of the eastern Mediterranean, *Int. J. Clim.*, 24, 1859–1871
- Wedepohl KH., (1995). The composition of the continental crust. *Geochim Cosmochim Acta* 59:1217–1232.
- Willey J. D., (1974). The effect of pressure on the solubility of silica in seawater at 0°C *Mur. Chem.* 2,239-250.

APPENDIX I

Chemical analysis of Nutrients_ Bonifacio Cruise

N.St	Depth (m)	Silicates ($\mu\text{m/l}$)
433	105	1,71
433	75	1,035
433	50	0,894
433	25	0,734
433	0	0,695
432	0	0,758
432	25	0,779
432	50	1,076
432	75	1,38
432	100	1,962
432	160	2,889
212	190	3,11
212	100	1,631
212	75	1,143
212	50	1,008
212	25	0,746
212	0	1,478
218	0	0,688
218	65	0,903
218	100	2,9
218	228	4,219
436	400	5,266
436	110	0,947
436	75	0,776
436	50	0,695
436	18	0,661
436	0	0,64
215	0	0,672
215	28	0,68
215	50	0,677
215	73	0,707
215	100	1,544
215	300	4,214
215	750	5,947
215	1199	6,612
Vector	3250	7,759

Vector	2500	7,711
Vector	2000	7,384
Vector	1000	6,38
Vector	500	5,05
Vector	200	3,376
Vector	100	1,429
Vector	68	0,849
Vector	50	0,754
Vector	25	0,755
Vector	0	0,731
51	0	1,488
51	25	0,768
51	45	0,791
51	75	1,347
51	100	1,763
51	200	3,574
51	500	5,146
51	1000	7,441
51	2000	7,277
51	2500	7,593
51	3250	7,715
51	3498	7,662

APPENDIX II

Chemical analysis of Nutrients_ Aeolian Cruise

N.St	Depth (m)	Silicates ($\mu\text{m/l}$)
Capo Granitola	5	0,46
Capo Granitola	15	0,558
Capo Granitola	30	0,26
Capo Granitola	45	0,345
Capo Granitola	70	0,455
Capo Granitola	110	0,369
Capo Granitola	200	2,959
Capo Granitola	250	2,577
Capo Granitola	350	4,974
Capo Granitola	600	4,875
Capo Granitola	800	3,875
Capo Granitola	1240	5,4
Palinuro 1	1760	7,565
Palinuro 1	1200	3,891
Palinuro 1	800	5,585
Palinuro 1	560	4,421
Palinuro 1	365	4,391
Palinuro 1	200	2,871
Palinuro 1	120	1,292
Palinuro 1	75	0,969
Palinuro 1	45	0,685
Palinuro 1	30	0,592
Palinuro 1	15	0,619
Palinuro 2	20	0,506
Palinuro 2	60	0,97
Palinuro 2	85	1,701
Palinuro 2	150	2,813
Palinuro 2	300	4,15
Palinuro 2	770	5,567
Palinuro 2	920	6,055
Palinuro 2	1185	6,4
Palinuro 2	1500	6,962
Palinuro 2	2300	7,398
Palinuro 2	2793	7,546
Marsili	2760	7,644

Marsili	1900	7,35
Marsili	1430	6,914
Marsili	1100	6,364
Marsili	890	5,89
Marsili	750	5,593
Marsili	500	4,844
Marsili	300	3,507
Marsili	100	1,268
Marsili	85	0,928
Marsili 1	30	0,547
Marsili 1	15	0,401

APPENDIX III

Chemical analysis of Trace Metals_ Bonifacio Cruise

Station	Depth	Al	Cu	Fe	Zn	V
51	0	1,15	0,58	3,11	1,36	3,54
51	25	0,35	0,11	1,06	0,39	1,35
51	45		0,09	1,10	0,98	1,89
51	75		0,02	0,62	0,34	1,15
51	100		0,10	2,24	0,50	3,06
51	200		0,06	0,24	0,20	0,85
51	500	0,55	0,11	1,25	1,69	1,99
51	1000		0,30	2,31	0,44	1,00
51	2000		0,27	1,02	0,42	0,85
51	2500		0,21	0,63	0,78	0,86
51	3250		0,30	0,39	0,23	0,80
51	3498	0,15	0,27		0,97	1,02
Vector	0	6,54	0,39	2,80	3,20	6,38
Vector	25	1,75	0,26			6,18
Vector	50	1,15	0,31	4,53	5,91	3,47
Vector	68	1,21	0,34		4,26	2,39
Vector	100	1,42	0,08	2,29	3,32	2,34
Vector	200	1,15	0,13	2,99		2,13
Vector	500	1,65	0,18	2,65		3,07
Vector	1000	4,09	0,59	3,94	4,68	2,22
Vector	2000	4,84	0,82	45,25	29,04	6,24
Vector	2500	0,47	0,09	0,55	0,55	0,80
Vector	3250	2,52	0,15	1,21	1,41	1,33
432	0	0,62	0,09	1,82	0,36	1,47
432	25	0,90	0,18	1,64	0,60	2,28
432	50	8,20	0,17	5,37	1,18	1,50
432	75	12,29	0,25	8,05	0,94	2,47
432	100	16,19	0,10	9,51	1,22	1,92
432	160	15,82	0,13	10,72	0,83	2,30
436	0	1,75	0,36	1,97	1,56	1,06
436	18	2,11	0,40	2,25	0,97	30,67
436	50		0,23	1,02	0,62	1,08
436	75	0,08	0,21	0,92	0,41	0,59
436	110	4,40	0,14	1,93	0,57	1,08

436	400	5,25		5,12	0,93	1,78
215	0	1,79	0,20	0,51	0,35	1,07
215	28	0,02	0,05	0,49	0,38	0,55
215	50		0,10	1,01	0,47	1,88
215	73	0,73	0,52	2,68	1,06	4,65
215	100		0,16	0,73	0,49	1,13
215	300	3,02	0,17	2,82	0,51	2,01
215	750	2,62	0,25	2,61	0,67	2,24
215	1199	1,48	0,10	1,30	0,29	1,39

APPENDIX IV

Silicon and Aluminum concentrations in the suspended particulate matter of the Rhone river

[Ollivier 2011]

DATE	Si	Al
28/11/2000	5,76	
12/12/2000	8,76	1,93
04/01/2001	7,97	
18/01/2001	6,75	2,4
07/02/2001	7,2	2,38
01/03/2001	6,35	
02/03/2001 (ore 11:00)	6,8	
02/03/2001 (ore 15:00)	6,59	
03/03/2001	6,42	
05/03/2001	5,88	
06/03/2001	6,92	1,85
09/03/2001(ore 11:40)	6,02	1,66
09/03/2001(ore 15:30)	5,42	1,79
12/03/2001	6,27	2,11
14/03/2001	6,47	
16/03/2001	6,45	2,02
20/03/2001	6,37	1,99
22/03/2001(ore 10:00)	7,29	2,11
22/03/2001(ore 15:00)	6,87	2,12
26/03/2001	6,99	2,37
29/03/2001	7,38	2,37
02/04/2001	7,1	2,19
03/04/2001	5046	2,32
20/04/2001	6,61	2,35
16/05/2001	6,09	2,13
10/07/2001	7,08	3,55
13/09/2001	7,77	3,39
05/10/2001	4,1	2,77
06/12/2001	7,44	3,06
07/01/2002		3,13
30/01/2002	7,19	2,4
18/02/2002		2,62
02/03/2002	7,99	2,5
28/03/2002		2,57
25/04/2002		1,97
07/05/2002		2,18
08/05/2002		2,24
22/05/2002		2,46

06/06/2002	6,53	2,64
16/08/2002	7,78	3,06
09/09/2002		2,49
10/09/2002 (ore 07:00)	7,42	2,47
10/09/2002 (ore 12:00)	7,07	2,36
10/09/2002 (ore 16:30)	6,45	2,21
11/09/2002	7,05	2,23
13/09/2002	6,9	2,55
27/09/2002		2,99
09/10/2002		5,24
08/11/2002		2,2
17/11/2002	6,2	
18/11/2002 (ore 11:00)	6,54	2,09
18/11/2002 (ore 17:00)	6,75	
19/11/2002 (ore 10:00)	6,76	1,99
19/11/2002 (ore 16:00)	6,04	1,97
20/11/2002 (ore 9:00)	6,52	1,96
21/11/2002	7,04	1,94
22/11/2002		1,93
25/11/2002		1,95
26/11/2002		1,97
27/11/2002		1,81
28/11/2002		1,81
29/11/2002		1,82
02/12/2002		1,88
01/04/2003		
23/05/2003		1,65
17/06/2003		3,07
01/12/2003		2,14
02/12/2003 (ore 9:00)		2,11
02/12/2003 (ore 12:35)		1,83
03/12/2003 (ore 10:30)		1,89
03/12/2003 (ore 17:30)		1,87
04/12/2003 (ore 12:15)		2,07
04/12/2003 (ore 19:45)		2,02
05/12/2003		1,84
06/12/2003		1,91
AVERAGE	6,73	2,3

